CALCULATION OF SPIN-HAMILTONIAN PARAMETERS FOR Gd^{3+} DOPING ISOSTRUCTURAL SERIES OF RARE-EARTH METAL TRICHLORIDE HEXAHYDRATES AND TRIFLUORIDES

Norman Robert Lewis

A Thesis

in

The Department

of

Physics

Presented in Partial Fulfillment of the Requirements
for the degree of Doctor of Philosophy at
Concordia University
Montréal, Québec, Canada

June 1982

ABSTRACT

CALCULATION OF SPIN-HAMILTONIAN PARAMETERS FOR Gd^{3+} DOPING ISOSTRUCTURAL SERIES OF RARE-EARTH METAL TRICHLORIDE HEXAHYDRATES AND TRIFLUORIDES

Norman Robert Lewis, Ph.D.
Concordia University, 1982

Spin-Hamiltonian parameters are calculated for Gd^{3+} doping the isostructural rare-earth metal series $RCl_3.6H_2O$ (R = Nd, Sm, Eu, Tb, Dy, Ho, Er, Tm) and RF_3 (R = La, Ce, Pr, Nd). The theory of spin-Hamiltonian parameters (SHPs) and of crystal-field parameters (CFPs) is presented, and the relationship between them is discussed. Consideration is given to the question of the validity of the crystal-field parameterization scheme and to the question of whether or not the SHPs arise solely from terms which are linear in the crystal field. The SHPs for the two series are calculated on the basis of the superposition model (SM) of Newman using a newly developed method which exploits the consistency of the model to determine distortions in the ionic positions. It is also shown how the SM may be reformulated so as to decouple the model parameter values from metal-ligand distance effects. In addition, the SHPs are calculated for the same two series using a model original to this work, called the point-charge plus induced-dipole model (PCID). This is based on the use of polarizability tensors whose symmetry conforms to that of the host crystal. These tensors are required in order to calculate the induced dipole moments at the various ion sites. Thus, the SHPs are expressed in terms of

point-charge sums and induced-dipole sums over the crystal, all sums being evaluated by Ewald's method. Although different polarizability values are found for each ion type for each host, these values are not arbitrary parameters as would arise in a purely empirical model. This is because they are subject to various physical constraints, as is discussed. Also, the polarizability values predicted by the model are found to vary with the host-ion radius in a way consistent with that predicted by the exchange charge model of Dick and Overhauser. Both the SM and the PCID model give results for the SHPs within experimental error. A review is given of existing polarizable dipole models. It is shown that all of these neither provide a rigorous treatment of the polarizability problem, nor do they agree well with experiment. Also there is presented a detailed treatment of Ewald's method including a newly developed technique for the evaluation of correction terms which occur in the theory. Conclusions are made regarding the validity and utility of the PCID model.

ACKNOWLEDGEMENTS

The author would like to thank Professor S. K. Misra for suggesting the thesis problem and for his continued aid and encouragement throughout the entire work. The author is also grateful to the personnel of the Concordia University Computer Center for much assistance and to the Natural Science and Engineering Research Council of Canada for partial financial support (Grant No. A4485).

TABLE OF CONTENTS

Table of Contents (Cont.)

LIST OF SYMBOLS

Symbols		See chapter
O_n^m	Stevens' Operator Equivalents	2
B_n^m, b_n^m	Spin-Hamiltonian parameters	2
	(Note: $b_2^m = 3\,B_2^m$, $b_4^m = 60\,B_4^m$)	
Z_n^m	Tesseral harmonics	3
A_n^m	Crystal-field coefficents	3
$A_n^m\langle r^n\rangle$	Crystal-field parameters	3
$K_n^m(\theta, \phi)$	Coordination factors	4
$\bar{A}_n$, $\bar{B}_n$, $\bar{b}_n$	Intrinsic parameters	4
t_n	Power law coefficent	4
R_N	Nearest-neighbour distance	4
α	Polarizability	5
Q'	Ionic core charge	6
Q''	Ionic shell charge	6
Q	Ionic charge	6

LIST OF FIGURES

LIST OF TABLES

List of Tables (Cont.)

Chapter 1

INTRODUCTION

The theory of the crystal field was first developed by Bethe[1] in 1929. Bethe considered the effect of the electrostatic (point-charge) field of an NaCl - type lattice on a given ion in the lattice. This classical approach, which deals with a basically long-range effect, is what is usually referred to as crystal-field theory. A different approach, which deals with inherently short-range effects, is that of ligand-field theory. Here, one is only concerned with a given metal ion and its immediate neighbours (ligands), the whole forming what is called a coordination cluster. In this context, the term 'ligand' refers not necessarily to a nearest neighbour, but rather to a neighbour which is such that there is no ion intervening between it and the metal ion. Thus, ligand-field theory includes all theories of chemical bonding between an ion and its neighbours.[2] In the present work, for convenience, the term 'crystal field' will be taken to include the ligand field.

Typical level splittings produced by a crystal field on an atom may be described in terms of crystal-field parameters (CFPs) which can be determined experimentally, usually from optical data. Also, the phenomenon of electron paramagnetic resonance (EPR) has been used as a primary tool in the investigation of the crystal field. In EPR, the energies are describable in terms of spin-Hamiltonian parameters (SHPs) which are also measurable.

In this area there are two long-standing problems. One relates to the question of what physical mechanisms give rise to the CFPs, and the

other is concerned with the relationship between the CFPs and the SHPs. With respect to the first problem, there have been, historically, two schools of thought as implied above in the distinction made between crystal-field theory and ligand-field theory. The proposition that the CFPs are due solely to the electrostatic point-charge field of the crystal is now taken to be untenable, as will be discussed later. In the past decade, the opposite contention, namely, the assertion that only short-range effects (for example, overlap and covalency) are of importance, has been the object of considerable attention. In this regard, perhaps the most successful theory has been the superposition model (SM) due to Newman. This model ascribes the origin of the CFPs solely to the neighbouring ligands.

It is clear that the point-charge-only approach ignores the quantum mechanical effects of near neighbours, while the ligand-only theory disregards the rest of the crystal. It should, however, be noted that in the point-charge plus induced-dipole (PCID) model, a model presented in this thesis, the magnitudes of the induced dipole moments are dependent on ionic polarizabilities. In a crystal, these in turn are dependent on covalency, exchange, and so on. Thus, the PCID model has features relating to both long- and short-range effects.

The fact that both the superposition model and the new PCID model meet with success implies that, despite their difference in outlook, they may be related to each other.

The second major question, mentioned above, dealt with the

relation between the CFPs and the SHPs. This work will also address this problem.

The EPR phenomenon, from which arise the SHPs, occurs only for transition ions. Of particular concern are those ions with a half-filled shell (S-state ions), as their splittings are not well understood. This work will concentrate on crystals of the lanthanide (rare-earth metal) transition series, doped by the S-state ion Gd^{3+}. A survey of the spectra of Gd^{3+} has been given by Buckmaster et al.[3] As they point out, the paramagnetic properties of Gd^{3+} have had an interesting history. Originally, interest in gadolinium compounds centered on their use in magnetic cooling and adiabatic demagnetization. Consideration of the paramagnetic properties of this ion was intensified in 1956 after it was used as the active material in the first solid-state maser. EPR measurements on Gd^{3+} are facilitated by the fact that it has an extremely long relaxation time which enables its EPR spectrum to be observed at temperatures as high as 290° K. This, combined with the fact that the Gd^{3+} splittings are readily measurable using EPR techniques at microwave frequencies with commonly available laboratory magnetic fields, means that there is a great variety of experimental data available.

This work will study the cases of Gd^{3+} doping single crystals of the series $RCl_3.6H_2O$ (rare-earth metal trichloride hexahydrates, hereafter RTH) where R = Nd, Sm, Eu, Tb, Dy, Ho, Er, Tm and RF_3, R = La, Ce, Pr, Nd. This is motivated by the fact that precise experimental values for the SHPs of these series are available. (See Chapter 4 for references.) Other more technical reasons for this choice will be given in due course.

Aside from the collateral aims previously mentioned, the main purpose of this work is to predict theoretically the values of the spin-Hamiltonian parameters for the above series. In outline form, the presentation will be as follows. Chapter 2 gives the theory leading to the spin-Hamiltonian parameters, while Chapter 3 treats that of the crystal-field parameters and discusses the relation between these and the SHPs. Chapter 4 deals with the theory and application of the superposition model and Chapter 5 deals with the theoretical development of the PCID model. Central to this is the question of the polarizability of ions in a crystal. This is considered separately in Chapter 6, and the application of the model is described in Chapter 7. Chapter 8 presents the conclusions and summary of this work. For convenience, detailed data and mathematics have been relegated to appendices.

Chapter 2

THE EPR PHENOMENON AND SPIN-HAMILTONIAN PARAMETERS

This chapter gives a brief outline of the phenomenon of electron paramagnetic resonance (EPR) and develops the concept of the so-called spin-Hamiltonian and the related spin-Hamiltonian parameters (SHPs). Although an excellent detailed treatment of this topic is given by Abragam and Bleaney,[4] the present account will serve as a basis for understanding, in the following chapter, the relation between the SHPs and the crystal-field parameters (CFPs).

Electron paramagnetism arises whenever an atom has an odd number of electrons, or, more specifically, when the electron shell has a resultant angular momentum. However, systems with an odd number of electrons are chemically highly reactive, and bond to form even-numbered systems which are not paramagnetic. On the other hand, transition atoms, which have partially filled inner shells, will remain paramagnetic because the chemistry affects only the outer shell. The odd electron in the unfilled shell will give the atom a net magnetic moment which can be set into precession by the application of an external static magnetic field. The EPR phenomenon consists of superposing a varying field (radiofrequency, microwave, etc.) on this and matching the applied frequency to that of the gyroscopic precession of the magnetic moment. This is done by varying either the frequency or the static external magnetic field. The advantage of the resonance method is its precise selectivity which allows one to concentrate on a particular contribution to the spectral splitting.

In EPR, one is dealing with the electronic Zeeman effect. An atom

with angular momentum $\vec{G}$ will have a magnetic moment $\vec{\mu}$ given by

$$\vec{\mu} = \gamma \vec{G} \tag{2.1}$$

where $\gamma \sim \frac{e}{mc}$ ($e = |e|$ and m is the mass of the electron). In a magnetic field, $\vec{H}$, the magnetic moment will precess with angular velocity

$$\vec{\omega} = -\gamma \vec{H} \tag{2.2}$$

The so-called Zeeman energy, W, is then given by

$$W = -\vec{\mu} \cdot \vec{H} \tag{2.3}$$

Now, γ may be expressed as

$$\gamma = -g\left(\frac{e}{2mc}\right) \tag{2.4}$$

where g (the 'g-factor') is a pure number measuring the relative contribution of orbital spin to the total angular momentum, $\vec{J}$. For an atom in a crystal, its value is determined experimentally. Defining the Bohr magneton, β, by

$$\beta = \frac{e\hbar}{2mc} \tag{2.5}$$

and using

$$\vec{G} = \hbar \vec{J} \tag{2.6}$$

one has, from Eqs. (2.1) and (2.3) to (2.6),

$$W = \beta g \vec{H} \cdot \vec{J} \tag{2.7}$$

Now, in the absence of $\vec{H}$, the levels of the ground-state term will be split by the crystal field by amounts known as zero-field splitting. However, for systems with an odd number of electrons, the zero-field splitting will leave a degeneracy. (This follows from Kramer's Theorem.[4]) One then assigns an 'effective' or 'ficticious' spin, S, to

the system so that the degeneracy equals 2S + 1. One then has an effective spin-Hamiltonian of the form

$$\mathcal{H} = \mathcal{H}_z + \mathcal{H}_c \tag{2.8a}$$

$$\mathcal{H}_z = \beta g \vec{H} \cdot \vec{S} \tag{2.8b}$$

where $\mathcal{H}_z$ is the electronic Zeeman term analogous to that given by Eq. (2.7), and $\mathcal{H}_c$ represents the crystal field. The expression for $\mathcal{H}_z$, as is, implies that the Zeeman effect depends only on the angle between $\vec{H}$ and $\vec{S}$. However, it also depends on the angle that $\vec{H}$ makes with the local crystal symmetry. Thus, g must be treated as a tensor, and Eq. (2.8b) is written as

$$\mathcal{H}_z = \beta \vec{H} \cdot \vec{g} \cdot \vec{S} \tag{2.9}$$

where

$$\vec{H} \cdot \vec{g} \cdot \vec{S} = g_{xx} H_x S_x + g_{xy} H_x S_y + \cdots \tag{2.10}$$

The crystal-field term in Eq. (2.8a) consists of a sum of terms containing combinations of higher powers of S_x, S_y, and S_z. These combinations, a given one designated by $\hat{O}$, behave as spin operators, and are chosen such as to behave in the same way as the spherical harmonics, Y_n^m. Thus, a given $\hat{O}$ would be written O_n^m. The advantage of this is that the formal form of the appropriate Hamiltonian can be written down without detailed calculation since it must reflect the symmetry of the crystal. Further, the number of such terms is limited by the fact that operators of degree $k > 2S$ can be omitted since they would have zero matrix elements, and those of odd degree are omitted because they are not invariant under time reversal. Thus, the spin-Hamiltonian is written as

$$\mathcal{H} = \beta \vec{H} \cdot \vec{g} \cdot \vec{S} + \sum_{n,m} B_n^m O_n^m \qquad (2.11)$$

For Gd^{3+} ($S = 7/2$), one has $n = 0, 2, 4, 6$ and $-n \leq m \leq n$. The form of the equivalent operators, O_n^m, most commonly employed (and used here) is due to Stevens.[5] They are listed in Ref. 4. Other forms for these operators are used by some authors. The relationships and conversion factors among the various representations are given by Dieke.[6]

The coefficents, B_n^m, are the spin-Hamiltonian parameters. They can be measured experimentally. The present thesis is concerned with their theoretical prediction.

Typical level splittings produced by a crystal field on an atom are of the order of 10^2 cm^{-1}. (Note that it is customary in this area to use the spectroscopists' unit of energy, the inverse centimeter, where one has 1 eV = 8108 cm^{-1}, although there will also be occasion to use GHz as a unit, where 1 GHz = 30 cm^{-1}.) This may be compared with the central field of the nucleus which gives splittings of 10^5 cm^{-1}, the Coulomb interaction with the other electrons in the atom (10^4 cm^{-1}), and spin-orbit coupling (10^2 to 10^3 cm^{-1}). On the other hand, there are smaller effects such as interactions with the nuclear spin ($< 10^{-1}$ cm^{-1}), and with the nuclear quadrupole moment ($\sim 10^{-3}$ cm^{-1}). However, here, these effects will not be considered, as current experimental procedures cannot resolve splittings of less than 10^{-1} cm^{-1} for the systems that are being investigated.

Chapter 3

THE CRYSTAL FIELD

This chapter develops expressions for the crystal-field parameters (CFPs), shows how they are related to the spin-Hamiltonian parameters of the previous chapter, and also discusses the ground-state splitting mechanisms of Gd^{3+}. It should be noted that these topics are subject to considerable dispute and that there is a lack of conventional mathematical notation in this area. Both of these factors dictate that the following be presented in some detail so as to avoid any confusion.

3.1 Crystal-Field Parameters

From the spherical harmonic addition theorem,[7] if ω is the angle between the vectors (r, θ_i, ϕ_i) and (R, θ_j, ϕ_j), one has

$$P_n^0(\cos\omega) = \frac{4\pi}{2n+1} \sum_{m=-n}^{n} (-1)^m Y_n^{-m}(\theta_j, \phi_j)\, Y_n^m(\theta_i, \phi_i) \qquad (3.1)$$

where P_n^0 is a Legendre polynomial, and Y_n^m are spherical harmonics. Now consider the electrostatic potential $V(\vec{r})$ due to an ion with charge q at position $\vec{R}$. If ω is the angle between $\vec{r}$ and $\vec{R}$, then one has[8]

$$V(\vec{r}) = \frac{q}{|\vec{R}-\vec{r}|} = \sum_{n=0}^{\infty} \frac{r^n}{R^{n+1}} P_n^0(\cos\omega), \quad R > r. \qquad (3.2)$$

In order to avoid using imaginary quantities, one defines Tesseral harmonics, Z, via[9]

$$\left.\begin{aligned} Z_{n0} &= Y_n^0 \\ Z_{nm}^c &= \frac{1}{\sqrt{2}}\left(Y_n^{-m} + (-1)^m Y_n^m\right) \\ Z_{nm}^s &= \frac{i}{\sqrt{2}}\left(Y_n^{-m} - (-1)^m Y_n^m\right) \end{aligned}\right\} \; m > 0 . \qquad (3.3)$$

Then, from Eq. (3.1),

$$P_n^o(\cos\omega) = \frac{4\pi}{2n+1} \sum_{m=0}^{n} \left\{ Z_{nm}^c(\theta_i,\phi_i)\, Z_{nm}^c(\theta_j,\phi_j) + Z_{nm}^s(\theta_i,\phi_i)\, Z_{nm}^s(\theta_j,\phi_j) \right\}. \tag{3.4}$$

This is usually written as

$$P_n^o(\cos\omega) = \frac{4\pi}{2n+1} \sum_{\alpha} Z_{n\alpha}(\theta_i,\phi_i)\, Z_{n\alpha}(\theta_j,\phi_j) \tag{3.5}$$

where the sum over α implies that, for each m, there are sums of products involving both Z_{nm}^c and Z_{nm}^s as in Eq. (3.4). Using this convention, the potential at (r,θ,ϕ) due to k charges q_j at (R_j,θ_j,ϕ_j), j = 1, ...,k is

$$V(r,\theta,\phi) = \sum_{n=0}^{\infty} \sum_{\alpha} r^n \gamma_{n\alpha}\, Z_{n\alpha}(\theta,\phi) \tag{3.6}$$

where

$$\gamma_{n\alpha} = \sum_{j=1}^{k} \frac{4\pi}{2n+1}\, q_j\, \frac{Z_{n\alpha}(\theta_j,\phi_j)}{R_j^{n+1}} \tag{3.7}$$

For a given magnetic ion, the total classical potential energy due to the crystalline magnetic field will be

$$W_c = -e \sum_i V(r_i,\theta_i,\phi_i) \quad (= \mathcal{H}_c) \tag{3.8}$$

where V is as in Eq. (3.6), and the summation is over the magnetic electrons. The corresponding crystal-field Hamiltonian, $\mathcal{H}_c$, is formed from this using the usual rules $x \to x_{op}$, etc. Thus, $\mathcal{H}_c$ is also given by Eq. (3.8) if V is now understood as an operator. That is, Eq. (3.6) may be put in the form

$$V(r,\theta,\phi) = \sum_{n,m} V_n^m \tag{3.9}$$

where V_n^m is an irreducible tensor operator of the form T_k^q. Such an operator is defined by its commutation relations with the angular momentum operators[10]:

$$[J_\pm, T_k^q] = \sqrt{k(k+1) - q(q\pm 1)}\; T_k^{q\pm 1}$$
$$[J_z, T_k^q] = q\, T_k^q \tag{3.10}$$

The T_k^q are the components of the tensor T_k of degree k with q components taking on the values: k, k - 1, ... , -k. The main advantage of treating V in terms of operators of this form is that the calculation of matrix elements of $\mathcal{H}_c$ is then facilitated by the Wigner-Eckart Theorem.[11] The type of representation one uses depends on the size of W_c relative to the other interactions in the ion. For the rare-earths, where W_c is less than spin-orbit coupling, one uses the L, S, J, J_M scheme.[12,13] Then the Wigner-Eckart Theorem gives[14]

$$\langle LSJJ_M | T_k^q | L'S'J'J_M' \rangle = \frac{(SJ \| T_k \| S'J')}{\sqrt{2J+1}} \langle J'kJ_M'q | JJ_M \rangle \qquad (3.11)$$

where $\langle J'kJ_M'q|JJ_M\rangle$ is a Clebsch-Gordan coefficent and $(SJ||T_k||S'J')$ is a reduced matrix element (which is independent of J_M and q). Applying Eq. (3.11) to the evaluation of the matrix elements of $\mathcal{H}_c$, gives

$$-e \sum_i \langle LSJJ_M | V(i) | L'S'J'J_M' \rangle =$$

$$-e \sum_{n,\alpha} \gamma_{n\alpha} \langle r^n \rangle (J'J_M' \| Z_n \| JJ_M) \langle JJ_M' | Z_{n\alpha}(\theta,\phi) | JJ_M \rangle \qquad (3.12)$$

where the radial and angular integrations have been separated. Now, the $Z_{n\alpha}$ may be replaced by operator equivalents as was done with the crystal-field term of the spin-Hamiltonian.[4,9] Then the reduced matrix element in Eq. (3.12) becomes $(J'J_M'||O_n||J J_M)$, which is usually denoted by θ_n (some authors use K_n). The values for θ_n for a given ion are found by directly integrating between single-electron wavefunctions. The last factor in Eq. (3.12) becomes of the form $\langle |O_n^m| \rangle$. The numerical values of these elements are (apart from normalization constants) just Clebsch-Gordan coefficents as is consistent with Eq. (3.11).

Explicitly, the relation between the $Z_{n\alpha}$ and the O_n^m (alluded to above) is defined via functions f_{nm}^c which are such that[9]

$$Z_{nm}^c = (\text{const})\, f_{nm}^c / r^n \qquad (3.13)$$

with

$$\sum_i f_{nm}^c(i) = \theta_n \langle r^n \rangle O_n^m \qquad (3.14)$$

Now, for most cases, the crystal symmetry is such that $\gamma_{nm}^s = 0$. Thus, one may write

$$-eV(x,y,z) = \sum_{n,m} A_n^m f_{nm}^c(x,y,z) \qquad (3.15)$$

where

$$A_n^m = \gamma_{nm}^c (-e) \times (\text{a numerical factor occuring in } Z_{nm}^c). \qquad (3.16)$$

Thus, $\mathcal{H}_c$ becomes

$$\mathcal{H}_c = \sum_i \sum_{n,m} A_n^m f_{nm}^c(x_i,y_i,z_i)$$

$$= \sum_{n,m} \{A_n^m \langle r^n \rangle \theta_n\} O_n^m \qquad (3.17)$$

The A_n^m in this expression are the crystal-field parameters. Explicitly, the A_n^m are given by

$$A_n^m = -|e| \sum_i \delta_i \left\{ \frac{Z_n^m(r_i)}{r_i^{n+1}} \right\} \qquad (3.18)$$

where (for n = 2,4) one has

$$Z_2^0 = \frac{3z^2 - r^2}{4r^2} \qquad (3.19A)$$

$$Z_2^2 = \frac{3}{4} \frac{x^2 - y^2}{r^4} \qquad (3.19B)$$

$$Z_4^0 = \frac{1}{64} \frac{35z^4 - 30z^2r^2 + 3r^4}{r^4} \qquad (3.19C)$$

$$Z_4^2 = \frac{5}{16} \frac{(7z^2 - r^2)(x^2 - y^2)}{r^4} \qquad (3.19D)$$

$$Z_4^4 = \frac{35}{64} \frac{x^4 - 6x^2y^2 + y^4}{r^4} \qquad (3.19E)$$

It is customary in calculating the A_n^m to take into account the fact that the magnetic electrons (in the 4f shell in the case of the rare earths) are shielded from the crystal field by the outer filled shell.

This is done by introducing a shielding constant[12], γ_n (not to be confused with the γ occuring in Eq. (3.7)). Thus, A_n^m is replaced by $A_n^m\gamma_n$ in Eq. (3.17). With this modification, if one compares Eq. (3.17) with Eq. (2.11), there is found the following relation between the spin-Hamiltonian parameters B_n^m and the crystal-field parameters A_n^m, namely,

$$B_n^m = A_n^m \langle r^n \rangle \gamma_n \theta_n \quad . \tag{3.20}$$

At this point there is great confusion in the literature. This is because many authors (in particular, Wybourne[15]) refer to 'crystal-field parameters' as being the product $A_n^m\langle r^n\rangle$ and then proceed to denote this product as B_n^m. Hence, it is often unclear if a given reference is referring to CFPs or to SHPs. Secondly, the A_n^m, per se, are not measurable experimentally. What is measurable is the product $A_n^m\langle r^n\rangle$. Thus, when measurements of CFPs are cited, it is this product, and not A_n^m by itself, which has been measured. Thirdly, the B_n^m (SHPs) are also measurable. However, from Eq. (3.20), a measurement of both CFPs and SHPs for the same crystal can, at best, give the ratio

$$\frac{B_n^m}{A_n^m\langle r^n\rangle} = \gamma_n \theta_n \quad . \tag{3.21}$$

But, for Gd^{3+}, the ground-state splitting is not fully understood (as will be discussed). Thus, one does not know what wavefunctions to use to calculate θ_n. Also, γ_n is not measurable. Hence the experimental results are not as helpful as one might think, in that they give only the product of two unknowns (γ_n and θ_n), not either separately.

3.2 The Validity of the Parameterization Scheme

The crystal-field parameterization scheme given above (Eqs. (3.17) and (3.18)) apparently makes two tacit assumptions: (1) that the extended ions can be replaced by point charges, and (2) that the interatomic forces in the crystal are of a Coulomb character. While the first assumption

is acceptable (with the proviso that one include induced dipoles), the second is false, as the actual interatomic potentials are known to deviate strongly from Coulomb behaviour. This has naturally led some to question the validity of the entire formulation. However, Newman has shown that, despite this, the resulting scheme is adequate and can incorporate other mechanisms (of non-Coulomb origin) related to the ligand aspects of the field, such as overlap and covalency. Newman's argument is given in detail in Appendix A.

Another criticism which has been made relates to the use of Eq. (3.20), this relation implying that the SHPs are linear in the CFPs, whereas it is known that, for S-state ions (Gd^{3+}, Eu^{2+}), the relative signs of B_n^m and A_n^m are different in similar hosts (e.g. YVO_4 and YPO_4[16]). On the other hand, there are many series of hosts for which one does have a linear relationship, for $n = 2$, with Gd^{3+} as the substituted ion. Examples are the lanthanide ethylsulphates,[3] hosts of the zircon structure,[16] plus studies on insulator data.[17] Also, Newman has indicated that there is good reason to believe that, generally, the $n = 2$ parameters are linear[16] and he further argues this for $n = 4$.[17] In addition, the assumption of linearity has been used successfully by a number of authors, for example, Bijvank et al.[19-21]

This apparent paradox has been discussed by Barnes et al.[22] They point out that, in general, the B_n^m versus A_n^m relation is linear for $n = 2,4$ for S-state lanthanide ions doping isostructural hosts, except for those of the hexagonal metal sequence Sc, Y, and Lu and the cubic metal sequence Pt, Pd, Ag, and Au. They propose that for these 'anomalous' metals there exists an extra metallic process for S-state splittings that is extremely sensitive to the electronic structure of the impurity

(Gd^{3+}) vis à vis that of the host metal. If this is the case, it would at least imply that the linearity assumption is valid for the series being investigated in this work, as the host metals are not among those described as being anomalous.

Another approach to this problem has been made by Adam et al.[23] They, in considering the problems inherent in the traditional crystal-field parameterization scheme, were led to develop a crystal-field Hamiltonian free of the assumption regarding the Coulomb nature of interatomic forces. This gave expressions for the CFPs consisting of a series of powers $\langle r^n \rangle$, rather than a pure $\langle r^n \rangle$ value as in $A_2^0\langle r^2 \rangle$, for example. Otherwise, their parametric expression for the crystal-field potential in terms of spherical (Tesseral) harmonics is the usual one. As this work (Ref. 23) is very recent, no numerical calculations have yet been published by the authors. However, it is possible that the various terms in the expressions for a given CFP could be competing in sign such that the overall sign varies from host-to-host in those cases where the B_n^m/A_n^m ratio varies. In other cases it may be such that one term dominates so the B_n^m versus A_n^m relation is linear.

From all of the above considerations it is evident that, while the basic processes are not well understood, the use of the relation given by Eq. (3.20) is justified for the hosts being considered in this work.

3.3 Ground-State Splitting Mechanisms for Gd^{3+}

This section briefly discusses the θ_2-value for Gd^{3+} as it is required for the calculations which will be described later.

The ground-state splitting of Gd^{3+} has long been an outstanding problem. The various attempts to provide a satisfactory explanation have

been reviewed by Wybourne,[15] Newman,[24] and by Buckmaster et al.[3] The problem is that Gd^{3+}, having a half-filled $4f^7$ shell, should have the ground term being $^8S_{7/2}$ (from Hund's rules[12]), giving L = 0. Thus, there should be no $\vec{L}\cdot\vec{S}$ coupling, and one should have $\chi_c = 0$ (working in the Russell-Saunders approximation). The fact that a spectrum is observed (over and above that of the electronic Zeeman splitting) means that there must be some higher states (terms) mixed in with the ground term. There are many mechanisms by which this mixing can occur. Newman[24] has discussed ten such mechanisms. However, there are only two which give a significant contribution to the observed splitting.[3] The first of these is ordinary intermediate coupling through which the higher-lying $^6P_{7/2}$ and $^6D_{7/2}$ terms are mixed in with the $^8S_{7/2}$ ground term. The contribution due to this has been calculated by Hutchison et al.[25] The second (Wybourne[26]) is due to relativistic effects. The sum of these effects gives θ_2 for Gd^{3+} as

$$\theta_2 = -\frac{12}{5}\frac{|e|\xi^3}{W_P^2 W_D}\langle r^2\rangle + \frac{16}{245}\frac{|e|\xi}{W_P}\langle R^2\rangle \qquad (3.22)$$

where, for Gd^{3+}, $\langle r^2\rangle = 0.785\ a_0^2$, $\xi = 1534\ cm^{-1}$ is the spin-orbit coupling parameter, W_P (= 32,200 cm^{-1}) and W_D (= 40,000 cm^{-1}) are the energy differences between the states ($^6P_{7/2}$, $^8S_{7/2}$) and ($^6D_{7/2}$, $^8S_{7/2}$), respectivly, and $\langle R^2\rangle = -0.07\ a_0^2$ ($a_0 = 0.52$ Å). The mechanisms which give rise to θ_4 and θ_6 are not yet understood.

Chapter 4

THE SUPERPOSITION MODEL

This chapter is concerned with the superposition model of Newman (hereafter denoted as SM). (See Refs. 16 - 18, 24, 26 - 30.) Sec. 4.1 briefly outlines the model and describes a method that has been developed to determine the model parameters. Secs. 4.2 and 4.3 describe the subsequent application of this method to RF_3 and RTH. Based on the results of this application, Sec. 4.4 shows how the SM may be formulated so as to decouple metal-ligand distance effects from other factors which may influence the model parameters.

4.1 Theory

The original motivation for the superposition model was the observation that the conventional electrostatic point-charge model simply cannot predict the experimentally observed values of the crystal-field parameters $A_n^m\langle r^n\rangle$.[24] It was concluded that the dominant effects contributing to the CFPs were essentially local in character — effects such as covalency and overlap. This being the case, it was assumed that the crystal field can be built up ('superposed') from the separate contributions of each ion in the crystal, although, in practice, only the so-called coordinated ions (ligands) are taken into account. The spherical symmetry of the ions then ensures that each contribution can be represented as a cylindrically symmetric field if the z axis of the coordinate system is aligned along the symmetry axis. A given CFP, $A_n^m\langle r^n\rangle$, is then expressed as

$$A_n^m\langle r^n\rangle = \sum_i \bar{A}_n(R_i)\, K_n^m(\theta_i,\phi_i) \qquad (4.1)$$

Here, the coordination factors $K_n^m(\theta_i, \phi_i)$ are explicit functions of the angular positions of the ligands, and the $\bar{A}_n(R_i)$, called intrinsic parameters, represent the axially symmetric field due to a single ligand at a distance R_i from the center of the substituted paramagnetic ion. (The expressions for $K_n^m(\theta, \phi)$ are given in Table I.) It is usually the case in a given crystal that the range of R-values for the ligands is quite small. Thus, it is assumed that the $\bar{A}(R_i)$ can be represented in terms of two parameters: a value $\bar{A}(R_o)$ at the average distance, R_o, of the ligands (from the substituted paramagnetic ion), and a power law, t_n, such that

$$\bar{A}_n(R) = \bar{A}_n(R_o)\left(\frac{R_o}{R_i}\right)^{t_n} \qquad (4.2)$$

If the coordinated ligands are of more than one type (e.g. some O^{2-}, and some F^-, say), then separate parameters ($\bar{A}_n(R_o)$, t_n) have to be introduced for each type.

As is evident from the above, the SM, in its original form, dealt only with CFPs. However, it can also be used to study SHPs if the relation between $A_n^m\langle r^n\rangle$ and B_n^m is linear. The question of linearity has been discussed in Chapter 3. If the relation is linear, then one may express Eqs. (4.1) and (4.2) in terms of SHPs, instead of CFPs, as

$$B_n^m = \bar{B}_n(R_o)\sum_i\left(\frac{R_o}{R_i}\right)^{t_n} K_n^m(\theta_i,\phi_i) \qquad (4.3)$$

As will be seen, the results of this present work support the contention that the second- and fourth-order parameters are linear. (As for the sixth-order parameters, they are very small and difficult to measure accurately. Also, because of the high powers involved (see Table I), they are extremely sensitive to small changes in the ionic positions.)

TABLE I. Values of the coordination factors $K_n^m(\theta, \phi)$ for m (even) ≥ 0.

n	m	K_n^m
2	0	$\frac{1}{2}(3\cos^2\theta - 1)$
2	2	$\frac{1}{2}(3\sin^2\theta\cos 2\phi)$
4	0	$\frac{1}{8}(35\cos^4\theta - 30\cos^2\theta + 3)$
4	2	$\frac{5}{2}(7\cos^2\theta - 1)\sin^2\theta\cos 2\phi$
4	4	$\frac{35}{8}(\sin^4\theta\cos 4\phi)$
6	0	$\frac{1}{16}(231\cos^6\theta - 315\cos^4\theta + 105\cos^2\theta - 5)$
6	2	$\frac{105}{32}(16\cos^4\theta - 16\sin^2\theta\cos^2\theta + \sin^4\theta) \times \sin^2\theta\cos 2\phi$
6	4	$\frac{63}{16}(11\cos^2\theta - 1)\sin^4\theta\cos 4\phi$
6	6	$\frac{231}{32}(\sin^6\theta\cos 6\phi)$

This relates to the main problem of the SM (and most models) — namely, that the substituted paramagnetic ion, being either undersized or oversized compared to the host paramagnetic ion, produces distortions which make the coordination factors $K_n^m(\theta_i, \phi_i)$ doubtful for just those ions which are supposed to make the largest contribution to the crystal field. Consequently, the sixth-order parameters will not be considered here.

The conventional way to determine the parameters $\bar{B}_n(R_o)$ and t_n is simply to apply a least-squares fitting procedure to the experimental data for each value of n. However, Misra et al.[31] have demonstrated a method of determining the parameter values by exploiting the self-consistency of the model. This is based on the fact that if one defines

$$P_n^m(t_n) = \sum K_n^m(\theta_i, \phi_i)\left(\frac{R_o}{R_i}\right)^{t_n} \tag{4.4}$$

then, taking the case of $n = 2$, $\bar{B}_2(R_o)$ can be expressed either as

$$\bar{B}_2(R_o) = B_2^o / P_2^o(t_2) \equiv \bar{B}_2(A) \tag{4.5}$$

or

$$\bar{B}_2(R_o) = B_2^2 / P_2^2(t_2) \equiv \bar{B}_2(B). \tag{4.6}$$

Clearly, consistency requires that the value of t_2 be such that $\bar{B}_2(A) = \bar{B}_2(B)$, or, equivalently, that

$$E(t_2) \equiv \frac{\bar{B}_2(A) - \bar{B}_2(B)}{\bar{B}_2(B)} = 0. \tag{4.7}$$

Now, if $E(t_2)$ values are calculated for a given crystal for various values of t_2, one need not expect to get a null result for Eq. (4.7) because local distortion effects will most likely have affected the K_2^m values in Eq. (4.4). However, it should be the case that one gets a t_2 value that minimizes $E(t_2)$. With this t_2 value having been determined, one then has two different $\bar{B}_2$ values (one for $m = 0$, and one for $m = 2$).

In order to bring them closer together one can consider distortions in the ionic positions. It is noted that, from Table I, if one were to vary only the ϕ_i values then only the $\bar{B}_2(B)$ values would change, as $\bar{B}_2(A)$ is independent of ϕ. (i.e. ϕ_i is the azimuthal angle for a given ion and the coordination factor K_2^0 is independent of ϕ, whereas K_2^2 is not.) A similar procedure can also be done for the fourth-order parameters.

The above analysis was applied by Misra et al.[31] to RF_3 and by Lewis and Misra[32] to RTH. This is described in the following sections. The details regarding the cell structure, lattice constants, and unit cell parameters for both of these systems are given in Appendix B.

4.2 Application to RF_3

The motivations for studying the system RF_3 (R = La, Ce, Pr, Nd) are: (i) the recent availability of very accurate SHPs as reported by Misra et al.[33] In Ref. 33, the parameters were evaluated by the application of a rigorous least-squares fitting procedure[34] in which all the resonant EPR line positions obtained for several orientations of the external magnetic field are simultaneously fitted. (ii) very accurate x-ray data are available on the RF_3 crystals[35] to permit a precise evaluation of the required coordination factors, (iii) the RF_3, being anhydrous, do not contain hydrogens (of H_2O molecules) whose positions are hard to determine by x-ray techniques, and (iv) since the RF_3 constitute a homologous series, they are ideal for the SM which is sensitive to small changes in atomic positions.

For RF_3, the ligands are the nine nearest-neighbour F^- ions. The positions of these ions for the four hosts are given in Table II. Eqs. (4.5) and (4.6) were applied to each host in order to evaluate $\bar{B}_2(A)$

TABLE II. Positions of the nine nearest-neighbour F^- ions for RF_3 used in superposition model fits. All angles are in degrees, all distances are in angstroms.

	Ions	1	2,3	4,5	6,7	8,9
	R	2.453	2.419	2.466	2.473	2.604
LaF_3	θ	0.0	118.13	90.56	69.19	150.07
	φ	. . .	166.55	279.04	32.44	72.64
	R	2.427	2.394	2.442	2.448	2.578
CeF_3	θ	0.0	118.13	90.56	69.19	150.06
	φ	. . .	166.54	279.04	32.45	72.65
	R	2.410	2.376	2.422	2.430	2.558
PrF_3	θ	0.0	118.13	90.56	69.19	150.08
	φ	. . .	166.56	279.05	32.42	72.63
	R	2.399	2.366	2.415	2.420	2.548
NdF_3	θ	0.0	118.13	90.56	69.20	150.04
	φ	. . .	166.53	279.04	32.47	72.66
	R	2.349	2.317	2.367	2.370	2.496
GdF_3	θ	0.0	118.13	90.56	69.20	150.02
	φ	. . .	166.52	279.02	32.50	72.67

and $\bar{B}_2(B)$. These results are given explicitly for Nd in Table III and plots of $E(t_2)$ vs. t_2 for the four hosts are given in Fig. 1. It is seen that the minima for $E(t_2)$ occur for $t_2 = 9 \pm 1$. The value of $t_2 = 9$ was used for further considerations. For the fourth-order parameters, the three values for $\bar{B}_4$ (corresponding to m = 0, 2, 4) were calculated. For $t_4 = 14$ the average deviation in the mean of these values was a minimum. (See Table III.) Thus, t_4 was taken to have the value 14. (Note that it is conventional to write $\bar{b}_2 = 3\,\bar{B}_2$, $\bar{b}_4 = 60\,\bar{B}_4$.)

Having determined the power laws, the values of ϕ_i for eight neighbours (Nos. 2 - 9 in Table II) were varied so as to bring $\bar{B}_2(B)$ into agreement with $\bar{B}_2(A)$. (Ion No. 1 has $\phi_1 = 0°$ and hence ϕ_1 is not defined.) The results are given in Table IV. It is seen there that variations of $\Delta\phi$ within $\pm 3°$ give fractional differences in the $\bar{B}$ values of the order of 0.2 %. These same sets of $\Delta\phi$ values are used to calculate the intrinsic parameters for the fourth-order case. (The results for all cases are given in Table V.) Them, for both orders, one can take the average value of the intrinsic parameters so determined and then use the previously determined t_n values in order to calculate the B_n^m values. These results are given in Table VI, which also lists the experimental values. It can be seen there that, taking into account the experimental error of ± 0.010 GHz, the agreement is perfect for all except the B_4^4 values in the cases of LaF_3 and CeF_3 where the agreement between theory and experiment can be considered reasonably close.

It is also noted, for future reference, that the $\bar{B}_2$ values so determined, are linear in the host-ion radius.

In almost all previous applications of the SM to Gd^{3+} SHPs, the crystal symmetry has been such that the parameter B_2^2 was identically

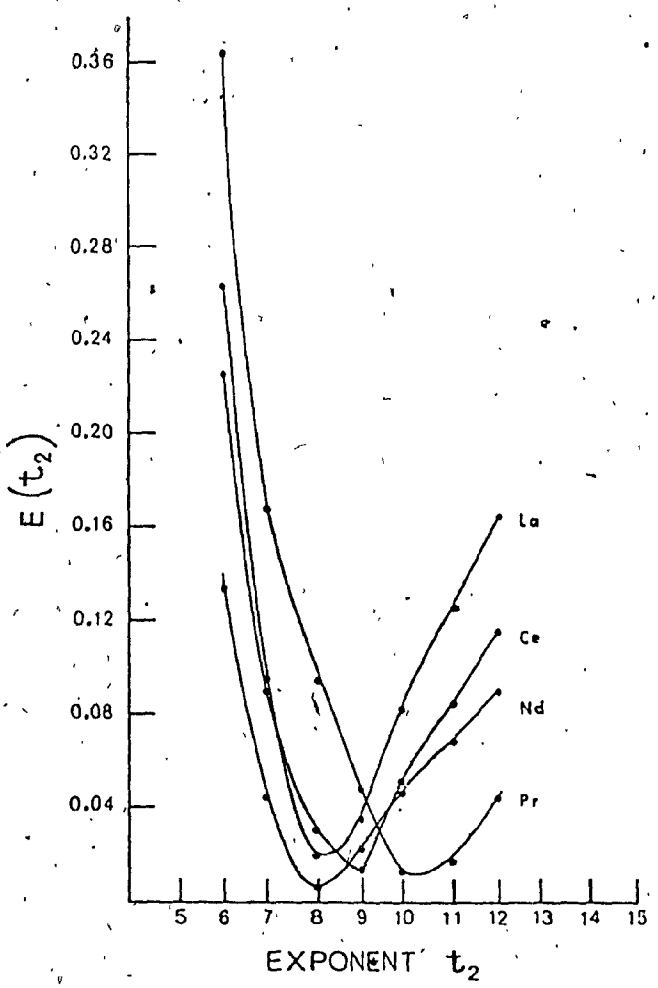

Fig. 1. Plot of $E(t_2)$ as a function of t_2 in various RF_3 hosts, R = La, Ce, Pr, Nd. (For definition of $E(t_2)$ see Eq. (4.7))

TABLE III. Values for $\bar{b}_2$ and $\bar{b}_4$ as a function of the power law exponent for Gd^{3+} in NdF_3 without distortions. All b_n^m are expressed in GHz. (Note: $\bar{b}_2 = 3\ \bar{B}_2$, $\bar{b}_4 = 60\ \bar{B}_4$)

t_n	b_0^0/P_2^0	b_2^2/P_2^2	b_4^0/P_4^0	b_4^2/P_4^2	b_4^4/P_4^4
1	3.510	0.743	0.0155	0.0349	0.0216
2	4.855	1.175	0.0159	0.0322	0.0218
3	7.473	2.627	0.0163	0.0300	0.0220
4	14.730	-14.764	0.0167	0.0283	0.0222
5	129.293	-2.019	0.0171	0.0269	0.0224
6	-21.231	-1.107	0.0176	0.0258	0.0226
7	-10.307	-0.774	0.0180	0.0248	0.0228
8	-7.022	-0.601	0.0185	0.0240	0.0230
9	-5.446	-0.495	0.0190	0.0234	0.0232
10	-4.526	-0.424	0.0195	0.0228	0.0234
11	-3.925	-0.372	0.0200	0.0224	0.0236
12	-3.505	-0.333	0.0205	0.0220	0.0238
13	-3.197	-0.303	0.0211	0.0216	0.0240
14	-2.963	-0.279	0.0216	0.0214	0.0242
15	-2.781	-0.259	0.0222	0.0211	0.0244
16	-2.636	-0.242	0.0228	0.0209	0.0246
18	-2.434	-0.216	0.0241	0.0207	0.0250
20	-2.291	-0.196	0.0255	0.0205	0.0254
22	-2.192	-0.181	0.0269	0.0204	0.0257
24	-2.124	-0.169	0.0285	0.0204	0.0261
26	-2.079	-0.158	0.0302	0.0205	0.0265

TABLE IV. The angular distortions $\Delta\phi_i$ ($i = 2,9$) to bring close together the $\bar{b}_2$ values as obtained from b_2^0 and b_2^2. $\Delta\bar{b}_2$ represents the per-cent difference $[\bar{b}_2(m = 2) - \bar{b}_2(m = 0)] \times [100/\bar{b}_2(m = 0)]$. $\bar{b}_n$ are expressed in GHz. The *'s indicate the deviations used for theoretical calculations of parameters b_n^m as given in Table VI.

Host	$\bar{b}_2(m = 0)$	$\bar{b}_2(\%)$	$\Delta\phi_2$	$\Delta\phi_3$	$\Delta\phi_4$	$\Delta\phi_5$	$\Delta\phi_6$	$\Delta\phi_7$	$\Delta\phi_8$	$\Delta\phi_9$
LaF_3	-4.457	0.18	-2°	-2°	-1°	3°	3°	3°	1°	1°
CeF_3	-4.879	0.54	-3°*	-2°*	0°*	-1°*	2°*	3°*	-1°*	-1°*
			-3°	-2°	0°	-1°	3°	2°	-1°	-1°
PrF_3	-4.936	0.01	-3°	-2°	-1°	-1°	1°	3°	-1°	0°
			-3°*	-2°*	-1°*	-1°*	1°*	3°*	0°*	-1°*
NdF_3	-5.472	0.13	0°	0°	-3°	-2°	3°	3°	-1°	3°
			0°	0°	-3°	-2°	3°	3°	3°	-1°
			0°*	0°*	-2°*	-3°*	-3°*	3°*	-1°*	3°*
			0°	0°	-2°	-3°	3°	3°	3°	-1°

TABLE V. The values of $\bar{b}_n$ (in GHz) as obtained for different m values using the deviations $\Delta\bar{\phi}_i$ given by Table IV.

	$\bar{b}_2$		$\bar{b}_4$		
Host	m = 0	2	0	2	4
LaF_3	-4.457	-4.465	0.018	0.018	0.031
CeF_3	-4.879	-4.853	0.020	0.020	0.035
PrF_3	-4.936	-4.935	0.019	0.020	0.026
NdF_3	-5.472	-5.479	0.022	0.021	0.025

TABLE VI. The values of the theoretical and experimental spin-Hamiltonian parameters b_n^m (GHz). The angular deviations as given in Table IV have been used for theoretical parameters. The $\bar{b}_n$ values used for theoretical parameters which are the averages of values for different m's are also given. (Expt. stands for experimental value, while theor. stands for theoretical value.)

	LaF_3		CeF_3		PrF_3		NdF_3	
	Expt.	Theor.	Expt.	Theor.	Expt.	Theor.	Expt.	Theor.
b_2^0	0.694	0.695	0.733	0.731	0.774	0.744	0.802	0.803
b_2^2	-0.083	-0.083	-0.055	-0.055	-0.081	-0.081	-0.148	-0.148
b_4^0	0.016	0.020	0.018	0.022	0.017	0.019	0.019	0.020
b_4^2	0.066	0.083	0.076	0.096	0.077	0.084	0.081	0.087
b_4^4	0.117	0.084	0.144	0.104	0.117	0.097	0.130	0.118
$\bar{b}_2$	-4.461		-4.866		-4.934		-5.476	
$\bar{b}_4$	0.022		0.025		0.022		0.022	

zero, unlike the situation with the RF_3 hosts considered here. Thus, the application of the SM to RF_3 hosts has subjected the model to a rigorous consistency test. The fact that the model succeeds in passing the test with such small distortions of the angular positions further establishes the validity of the model for the RF_3 hosts.

4.3 Application to RTH

The crystals $RCl_3.6H_2O$ (RTH), R = Nd, Sm, Eu, Tb, Dy, Ho, Er, Tm form a homologous series containing rare-earth ions whose ionic radii are both larger and smaller than that of the substituted Gd^{3+} ion. This contrasts with the previous system (RF_3) where the host radii were all larger than Gd^{3+}. Precise experimental values for the relevant SHPs have been reported by Misra and Sharp[36] and by Misra et al.[37] The ligands are six oxygen ions (O^{2-}), the positions of which are given in Table VII. The procedure described in Sec. 4.1 was applied to this series by Lewis and Misra.[32] In contrast to the RF_3 case, it was found that there are values of t_2 for each host for which $E(t_2)$ is identically zero. Thus, one immediately gets the corresponding value for B_2^2. The results are given in Table VIII. Because of the null values obtained for $E(t_2)$, no attempt was made to introduce angular distortion in this case.

In regard to the fourth-order parameters, the values for t_4 obtained by this method were extremely large in magnitude, negative ($t_4 \sim -100$), and widely different from host to host. This was taken to be unreasonable and was attributed to the distortion sensitivity of the fourth-order parameters for this particular crystal, or to the fact that O^{2-} ions are extremely sensitive to changes in ionicity which may be induced as one goes from host to host.[18] From Table VIII it is

TABLE VII. Positions for the six nearest-neighbour O^{2-} ions for RTH used in superposition model fits. The value of the radius vector, r, is also given. All units are in angstroms. For a given host, only the positions (x, y, z) for three ions are given. The coordinates for the other three may be obtained from (-x, -y, z).

Host	x	y	z	r
Nd	2.0529	1.0741	-0.6930	2.4183
	-1.5882	0.1594	1.8038	2.4086
	0.0366	-2.2355	0.9682	2.4364
Sm	2.1330	0.9481	-0.6878	2.4334
	-1.5802	0.2531	1.7901	2.4011
	-0.1216	-2.2292	0.9609	2.4305
Eu	2.1611	0.8822	-0.6857	2.4329
	-1.5722	0.3022	1.7846	2.3975
	-0.1887	-2.2261	0.9580	2.4308
Tb	2.0896	0.9936	-0.6836	2.4127
	-1.5747	0.2141	1.7792	2.3856
	-0.0584	-2.2194	0.9550	2.4169
Dy	2.0972	0.9636	-0.6815	2.4064
	-1.5680	0.2345	1.7737	2.3790
	-0.0868	-2.2136	0.9521	2.4122
Ho	2.0976	0.9414	-0.6794	2.3974
	-1.5602	0.2478	1.7683	2.3712
	-0.1052	-2.2054	0.9491	2.4033
Er	2.1135	0.9050	-0.6794	2.3974
	-1.5552	0.2741	1.7683	2.3707
	-0.1445	-2.2016	0.9491	2.4018
Tm	2.1236	0.8656	-0.6773	2.3912
	-1.5464	0.3008	1.7628	2.3642
	-0.1821	-2.1939	0.9462	2.3961

seen that the t_2 values obtained (except for one) are negative. One would anticipate a priori that they should be positive (ions farther away contributing less), but there is no absolute restriction that this need be so. Indeed, Edgar and Newman[30] have reported $t_2 < 0$ for Gd^{3+}: CaF_2 and Buzaré et al.[38] have reported $t_4 < 0$ for $RbCaF_3$. Also, Newman et al.[17] have explicitly stated that t_2 can be negative for Gd^{3+} and Eu^{2+}.

Also, from Table VIII, one notes that the way in which t_2 varies depends on whether the ionic radius, r, of the corresponding rare-earth host is greater or less than that of the substituted Gd^{3+} ion (r_{Gd} = 0.938 Å). This may be seen from Fig. 2 where plots of t_2 vs. r give separate straight lines in the two regions: $r < r_{Gd}$ and $r > r_{Gd}$. If one now considers R_N ($\equiv R_N(i)$), the distance of the nearest O^{2-} ion from Gd^{3+} for a given host, one finds that a plot of r vs. R_N for the various hosts (see Fig. 3) gives two separate straight lines of slightly different slope if the cases $r < r_{Gd}$ and $r > r_{Gd}$ are considered separately. Thus, plots of t_2 vs. R_N also give separate straight lines as shown in Fig. 4. If one considers the t_2 vs. R_N equations for these lines, as determined from a least-squares fit, one finds (defining $t_<$ ($\equiv t_<(i)$) as being values of t_2 for which $r < r_{Gd}$, and similarly for $t_>$):

$$t_< = 391.345\,(R_N - 2.395) \qquad (4.8)$$

$$t_> = 1631.126\,(R_N - 2.409) \qquad (4.9)$$

The numbers in the brackets in Eqs. (4.8) and (4.9) have an average value of 2.402 Å. This may be compared with the value of R_o for RTH which is

TABLE VIII. Superposition model results for the parameters $\bar{b}_2$ (GHz) and t_2 for RTH. The values for the host-ion radii (Å) are also given.

Host	t_2	$\bar{b}_2$(GHz)	r(Å)
Nd	0.166	-3.106	0.995
Sm	-13.050	-2.229	0.964
Eu	-17.412	-1.964	0.950
Tb	- 3.943	-2.851	0.923
Dy	- 5.704	-2.796	0.908
Ho	- 5.701	-2.870	0.894
Er	-10.247	-2.772	0.881
Tm	-12.244	-2.784	0.869

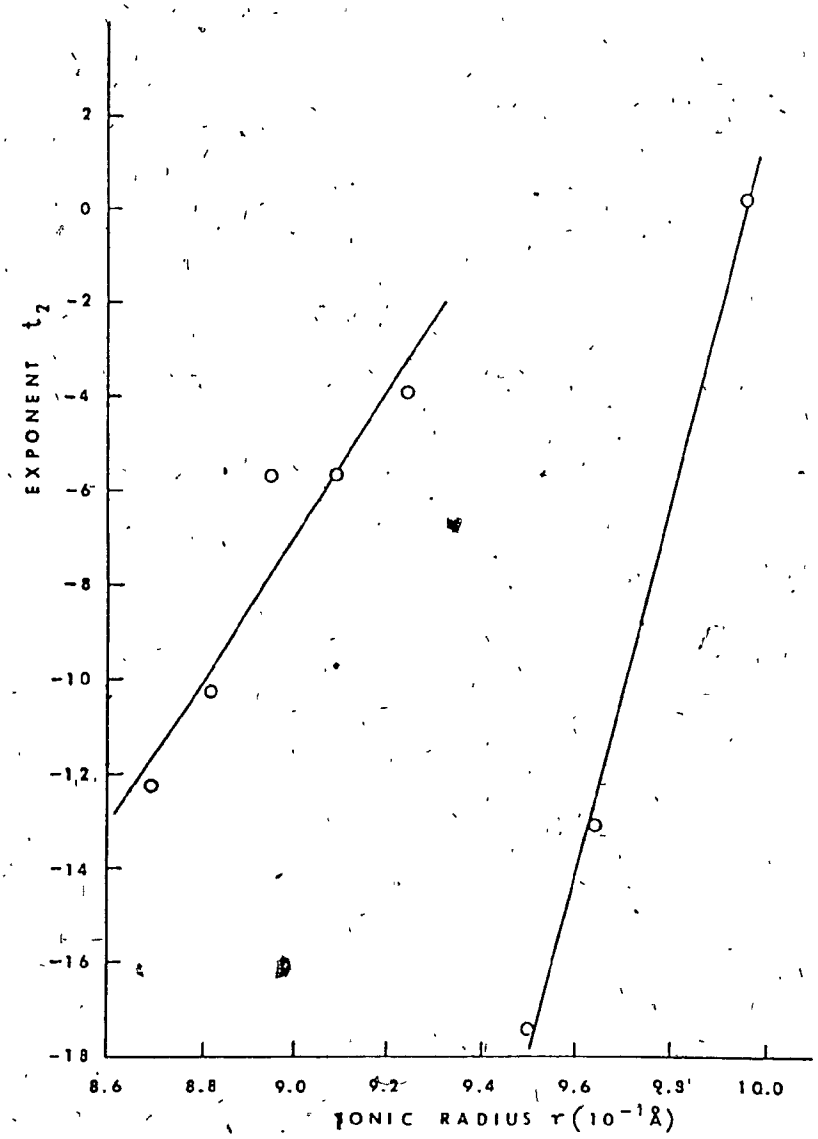

Fig. 2. Graph of the values of t_2, as determined from Eq. (4.7), vs the host-ion radius r (10^{-1} Å). The cases $r < r_{Gd}$ and $r > r_{Gd}$ are plotted separately.

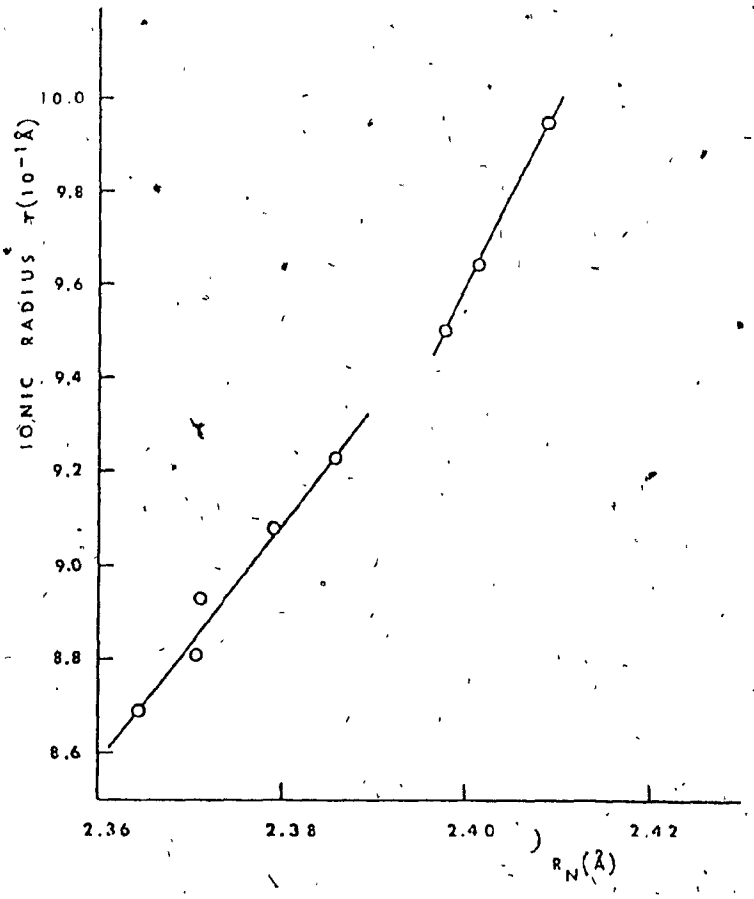

Fig. 3. Graph of the host-ion radius r (10^{-1} Å) vs R_N (Å). R_N is defined in Sec. (4.3). The cases $r < r_{Gd}$ and $r > r_{Gd}$ are plotted separately.

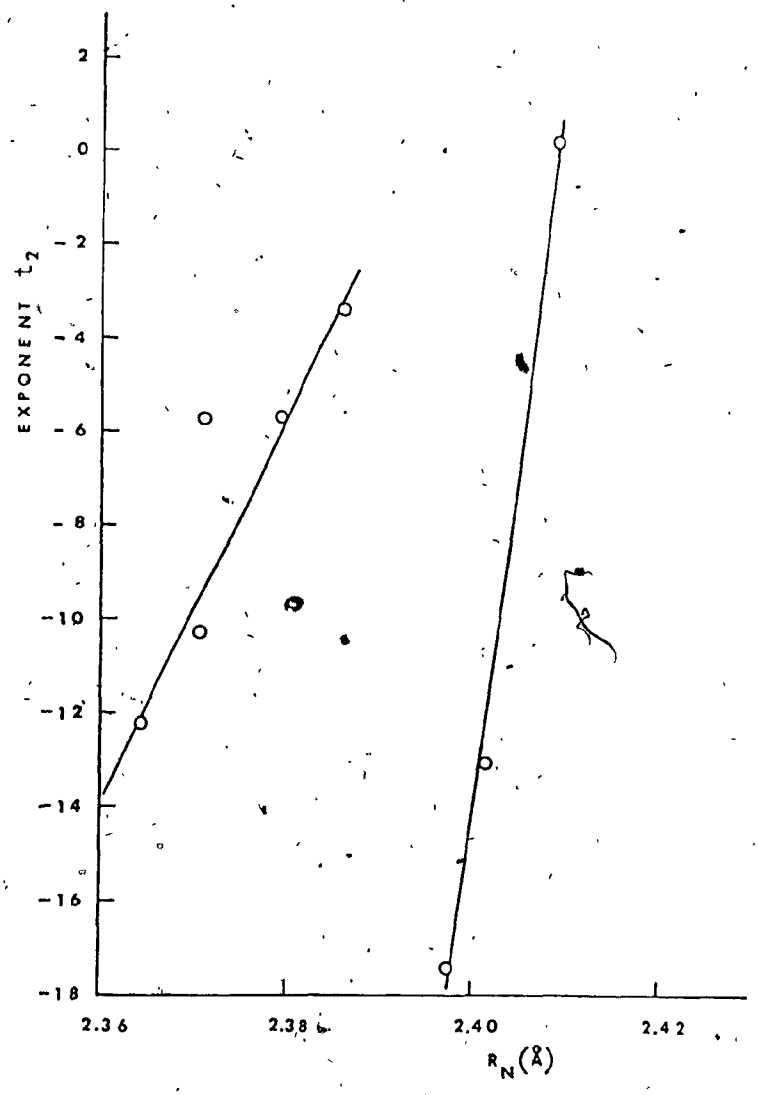

Fig. 4. Graph of the values of t_2, as determined from Eq. (4.7), vs R_N (Å). R_N is defined in Sec. (4.3). The cases $r < r_{Gd}$ and $r > r_{Gd}$ are plotted separately.

2.404 Å. One may then approximate Eqs. (4.8) and (4.9) as

$$t_{2} = k_{2} (R_N - R_o) . \quad (4.10)$$

Eq. (4.10) has the advantage that it decouples, from t_2, variations due to metal-ligand distance effects thus enabling one to concentrate on other factors which give rise to the specific value of k_2. It could also explain why, for some series, success has been obtained by taking t_2 to be roughly constant, whereas for RTH there is a wide variation from host-to-host. For example, as mentioned in Sec. 4.2 for RF_3, the values found for t_2 were in the range 9 ± 1. The average change in the value of $R_N - R_o$ (for an undistorted lattice) in going form host to host in that series is about 25 %. In the present case (RTH), the corresponding change is about 65 %.

In regard to the $\bar{B}_2$ values, it is seen from Table VIII that the value for $\bar{B}_2$ for Δr ($\equiv r_R - r_{Gd}$) < 0 is constant; i.e. $\bar{B}_2(\Delta r < 0) = 2.815 \pm 0.037$ GHz, with an average deviation from the mean of 1.3 %. For $\Delta r > 0$, it is also seen from Fig. 5 that $\bar{B}_2(\Delta r > 0)$ varies linearly with the host-ion radius. Hence, it will also vary linearly with R_N. The relation, from a least-squares fit, is given as

$$\bar{B}_2(\Delta r > 0) = -106.475 (R_N - 2.380) . \quad (4.11)$$

The number in the bracket may be compared with the average value of R_N for the various hosts, $\bar{R}_N$ = 2.385 Å. Hence, one may express Eq. (4.11) as

$$\bar{B}_{2>} = k_{i>} (R_N - \bar{R}_N) . \quad (4.12)$$

Similarly, for $\Delta r < 0$,

$$\bar{B}_{2<} = k_{i<} . \quad (4.13)$$

where i refers to 'intrinsic'. Eqs. (4.12) and (4.13) indicate that one is able to separate out the distance dependence of $\bar{B}_2$ from other effects.

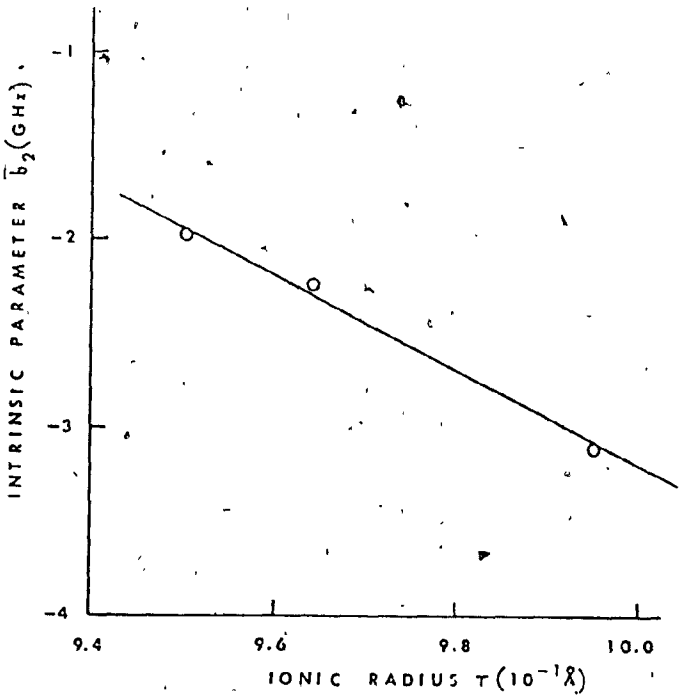

Fig. 5. Graph of the intrinsic parameter $\bar{b}_2$ (GHz), as determined via Eq. (4.7), vs the host-ion radius r (10^{-1} Å) for those hosts for which $r > r_{Gd}$.

Relations similar to Eqs. (4.10) and (4.12) are also found for RF_3. It was mentioned in Sec 4.2 that $\bar{B}_2$ (for RF_3) was linear in r (and hence in Δr). Also, for RF_3, t_2 is linear in r (except for Nd — an anomaly conceivably related to distortion effects).

4.4 Analysis

The results of the above application of the SM to two crystal systems suggest that one can reformulate the model equations in such a way as to decouple metal-ligand distance effects from other factors which influence the model parameters. This has been demonstrated by Lewis and Misra[32]. Taking into account that $\bar{B}_2(R_o)$ is host (R)- dependent, one may put it as $\bar{B}_2(R, R_o)$. Defining $\delta_i \equiv R_i - R_o$, Eq. (4.3) may be written as

$$B_2^m = \sum_i \bar{B}_2(R,R_o)\left\{1 - \frac{\delta_i}{R_i}\right\}^{t_2} K_2^m(i) \quad (4.14)$$

Clearly, $\frac{|\delta_i|}{R_i} << 1$. Hence, Eq. (4.14) may be written as

$$B_2^m = \sum_i \bar{B}_2(R,R_o)\left\{1 - t_2\frac{\delta_i}{R_i}\right\} K_2^m(i) \quad (4.15)$$

Define now

$$\delta_{\bar{N}} \equiv R_N - \bar{R}_N \quad (4.16)$$

and

$$\delta_{N_o} \equiv R_N - R_o \quad (4.17)$$

Combining Eqs. (4.15) to (4.17) with Eqs. (4.10), (4.12), and (4.13) gives

$$B_2^m = \sum_i k_2 \delta_{\bar{N}}\left\{1 - k_{22}\delta_{N_o}\left(\frac{\delta_i}{R_i}\right)\right\} K_2^m(i) \quad (4.18)$$

Substituting for δ_i and rearranging gives

$$B_2^m = \sum_i \left\{k_2\delta_{\bar{N}}(1 - k_{22}\delta_{N_o}) + k_2\delta_{\bar{N}}k_{22}\delta_{N_o}\left(\frac{R_o}{R_i}\right)\right\} K_2^m(i), \quad (4.19)$$

or

$$B_2^m = \sum_i \left\{A + B\left(\frac{R_o}{R_i}\right)\right\} K_2^m(i) \quad (4.20)$$

where

$$A = k_g \delta_{\bar{N}} (1 - k_z \delta_{N_o}) \quad (4.21)$$

$$B = (k_g \delta_{\bar{N}})(k_z \delta_{N_o}) \quad (4.22)$$

The advantage of this formulation over the conventional one is that all distance relations are given by $\delta_{\bar{N}}$ and δ_{N_o}, which can be easily calculated if one knows the crystal structure and unit cell parameters. This enables further analysis to concentrate on the origin of the k_g and k_z.

Chapter 5

THE POINT-CHARGE PLUS INDUCED-DIPOLE MODEL

This chapter describes the point-charge plus induced-dipole (PCID) model. Sec. 5.1 reviews the literature related to this sort of an approach, and Sec. 5.2 presents the details of the PCID model. The matter of atomic polarizabilities, which is of importance to the model, is discussed in the next chapter. The application of the model is described in Chapter 7.

5.1 Review

Ever since the pioneering work of Bethe,[1] mentioned at the outset, there has existed the question of whether or not, in fact, the parameters A_n^m arise solely from the electrostatic point-charge field of the various ions in the crystal. Even with the advent of electronic computers, a 'brute-force' method to compute the required lattice sums is prohibitively expensive. Thus, one is led to employ various summation methods which are such that the series involved converge rapidly. The most widely used and efficent of these methods is that due to Ewald.[39] This method is discussed in detail in Appendix C which also includes extensions to the Ewald method which are required in the present work.

The conclusion of the efforts of various investigators over the last fifteen years is that the point-charge sums per se are simply insufficient to explain the parameters.[24,37] The logical extension of this is to consider also the induced dipole field. There are primarily three groups of investigators which have considered this problem. (All of these use Ewald's method.) Each will here be discussed briefly.

First, Faucher et al.[40] have presented a polarizable dipole model

which was applied to Nd_2O_3 and NdO_2S. They found that, while consideration of dipole contributions improved the results (over those for monopoles only), the calculated value for $A_2^0\langle r^2\rangle$ was off by about 100 %, and that for $A_4^0\langle r^4\rangle$ was off by about 50 %.

As will be discussed in detail later, one needs, for any dipole calculation, the values for the atomic polarizabilities for the various ions in the crystal. Indeed, this is the crux of the dipole problem, as these values are neither known, nor directly measurable, nor calculable. Polarizability values are available for free atoms (or ions), but these change when that atom is placed in a molecule or in a crystal. This is known from the fact that molecular polarizabilities do not equal (i.e. are less than) the sum of the constituent free atom polarizabilities. In other words, polarizabilities are not additive. Also, polarizabilities (in situ) should be represented by tensor quantities, not scalars. Further, from Neumann's theorem,[41] these tensors should conform to the symmetry of the crystal involved. However, Faucher et al. have employed scalars and assumed additivity. They use the Lorentz formula:[42]

$$\alpha = \frac{3V}{4\pi}\,\frac{n^2-1}{n^2+1}\,, \qquad (5.1)$$

where α is the polarizability of the unit cell, V is the unit cell volume, and n is the index of refraction of the material (n = 1.91 for Nd_2O_3). Then, from this, having calculated α (= 8.5 $\mathring{A}^3$) for the unit cell, they assumed $\alpha(Nd^{3+}) < \alpha(O^{2-})$ and set $\alpha(O^{2-}) = 2\ \mathring{A}^3$, $\alpha(Nd^{3+}) = 1\ \mathring{A}^3$. (i.e. $2\times1 + 3\times2 \simeq 8$). This method has four major shortcomings: (i) the Lorentz formula holds only for crystals with cubic symmetry,[43] (ii) the indices of refraction employed are those as measured at optical

frequencies, whereas in EPR one is usually employing microwave frequencies. The polarizability values are subject to dispersion relations in that they depend on the applied frequency. (iii) Polarizabilities are not additive. (iv) No attempt has been made to account for the tensor nature of polarizability.

The second group working on a polarizable dipole model is that of Malkin and co-workers.[44-47] They have attempted to employ tensor polarizabilities in working with garnets. However, their tensors do not conform to the symmetry of the crystal and it is unclear from their publications just how their tensor components were determined. Also, their results do not agree well with the experimental values.

The third group is that of Bijvank et al.[19-21] They employ scalar polarizabilities and allow for considerable distortion in the positions of a large number of ions. Their results (Gd^{3+} - M^+: CaF_2, M^+ = Li, Na, ... , Cs) for B_2^0 are off by 50 to 1000 %, and those for B_2^2 are of the wrong sign and are off in magnitude by 200 to 800 %. They claim, nevertheless to have presented, for the first time, a "clear-cut theoretical explanation" of the Gd^{3+} crystal-field splitting.

As will be seen, the present work produces theoretical results (from the PCID model for RF_3 and RTH) which are within experimental error. Conclusions and claims which may be drawn from this will be discussed in due course. The present model will now be presented.

5.2 Details of the Present Model

In order to extend the expression for the A_n^m (Eq. (3.18)) to include dipoles, one may write[40]

$$A_n^m = -|e| \sum_i q_i \left(\frac{Z_n^m(\hat{r}_i)}{r_i^{n+1}} \right) - |e| \sum_i \vec{p}_i \cdot \nabla \left(\frac{Z_n^m(\hat{r}_i)}{r_i^{n+1}} \right) \qquad (5.2)$$

This may be evaluated, in principle, only if one knows the value for $\vec{p}_i$ ($\equiv p_\beta(i)$, $\beta = x, y, z$), the induced dipole moment at the site of the ion i. (r_i ($\equiv |\vec{r}_i|$) is the magnitude of the radius vector of ion i with respect to the substituted Gd^{3+} ion taken as origin.) To determine $\vec{p}_i$, one requires the value of the electric field, $\vec{E}(i)$, at that ion site. This field, denoted as $\vec{E}_{tot}(i)$ or as $\{E_\alpha(i)\}_{tot}$ ($\alpha = x, y, z$), will be the sum of the monopole field, $E_\alpha(i)$, and the dipole field, $E'_\alpha(i)$, at that site.

$$\{E_\alpha(i)\}_{tot} \equiv E_\alpha(i) + E'_\alpha(i) \qquad (5.3)$$

The monopole field at site i due to ions at other sites k (k runs over all the ions in the crystal) is given by

$$E_\alpha(i) = \nabla_\alpha \left\{ \sum_{k \neq i} q_k \frac{1}{|\vec{r}_k - \vec{r}_i|} \right\} \qquad (5.4)$$

where q_k is the charge at site k. This sum may be evaluated, for each i, using Ewald's method (see Appendix C). In practice, the required number of different values of i is restricted by symmetry considerations; this will be discussed later.

The dipole potential, Φ', at the site of ion i (due to ions at other sites, k) is given by

$$\Phi' = -\sum_{k \neq i} \vec{p}_k \cdot \left(\nabla \frac{1}{|\vec{r}_k - \vec{r}_i|} \right) \qquad (5.5)$$

Hence, the corresponding electric dipole field is

$$\vec{E}' = -\nabla \Phi'$$

$$= \sum_{k \neq i} \frac{3\{\vec{p}_k \cdot (\vec{r}_k - \vec{r}_i)\}(\vec{r}_k - \vec{r}_i) - \vec{p}_k |\vec{r}_k - \vec{r}_i|^2}{|\vec{r}_k - \vec{r}_i|^5} \qquad (5.6)$$

Defining

$$Q_{\alpha\beta}(ki) \equiv \frac{3R_\alpha R_\beta - R^2\delta_{\alpha\beta}}{R^5} = \frac{\partial^2}{\partial x_\alpha \partial x_\beta}\left(\frac{1}{R}\right), \quad (5,7)$$

where $R = |\vec{R}| = |\vec{r}_k - \vec{r}_i|$; $(\alpha, \beta = x, y, z)$, one may write Eq. (5.6) in component form as

$$E'_\alpha(i) = \sum_{k\neq i}\sum_\beta Q_{\alpha\beta}(ki)\, p_\beta(k) \quad (5.8)$$

Now, the induced dipole moment (component) at the site of a given ion, k, is proportional to the total electric field at that site, the proportionality constant being the polarizability, α. However, the value of α is directionally dependent for an ion in a crystal. Hence, one must speak of the tensor $\alpha_{\beta\gamma}(k)$ $(\beta, \gamma = x, y, z)$ at ion site k. Thus, the dipole moment, $p_\beta(k)$, induced at the site of ion k by the total electric field, $\{E_\gamma(k)\}_{tot}$, is given by

$$p_\beta(k) = \sum_\gamma \alpha_{\beta\gamma}(k)\{E_\gamma(k)\}_{TOT} \quad (5.9)$$

or, in the present notation, by

$$p_\beta(k) = \sum_\gamma \alpha_{\beta\gamma}(k)\{E_\gamma(k) + E'_\gamma(k)\}. \quad (5.10)$$

This may be inverted to give

$$\sum_\beta \alpha^{-1}_{\beta\gamma}(k)\, p_\beta(k) = E_\gamma(k) + E'_\gamma(k) \quad (5.11)$$

where α^{-1} denotes the (matrix) inverse of α. The left-hand side of Eq. (5.11) may be expressed as

$$\sum_\beta \alpha^{-1}_{\beta\gamma}(k)\, p_\beta(k) = \sum_{k'}\sum_\beta \alpha^{-1}_{\beta\gamma}(k)\, p_\beta(k')\delta_{kk'} \quad (5.12)$$

Also, Eq. (5.8) may be written as

$$E'_\gamma(k) = \sum_{k'} \sum_{\beta} Q_{\gamma\beta}(kk') p_\beta(k') \qquad (5.13)$$

Combining Eqs. (5.12) and (5.13) with Eq. (5.11) gives

$$\sum_{k'} \sum_{\beta} \left\{ \alpha^{-1}_{\beta\gamma}(k) \delta_{kk'} - Q_{\gamma\beta}(kk') \right\} p_\beta(k') = E_\gamma(k) \qquad (5.14)$$

This is an equation for each value of k and for each value of γ (γ = x, y, z), where k labels successively each of a total number of ℓ ions in the unit cell. Thus, Eq. (5.14) constitutes a set of linear equations, 3ℓ in number, in the unknowns $p_\beta(k')$, where k' also ranges over the ions in the unit cell. This system can thence be solved for the $p_\beta(k')$, given the values of $\alpha_{\beta\gamma}(k)$ and $E_\gamma(k)$ for each k, and $Q_{\gamma\beta}(kk')$ for each set k, k'. The determination of the values to be used for the $\alpha_{\beta\gamma}(k)$ will be discussed in Chapter 6. As previously mentioned, the values for $E_\gamma(k)$ (see Eq. (5.4)) can be evaluated by Ewald's method. The same is true for the $Q_{\gamma\beta}(kk')$ values.

In practice, the number of unknowns in Eq. (5.14) may be greatly reduced from 3ℓ (in number) by symmetry considerations. In general, the positions of the ions in the unit cell correspond to several species or sublattices, labelled j, say; each of which will have a number of equivalent positions, say m. (For example, see Appendix B.) Each sublattice corresponds to a subgroup of the overall space group of the crystal being considered. The m equivalent positions of a given sublattice can be generated by the group operations associated with the corresponding subgroup. In fact, the number m is equal to the number of elements (operations) of the subgroup, and ℓ is equal to the number of subgroups of the space group that occur for that crystal. Now

suppose that, in a given sublattice, a given atomic position vector component is denoted by $R(j, m, \alpha)$, where j labels the sublattice, m labels the equivalent position within that sublattice, and $\alpha = x, y, z$. Then the above discussion implies that the $R(j, m, \alpha)$ for all m (for a given j, α) can be generated from any one of them, e.g. that corresponding to m = 1, by operating on $R(j, m, \alpha)$ with the corresponding group operators. These operations will consist either of translations, denoted by $T(j, m, \alpha)$, which represents a column vector, or by reflections or rotations, denoted by the matrix $S(j, m, \alpha', \alpha)$. That is, for each (j, m) combination, one has

$$R(j,m,\alpha) = T(j,m,\alpha) + \sum_{\alpha'} S(j,m,\alpha,\alpha') R(j,1,\alpha') \quad (5.15)$$

Now, as follows from Neumann's theorem, the dipole moments must correspond to the same symmetry elements as the atomic position parameters. Neumann's theorem states that the symmetry operations of any property of a crystal must include the symmetry operations of the point group of the crystal. In Eq. (5.15), the symmetry operations of the point group correspond to those operations which do not involve translations. Thus, in generating the values of the dipole moments for lattice sites within a given sublattice, given the value of the dipole moment for one particular lattice site, one may ignore the $T(j, m, \alpha)$ operator in Eq. (5.15). The physical reason for this is that in measuring a macroscopic property one would not expect to detect the effect of a translation that is only a fraction of a unit cell.[48] That is, no distinction could be made between $\{S|T\}$ and $\{S|0\}'$ (where $\{S|T\}R = SR + T$). Thus, in Eq. (5.14), one may take as unknowns only one $p_\beta(k')$ for each sublattice. (This unknown will be called the reference unknown for

a particular sublattice.) The values for the other dipole moments in that sublattice can be generated from this via relations of the form of Eq. (5.15). Thus the number of unknowns in Eq. (5.14) is reduced from 3ℓ to $3j$ (recalling that ℓ is the number of atoms in the unit cell, whereas j is the number of different sublattices in the unit cell). This may be reduced even further, because, if within a given sublattice the group operation consists only of a translation, then the corresponding dipole moment will be zero. Thus, knowing in advance that this will be the case, one can exclude these unknowns to begin with.

For a given sublattice, Eq. (5.15) becomes, for the dipole moments,

$$p_\alpha(k') = \sum_\beta S_{\alpha\beta}(kk')\, p_\beta(k) \qquad (5.16)$$

where $p_\beta(k)$ is the reference unknown for that sublattice, and $S_{\alpha\beta}(kk')$ is the matrix relating the components at site k to those at site k'. These matrices may be determined by inspection from the listings of the equivalent positions for the 230 space groups as given in the International Tables.[49]

In the unit cell of ℓ atoms, one can assign a number, called here a k-label, to each atom. That is, the atoms can be labelled by $k = 1, 2, \ldots, \ell$. These atoms will be grouped into sublattices which can also be labelled using the index $j = 1, 2, \ldots$ where the maximum value of j equals the number of sublattices in the unit cell. One can then define f_j as being the k-label of the first atom in the jth sublattice. For example, in the case of RF_3 (see Appendix B) there are 24 ions in the unit cell. Ions No. 1 - 12 correspond to one fluorine (F(I)) sublattice, Nos. 13 - 16 to fluorine (F(II)), Nos. 17 - 18 to F(III), and Nos. 19 - 24 to the rare-earth metal sites. Thus, k takes on the

values 1 to 24 (number of ions in the unit cell), j takes the values 1 to 4 (number of different sublattices), and f_j takes the values 1, 13, 17, 19 corresponding to the k-label of the first atom in each of the sublattices. Now define

$$\mathbb{P}_{\gamma\beta}(kk') \equiv \alpha^{-1}_{\gamma\beta}(k)\,\delta_{kk'} - Q_{\gamma\beta}(kk') \tag{5.17}$$

Then, using Eq. (5.16) in Eq. (5.14), the sum in Eq. (5.14) will break up into separate sums over each of the sublattices, and each of these sums will contain only one unknown, namely $p_\beta(f_j)$, the dipole moment of the first atom in a given sublattice.

$$\text{i.e.} \quad \sum_{i=1}^{j} \sum_{k'=f_i}^{f_{i-1}} \sum_{\beta} \sum_{\delta} \mathbb{P}_{\gamma\beta}(kk')\, S_{\beta\delta}(f_i k')\, p_\delta(f_i) = E_\gamma(k) \tag{5.18}$$

where $k = f_1, f_2, \ldots$. Thus, one has 3j equations in 3j unknowns. (For some cases, for a given f_i and γ, it may be known that $p_\gamma(f_i) = 0$, from symmetry. Thus the actual number of unknowns may be less than 3j.)

As has been mentioned, all the factors in Eq. (5.18) are either known, or can be explicitly calculated using Ewald's method, with the exception of the elements, $\alpha_{\beta\gamma}(k)$, of the polarizability tensor at a given site.

Chapter 6

POLARIZABILITY

This chapter provides the theoretical background for a number of criteria that may be used in the determination of atomic polarizabilities in crystals. Sec. 6.1 develops a model which demonstrates the reasons why in-crystal polarizabilities differ from those of a free ion. The next section discusses the symmetry constraints placed on the polarizability tensor, while Sec. 6.3 treats some general guidelines. The last section deals with how polarizabilities differ in a homologous series of hosts.

6.1 The Shell Model

The purpose of this section is not to derive an explicit expression for the polarizability tensor of a given ion. This is not yet a feasible proposition[50] as there are simply too many complexities involved. Rather, the purpose is to demonstrate how the tensorial character of polarizability in a crystal arises, and how this is related to the free-ion polarizability. The treatment is based on the shell model of Dick and Overhauser.[51] They point out that the equivalence of the shell model to a more formal quantum mechanical description has been demonstrated. Thus, given the purposes indicated above, it is sufficient here to consider only a classical treatment of the problem.

As has already been noted (Eq. (5.9)), the atomic dipole moment, $\vec{p}$, induced by a field, $\vec{E}$, is given by

$$\vec{p} = q\vec{r} = \alpha\vec{E} \qquad (6.1)$$

where α is the polarizability, and q is the charge of the electron

cloud (shell) of mass m which is being displaced relative to the atomic core by an amount $-\vec{r}$. There is a restoring force between the core and the shell which is represented by an effective force constant, k (shell-core spring constant). There will also be a velocity-dependent damping term, β. (In a more general treatment, β would be seen to be of quantum-mechanical origin.) Thus, if one has an external field acting of the form $E_o e^{i\omega t}$ (ω is typically in the microwave region for EPR), the equation of motion (in one dimension) of the shell will be

$$m\frac{d^2x}{dt^2} + \beta\frac{dx}{dt} + kx = qE_o e^{-i\omega t} \qquad (6.2)$$

This is just the equation for a forced oscillator (the shell) with damping. Thus, the displacement, x, will be of the order of

$$x \simeq \frac{qE_o}{m}\left\{(\omega_o^2-\omega^2)^2 + (\beta\omega)^2\right\}^{-1/2} \qquad (6.3)$$

Comparing this with Eq. (6.1) gives

$$\alpha \simeq \frac{q^2}{m}\left\{(\omega_o^2-\omega^2)^2 + (\beta\omega)^2\right\}^{-1/2} \qquad (6.4)$$

In the static case ($\omega = 0$, $\alpha = \alpha_o$), one has (defining $\omega_o^2 = k/m$)

$$\alpha_o = q^2/k. \qquad (6.5)$$

When polarizability values are quoted by various authors, it is this static value that is being cited. As is seen from Eq. (6.3), the actual value of interest in EPR dipole moments will be frequency-dependent.

Now consider an ion in a crystal as being made up of a core of charge Q_K' and a shell of charge Q_K'', with the ionic charge being Q_K ($= Q_K' + Q_K''$). Under the action of an electric field, the shell is

assumed to move with respect to the core while maintaining its shape.[51] As before, one has a shell-core force constant, now denoted as k_K, but, in the crystal, there will also be a short-range force coupling this shell to a neighbouring shell associated with ion K', say. The shell-shell force constant corresponding to this force will be tensorial in form, depending on the direction of K' relative to the electric field. Thus, this tensor force constant will be denoted $S_{\alpha\beta}(KK')$ (α, β = x, y, z). Further, let $\vec{D}(K)$ be the displacement of the Kth shell relative to its core. Under the action of a field, the force $Q_K'' \vec{E}(K)$ acting on the Kth shell will be balanced by the shell-core restoring force $k_K \vec{D}(K)$ and by the shell-shell forces due to neighbouring shells K'. Each of the latter will be of the form of the product of S(KK') with $\vec{D}(K) - \vec{D}(K')$, the relative displacement of core K' with respect to core K. Thus one has

$$Q_K'' E_\beta(K) = k_K D_\beta(K) + \sum_{K' \neq K} \sum_\gamma S_{\beta\gamma}(KK') \{ D_\gamma(K) - D_\gamma(K') \} \quad (6.6)$$

or

$$Q_K'' E_\beta(K) = \sum_{K' \neq K} \sum_\gamma \{ k_K \delta_{KK'} \delta_{\beta\gamma} + S_{\beta\gamma}(KK') \} D_\gamma(K) - \sum_{K' \neq K} \sum_\gamma S_{\beta\gamma}(KK') D_\gamma(K') . \quad (6.7)$$

In the last term in Eq. (6.7), for ions K' situated around ion K, the factors $D_\gamma(K')$ will tend to cancel in the sum (the force constants, S, are intrinsically positive). It is thus assumed that this sum is negligible in comparison to the first sum in Eq. (6.7). Now, in the current notation, the dipole moment of ion K is given by

$$p_\beta(K) = Q_K'' D_\beta(K) . \quad (6.8)$$

But, $D_\beta(K)$ may be obtained from the matrix inverse of Eq. (6.7) (keeping

only the first term in that equation).

$$D_\beta(k) = Q''_k \sum_{k' \neq k} \left\{ k_k \, \delta_{kk'} \, \delta_{\beta\gamma} + S_{\beta\gamma}(kk') \right\}^{-1} E_\gamma(k) \qquad (6.9)$$

The polarizability elements for ion K may be written as

$$\alpha_{\beta\gamma}(k) = p_\beta(k) \; E_\gamma^{-1}(k) \qquad (6.10)$$

Substituting Eq. (6.9) into Eq. (6.8), and then Eq. (6.8) into Eq. (6.10) gives

$$\begin{aligned} \alpha_{\beta\gamma}(k) &= \left\{ Q''_k \, D_\beta(k) \right\} E_\gamma^{-1}(k) \\ &= \left\{ Q''_k \left[Q''_k \sum_{k'' \neq k} \left(k_k \, \delta_{kk'} \, \delta_{\beta\gamma} \right.\right.\right. \\ &\quad \left.\left.\left. + S_{\beta\gamma}(kk') \right)^{-1} E_\gamma(k) \right] \right\} E_\gamma^{-1}(k) \\ &= Q''^2_k \left(k_k \, \delta_{\beta\gamma} + \sum_{k' \neq k} S_{\beta\gamma}(kk') \right)^{-1} \qquad (6.11) \end{aligned}$$

Noting Eq. (6.5), Eq. (6.11) may be expressed as

$$\alpha_{\beta\gamma}(k) = \alpha_o(k) \left(\delta_{\beta\gamma} + \frac{1}{k_k} \sum_{k' \neq k} S_{\beta\gamma}(kk') \right)^{-1} \qquad (6.12)$$

(Here, the exponent denotes the matrix inverse. In this context, α_o is written in the form of a diagonal matrix with each diagonal element equal to α_o.) From this it can be seen that the free-ion polarizability is modified by the neighbouring ions in the crystal such that the resulting polarizability is in the form of a tensor.

Eq. (6.12), as is, does not include exchange effects arising from the Pauli exclusion principle. For the ions to repel, they must overlap, and, in the region of overlap, the exclusion principle will act to

reduce the electron charge density and to redistribute the charges on the ions. The region of reduced charge may be considered, electrostatically, to be a region of superposed positive charge which may be modelled by placing a positive 'exchange charge', q_{ex}, on the line joining the centers of adjacent ion shells. Total electric neutrality is preserved by a slight enhancement of the shell charges. This is equivalent to replacing Q''_K, in Eqs. (6.11) and (6.12), by $Q''_K + Q_D$, where Q_D is referred to as the exchange charge parameter.

6.2 Symmetry Considerations

Having shown that the polarizability, α, must be in the form of a tensor, it is now considered how symmetry constraints reduce the number of independent elements $\alpha_{\beta\gamma}$.

First, time-reversal invariance requires that the tensor be symmetric.[52] i.e. $\alpha_{\beta\gamma} = \alpha_{\gamma\beta}$. This may also be argued to be the case on the grounds that the electric field is conservative.[53]

Second, it has been noted (Sec. 5.2) that the position coordinates r_α of an ion in a given sublattice are related to the other equivalent positions r_β in that sublattice by

$$r_\beta = \sum_\alpha S_{\beta\alpha} r_\alpha \qquad (6.13)$$

where $S_{\alpha\beta}$ are the elements of one of the point group operators for that sublattice. Similarly, it has been seen that any vector describing a physical property of a crystal must also transform in the same way as do the r_α. Let p and q be two such vectors. Then

$$p_\alpha' = \sum_\beta S_{\alpha\beta} p_\beta \qquad (6.14)$$

The corresponding inverse transformation for q is (noting that S is

unitary)

$$q_\alpha = \sum_\beta S_{\beta\alpha} q'_\beta \tag{6.15}$$

Now suppose that p and q are related by a (second rank) tensor, T. Then

$$p_\alpha = \sum_\beta T_{\alpha\beta} q_\beta \tag{6.16}$$

The transformed equation is then

$$p'_\alpha = \sum_\beta T'_{\alpha\beta} q'_\beta \tag{6.17}$$

But, from Eqs. (6.14) - (6.16),

$$p'_\alpha = \sum_\beta S_{\alpha\beta} p_\beta$$

$$= \sum_\beta S_{\alpha\beta} \left(\sum_\gamma T_{\beta\gamma} q_\gamma \right)$$

$$= \sum_\beta S_{\alpha\beta} \left(\sum_\gamma T_{\beta\gamma} \left(\sum_\delta S_{\delta\gamma} q'_\delta \right) \right) \tag{6.18}$$

Comparison of Eqs. (6.17) and (6.18) gives (on relabelling the dummy subscripts)

$$T'_{\alpha\beta} = \sum_{\gamma\delta} S_{\alpha\gamma} T_{\gamma\delta} (S_{\delta\beta})^\dagger = \sum_{\gamma\delta} S_{\alpha\gamma} S_{\beta\delta} T_{\gamma\delta} \tag{6.19}$$

Now recall that the operators, S, are operators of the point group of the cell and that Neumann's theorem requires that the transformed T be indistinguishable from the original. Thus, the prime in Eq. (6.19) may

be omitted:

$$T_{\alpha\beta} = \sum_{\gamma\delta} S_{\alpha\gamma} S_{\beta\delta} T_{\gamma\delta} \quad . \tag{6.20}$$

That this places severe constraints on T may be seen by considering an example — the monoclinic crystal system. This is characterized by invariance under a 180° rotation about the y axis. Thus one has

$$S_{\alpha\beta} = \begin{pmatrix} -1 & 0 & 0 \\ 0 & 1 & 0 \\ 0 & 0 & -1 \end{pmatrix} . \tag{6.21}$$

Applying Eq. (6.20), and using the value for $S_{\alpha\beta}$ as given by Eq. (6.21) gives $T_{11} = a_{11}a_{11}T_{11} + a_{11}a_{12}T_{12} + \ldots = (-1)(-1)T_{11} + 0$ or $T_{11} = T_{11}$. On the other hand, one gets $T_{12} = -T_{12}$ which requires $T_{12} = 0$. Proceeding in a similar fashion, it is seen that tensors describing the physical properties of a monoclinic crystal must be of the form

$$T_{\alpha\beta} = \begin{pmatrix} T_{11} & 0 & T_{13} \\ 0 & T_{22} & 0 \\ T_{13} & 0 & T_{33} \end{pmatrix} . \tag{6.22}$$

Thus the number of independent elements is, in this case, reduced to four.

6.3 General Considerations

Having seen that the polarizability tensor for a given ion must conform to the symmetry of the crystal, and that this reduces the number of independent elements, there still remains the question as to the numerical value to be assigned to these elements. It is not possible to answer this question via an ab initio approach.[50] Among the complicating factors is the fact that the shell-shell interaction, mentioned in Sec. 6.1, redistributes the charge on the ions. This causes a change in the polarization of the ions which in turn alters the short-range shell-shell interaction. Hence, one has a non-linear feedback effect. This is further complicated by the fact that it is not known how much of the ion's charge (electron cloud) is participating in the process. That is, the

values for Q''_K in Eq. (6.12) are not known. Also, the positions of the ions are not known exactly because of distortions produced by the substituted paramagnetic ion which will be either under- or over-sized compared to the host paramagnetic ion. These distortions will modify shell-shell distances and hence the strength of the shell-shell coupling, which in turn will affect the polarizability values. Thus one may expect that, even in an isostructural homologous series, polarizabilities will vary due to variations in host-ion radii. This is discussed separately in the next section.

As has been mentioned in Sec. 5.1, it is well known that polarizabilities are not additive.[50,51,54] That is, molecular polarizabilities have been found to be less that the sum of the free-atom polarizabilities of the constituent atoms: This result is also predicted by most models dealing with the polarizabilities of ions in crystals. Because of this, it is usually taken to be the case that the polarizability of an ion in a crystal is less than its free-ion value. This may be seen from Eq. (6.12) (recall that k and S in that equation are positive quantities). However, it is conceivable that, in a crystal, a given ion may have its polarizability increase (over its free-ion value), while that of another species decreases, so that the overall polarizability is still less than the sum of the free-ion values. This could occur, with reference to Eq. (6.11), if there were, for one ion type, an increase in its Q''_K value — i.e. an increase in the effective charge which participates in the polarization process.

Another factor that can be taken as a guide in determining the components of $\alpha_{\beta\gamma}$ is the fact that the free-ion polarizability (units, Å^3) is of the order of magnitude of the cube of the atomic radius.[55] With

reference to Eq. (6.12), this, in the case of an ion in a crystal, may be taken as applying to the approximate magnitude of the diagonal elements of the tensor.

A further factor that can be used as a rough indicator is the Lorentz relation (Eq. (5.1)). From this it can be seen that α is related to optical indices of refraction. Thus if one considers the measured indices of refraction of a crystal along different symmetry axes (especially in the case of birefringent crystals), the ratios of these indices can give a rough estimate of the relative size of the diagonal tensor components.

6.4 Polarizability Versus Host-Ion Radius

It was mentioned in the last section that one should expect that polarizabilities will vary with host-ion radius. That is, the polarizability of a given ion (say F^-) will be different in different crystals (in an isostructural series) depending on how great a difference there is between the ionic radius of the host metal ion and the substituted metal ion.

A case relating to this has been reported in the study of the electric field effect[56] where a large effect was observed when the substituted paramagnetic ion (Gd^{3+}) was small in relation to the cation it displaced. In Ref. 56 it was taken as being reasonable to associate this as resulting from an increase in polarizability with decreasing difference in the host rare-earth ion radius (r_R) and the Gd^{3+} ion radius (r_{Gd}). This may be interpreted in light of the above discussion on shell-shell interactions. (See Eq. (6.12).) As Δr ($\equiv r_R - r_{Gd}$) increases, there will be a greater tendency for the ions to collapse towards the under-

sized substituted Gd^{3+} ion. This will lead to smaller inter-shell distances and thus to increased shell-shell interactions. This will give larger S(KK') values in Eq. (6.12) which will give smaller $\alpha(K)$ values. Thus, one may conclude that a plot of polarizability versus Δr for a given ion should have a negative slope for $r_R > r_{Gd}$.

Support for this conclusion may be drawn from the following discussions, which relate to the notion of exchange charge. The exchange charge, q_{ex}, between two atoms may be expressed in terms of overlap integrals. If a given atom, A, has occupied states u_i ($i = 1, 2, \ldots, n_A$) and atom B has occupied states u_j ($j = 1,$ then the total exchange charge is[51]

$$q_{ex} = 2|e| \sum_{i,j} S_{ij}^2 \tag{6.23}$$

where S_{ij} is the overlap integral

$$S_{ij} = \int u_i(r)\, u_j(r)\, d\tau \tag{6.24}$$

The values of S_{ij} are critically dependent on the ion separation and hence are very sensitive to distortion effects. The integrals S_{ij} have been evaluated by Löwdin[57] for LiCl and NaCl for a number of internuclear separations, but it is only recently that the specific effects of distortion have been examined. This has been done by Satoh et al.[54] They show that the electric dipole moment due to the exchange charge may be written as a function of ϵ, where ϵ is the fractional change in the interionic separation produced by distortion. That is, if 'a_o' is the undistorted separation, and 'a' is the distorted separation, one has

$$a = a_o(1 + \epsilon) \tag{6.25}$$

The relation is

$$\mu = \xi + \eta\epsilon + \zeta\epsilon^2 \tag{6.26}$$

where μ is the dipole moment and ξ, η, and ζ are combinations of overlap integrals. In their analysis of six alkali halides they found that, generally, one had: $\xi \simeq -0.03$, $\eta \simeq +0.1$, $\zeta \simeq -0.5$. Presumably, for any pair of closed-shell metal-non-metal ions, the signs of these parameters would remain the same. Also, if one roughly takes

$$\mu = \alpha E \tag{6.27}$$

where α is the (scalar) polarizability, then Eq. (6.26) could be written as

$$\alpha = A + B\epsilon + C\epsilon^2 \tag{6.28}$$

where A, B, C have the same sign as ξ, η, ζ respectively. When one substitutes a paramagnetic ion (say Gd) with radius r_{Gd} which is such that $r_{Gd} < r_R$ where r_R is the radius of the host paramagnetic ion (i.e. $\Delta r \equiv r_R - r_{Gd} > 0$), the ions will tend to collapse towards the resulting partial vacancy. Thus, ϵ will be negative; $\epsilon \propto -\Delta r$ or

$$\frac{\Delta a}{a_0} \equiv \epsilon = -k\frac{\Delta r}{r_R} \tag{6.29}$$

where k is a positive constant of proportionality. Differentiating Eq. (6.28) with respect to ϵ, gives

$$\frac{\partial \alpha}{\partial \epsilon} = B + 2C\epsilon \tag{6.30}$$

Using Eq. (6.29) gives

$$\frac{\partial \alpha}{\partial\left(\frac{k\Delta r}{r_R}\right)} = B + 2C\left(-k\frac{\Delta r}{r_R}\right)$$

or

$$\frac{\partial \alpha}{\partial(\Delta r)} = -\left(\frac{k}{r_R}\right)B + 2\left(\frac{k}{r_R}\right)^2 C\,\Delta r$$

or

$$\frac{\partial \alpha}{\partial(\Delta r)} = -B' + C'(\Delta r) \tag{6.31}$$

where $B' > 0$ and $C' < 0$ (from the signs of η and ζ). Thus, for $\Delta r > 0$, one has definitely $\frac{\partial \alpha}{\partial(\Delta r)} < 0$. For $\Delta r < 0$, the sign of $\frac{\partial \alpha}{\partial(\Delta r)}$ will depend on the magnitude of C' relative to B' which may vary from crystal to

crystal. It is thus the case that a plot of α vs. Δr for $r > 0$ should give a negative slope, as was concluded at the beginning of this section based on the electric field effect results.

Chapter 7

APPLICATION OF THE PCID MODEL

This chapter describes the application of the theory of the previous two chapters to the isostructural series RTH and RF_3. These are the same systems which were discussed in regard to the superposition model in Chapter 4. The first section gives an outline of the steps involved in the calculation. Sec. 7.2 describes and analyses the results for RTH, while the last section does the same for RF_3.

7.1 Outline of the Procedure for RTH

The point-charge plus induced-dipole model (PCID), as described in Chapters 5 and 6, was applied by Lewis and Misra[58] to Gd^{3+}: $RCl_3.6H_2O$ (RTH), R = Nd, Sm, Eu, Tb, Dy, Ho, Er, Tm; the details regarding the unit cell structure of RTH and the summation method are described in Appendices B and C respectively.

In short, the procedure is: (i) calculate the values of $E_\alpha(k)$ (Eq. (5.4)) for those values of α and k in the unit cell for which one knows, a priori, from symmetry, that the result (for $E_\alpha(k)$) is non-zero, (ii) calculate the values of $Q_{\alpha\beta}(ki)$ (Eq. (5.7)), (iii) use the considerations of Ch. 6 to determine trial values of $\alpha_{\beta\gamma}(k)$, and, then, with the resulting $Q_{\alpha\beta}(ki)$, determine the values of $P_{\alpha\beta}(kk')$ as given by Eq. (5.17), (iv) use the $E_\gamma(k)$ and $P_{\gamma\beta}(kk')$ values to determine the dipole moments from the system of linear equations given by Eq. (5.18), (v) use these dipole moments in Eq. (5.2) to determine the A_n^m values, and finally (vi) use the considerations of Sec. 3.2 to betermine the B_n^m values. (In the above, steps (i), (ii), and (v) employ Ewald's method.)

In dealing with the water molecules in RTH, one needs to know the values of the charges on the oxygen and hydrogen ions. The charge distribution is not uniquely known. For the present calculations, the charges $-2\eta|e|$ and $+\eta|e|$ were taken for the oxygen and hydrogen ions, respectively. Using $\eta = 1$, it was found that the magnitudes of the dipole sums for B_2^0 and B_2^2 were large, and of opposite sign, compared to their counterparts for the point-charge sums. The value of η was then reduced. The effect of this was to greatly reduce the magnitude of the dipole contributions, while giving a relatively small change in the point-charge contributions. By further reduction of η it was possible to reduce the dipole values to such an extent that they, plus the point-charge values, were in approximate agreement with experiment. The polarizability trial values were then adjusted so as to bring the results to within experimental error.

The value of η which was found to give good results was $\eta = 0.21$. This compares with the result of Burns[59] who took $\eta = 0.30$ to reproduce the values of the dipole moment in gaseous H_2O. The value of $\eta = 0.30$ can also be deduced from Pauling's work[60] on the ionic character of bonds. However, both of these references refer to molecular H_2O, and the values are subject to considerable uncertainty. This is all the more the case when the H_2O appears as water of hydration in a crystal.

Regarding the polarizability values, the symmetry of RTH (monoclinic) requires a tensor of the form[61]

$$\begin{pmatrix} \alpha_{xx} & 0 & \alpha_{xz} \\ 0 & \alpha_{yy} & 0 \\ \alpha_{zx} & 0 & \alpha_{zz} \end{pmatrix}$$

As the RTH crystals are not birefringent, it was assumed, for simplicity, that $\alpha_{xx} = \alpha_{yy} = \alpha_{zz} \equiv \alpha_d$. Also, one writes $\alpha_o \equiv \alpha_{xz} = \alpha_{zx}$. The values of α_d were taken initially to be equal to the free-ion values of the ions in question. For the rare-earths, these are (in units of Å^3)[62]: Nd (1.23), Sm (1.11), Eu (1.06), Tb (0.97), Dy (0.94), Ho (0.90), Er (0.86), and Tm (0.83). Those for chlorine and oxygen are[63]: Cl^- (2.97, also reported 3.05, 3.53), O^{2-} (3.88). No value is available for H^+, although the molecular polarizability of the H_2 molecule is given by Birge[50] as 0.79 Å^3, so the polarizability of H^+ should be of the order of 0.40 Å^3. (Note that the symbol H^+, in this context, does not denote a proton. The hydrogen is bonded covalently to the oxygen and thus has an effective fractional charge, as has been discussed above. Hence, to speak of the polarizability of H^+ is to refer to the deformability of the electron cloud in which the hydrogen is situated.) These initial trial values for α_d were allowed to vary from host-to-host so as to agree best with the experimental values for the spin-Hamiltonian parameters.

All of the above is with reference to the second-order parameters (B_2^0 and B_2^2). For the fourth-order parameters (B_4^0, B_4^2, B_4^4) the procedure is identical, except that the value for θ_4 (see Sec. 3.3) is not known. However, one may determine the values for A_4^m (m = 0, 2, 4) using the same polarizabilities for each ion as were used for the second-order parameters. Having done this, it was found that good results were obtained by taking $B_4^m = c\, A_4^m$ (m = 0, 2, 4) where $c = 3.524 \times 10^{-5}$ Å^4 is the same for all hosts and is independent of m.

7.2 Results and Analysis for RTH

It was found that the polarizabilities (α_d), listed in Table IX, gave values of B_2^0, B_2^2, and B_4^0 within experimental error for all hosts. Although some simplification has been made in choosing all the diagonal elements to be the same, for a given ion, this still represents an improvement over previous choices in that the non-zero off-diagonal elements (α_o) are also taken into account. For a given ion, the same value of α_o was chosen for all the hosts. The best values for α_o were found to be 0.00, 0.34, 2.22, and 0.31 $\AA^3$ for (any) rare-earth (R^{3+}), chlorine (Cl^-), oxygen (O^{2-}), and hydrogen (H^+) ions respectively. Plots of α_d versus Δr are given in Fig. 6. On the basis of these, the computed values for B_2^0 and B_2^2 are as listed in Table X, and those for B_4^0, B_4^2, and B_4^4 are in Table XI.

The polarizability values of Table IX are consistent with the discussion of Sec. 4.3 in that these values are considerably smaller than the free-ion values. For H^+, the values are in the range 0.42 ± 0.03 $\AA^3$, to be compared with the crude free-ion estimate of 0.40 $\AA^3$ given in Sec. 7.1. For Cl^-, the values are within 3.04 ± 0.40 $\AA^3$; this is to be compared with the reported free-ion values of 2.97, 3.05, and 3.53 $\AA^3$. For O^{2-}, the value is 3.79 $\AA^3$ as compared to the free-ion value of 3.88 $\AA^3$. For the rare-earth hosts, all the values are considerably smaller than their free ion counterparts and show approximately the same trend as the free-ion values except as discussed below. With regard to the changes in α_d as the host lattice is varied, one sees that, for $r_R > r_{Gd}$, both Cl^- and H^+ have a negative slope (Fig. 6). This is in accordance with the analysis of Sec. 6.4.

TABLE IX. Polarizabilities (α_d) for the various ions in RTH hosts ($Å^3$).

Host	R^{3+}	Cl^-	O^{2-}	H^+	$\Delta r (\times 10^{-2}$ Å)
Nd	0.85	2.68	3.79	0.414	+5.7
Sm	0.75	3.18	3.79	0.441	+2.6
Eu	0.70	3.44	3.79	0.460	+1.2
Tb	0.65	2.69	3.79	0.416	-1.5
Dy	0.63	2.72	3.79	0.415	-3.0
Ho	0.62	2.73	3.79	0.408	-4.4
Er	0.59	2.91	3.79	0.412	-5.7
Tm	0.58	3.05	3.79	0.412	-6.9

TABLE X. Second-order spin-Hamiltonian parameters b_2^m (GHz) for RTH.

Experimental error = ± 0.01 GHz.

Host	Index	Point Charge	Dipole	Total	Experiment	Difference
Nd	20	-0.8074	2.6655	1.8580	1.8550	0.0030
	22	1.4600	-2.5186	-1.0585	-1.0650	0.0065
Sm	20	-0.8088	2.6752	1.8664	1.8640	0.0024
	22	1.5398	-2.6572	-1.1174	-1.1120	-0.0054
Eu	20	-0.7848	2.6412	1.8564	1.8540	0.0024
	22	1.5367	-2.6809	-1.1442	-1.1500	0.0058
Tb	20	-0.8081	2.6862	1.8781	1.8820	-0.0039
	22	1.5489	-2.7406	-1.1917	-1.1910	-0.0007
Dy	20	-0.8087	2.6834	1.8756	1.8830	-0.0074
	22	1.5574	-2.7758	-1.2183	-1.2280	0.0097
Ho	20	-0.8157	2.7038	1.8881	1.8900	-0.0019
	22	1.5656	-2.8068	-1.2412	-1.2410	-0.0002
Er	20	-0.8240	2.6754	1.8514	1.8430	0.0084
	22	1.5653	-2.8428	-1.2775	-1.2760	-0.0015
Tm	20	-0.8237	2.7083	1.8846	1.8800	0.0046
	22	1.5691	-2.8744	-1.3053	-1.3110	0.0057

TABLE XI. Fourth-order spin-Hamiltonian parameters b_4^m (10^{-2} GHz) for RTH. Experimental error = ± 0.01 GHz.

Host	Index	Point Charge	Dipole	Total	Experiment	Difference
Nd	40	-3.07	-0.22	-3.30	-3.30	0.00
	42	-0.32	3.69	3.37	3.50	0.13
	44	-6.84	0.56	-6.28	-1.40	-4.88
Sm	40	-3.11	-0.25	-3.36	-3.50	0.14
	42	-1.32	3.51	2.20	2.30	-0.10
	44	-5.32	0.86	-4.46	1.00	-4.56
Eu	40	-3.12	-0.25	-3.37	-3.40	0.03
	42	-1.75	3.11	1.56	3.40	-1.84
	44	-4.73	0.87	-3.86	0.40	-4.26
Tb	40	-3.15	-0.25	-3.40	-3.70	0.30
	42	-0.94	3.75	2.81	2.40	0.41
	44	-5.79	0.78	-5.00	-0.40	-4.60
Dy	40	-3.17	-0.26	-3.43	-3.50	0.07
	42	-1.15	3.73	2.58	3.10	-0.52
	44	-5.46	0.79	-4.68	-0.50	-4.18
Ho	40	-3.19	-0.27	-3.46	-3.30	-0.16
	42	-1.31	3.80	2.49	5.20	-2.71
	44	-5.23	0.77	-4.46	-3.30	-1.16
Er	40	-3.19	-0.27	-3.46	-3.60	0.14
	42	-1.59	3.72	2.14	9.20	-7.06
	44	-4.85	0.80	-4.06	6.90	11.00
Tm	40	-3.21	-0.27	-3.49	-3.50	0.01
	42	-1.88	3.69	1.81	5.40	-3.59
	44	-4.45	0.81	-3.64	3.10	-6.74

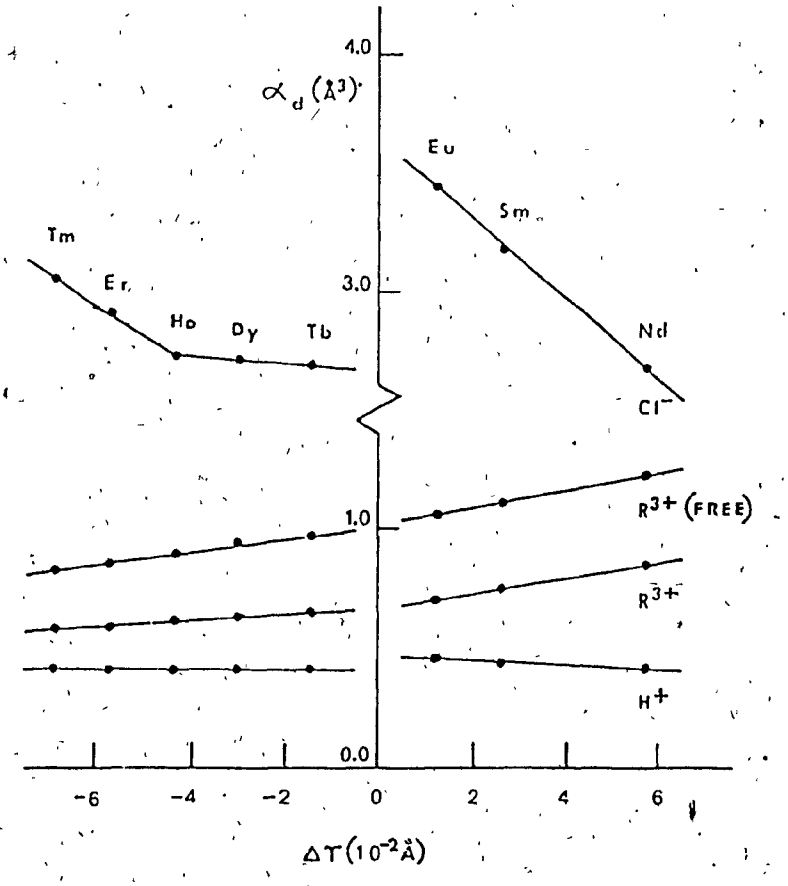

Fig. 6. Graph showing the polarizability α_d (Å^3) for chlorine (Cl^-), hydrogen (H^+), and rare-earth (R^{3+}) ions in the isostructural series of RTH as a function of Δr (10^{-2} Å). ($\Delta r \equiv r_R - r_{Gd}$) Also shown are the free-ion polarizabilities for the rare-earth ions.

For the rare-earth ions, for $r_R > r_{Gd}$, the slopes for α_d versus Δr is less that that for the free-ion values (plotted against Δr). Thus one finds that the polarizabilities of rare-earth ions in RTH crystals decrease with r less quickly than do the corresponding free-ion values. This is also in accord with Sec. 6.4. Hence, taking this factor into account, it can be seen from Fig. 6 that the slopes (α vs. Δr) for R^{3+}, Cl^-, and H^+ exhibit the same trend for $r > r_{Gd}$. For $r < r_{Gd}$, the trends are similar in that the slopes for R^{3+}, Cl^-, and H^+ all have the same sign as the slopes for $r > r_{Gd}$, but the magnitudes of the slopes for $r < r_{Gd}$ are smaller for all three graphs. This result is predicted by Eq. (6.31).

Regarding the off-diagonal elememts, α_o (same for all hosts), the value of zero is found for all rare-earths. This is not unreasonable, since the free-ion value is rather small to begin with, and also the 4f electrons are screened by the outer (n = 5) shell. For Cl^-, the value of 0.34 $\AA^3$ is small compared to the free-ion value. One would expect this value to be small because Cl^- is a closed shell configuration of spherical symmetry, and is thus less susceptible to an asymmetric distortion.

For O^{2-}, the value of 2.22 $\AA^3$ for the off-diagonal elements, α_o, is of the same order of magnitude as α_d; this may be expected in that O^{2-} has two covalent bonds with the hydrogens and thus is not in an isotropic state. It will thus respond in a skewed fashion to an external field because of the constraints imposed by these bonds on its electron cloud which is initially asymmetrical. For H^+, the value of 0.031 $\AA^3$ is small; this is because of a small but non-zero α_d (due to covalent bonding) for this ion.

As far as the fourth-order parameters are concerned, it is noted that the experimental values for B_4^2 and B_4^4 are somewhat uncertain.[33] Further, these values are extremely sensitive to the ionic positions in the host crystal. Thus, if ionic distortions, caused by the substitution of the paramagnetic ion, are to be taken into account, it is plausible that the computed values for the parameters can be found to be in agreement with the experimental ones. However, here such distortions have not been taken into account.

In the procedure described, it may be argued that, for each host, one is fitting three data points (B_2^0, B_2^2, B_4^0) with three parameters (the α_d-values for R^{3+}, Cl^-, and H^+). However, there are actually five data points, and, in any case, the fit is not in the nature of a least-squares fit, or a purely empirical fit where one does an arbitrary search. This is because the values of α_d are fairly strictly limited according to the constraints mentioned in Chapter 6. Specifically, the values correlate with the free-ion values, they vary linearly with Δr, and the slopes are consistent with those described in Sec. 6.4.

7.3 Application to RF_3

The prescription outlined in Sec. 7.1 was also applied to Gd^{3+}: RF_3 (R = La, Ce, Pr, Nd). In principle, the only difference in procedure arises from the different symmetry of RF_3 (trigonal) as compared to RTH (monoclinic). This dictates that one should (for RF_3) also include parameters, B_n^m, having $m < 0$. However, as reported in Ref. 33, the parameters for negative m are, for the most part, very small in magnitude — namely, of the order of the experimental error. They were, therefore, not taken into account in the present calculation.

Trigonal symmetry requires a tensor of the form[61]

$$\alpha = \begin{pmatrix} \alpha_o & \alpha_o & 0 \\ 0 & \alpha_o & \alpha_e \end{pmatrix}$$

where $\alpha_o = \alpha_{11}$ $(= \alpha_{22})$ and $\alpha_e = \alpha_{33}$ with α_{ij} $(i \neq j) = 0$. The subscripts allude to the so-called 'ordinary' and 'extraordinary' rays, which refer to the fact that RF_3 is birefringent; i.e. the optical index of refraction as measured along the z axis (n_e) is different from that measured along the x or y axis (n_o). The polarizabilities are crudely related to these indices by the Lorentz relation. Since the measured values for n_o and n_e for RF_3 differ by less than 0.1 %,[64] it is assumed, for the present calculations, that one may take $\alpha_o = \alpha_e$ for all the ions in the crystal.

In the calculation one needs the values for the polarizability of the fluorine ion (F^-) for each of the four hosts in the series and for R^{3+} (R = La, Ce, Pr, Nd). As was done previously with RTH, the free-ion values were used as a first estimate. These are[62] (in units of $Å^3$) 1.41, 1.35, 1.29, 1.23, and 0.76 for La, Ce, Pr, Nd, and F[63] respectively. It was found that, in order to get agreement with experiment, the polarizability values for the various R^{3+} ions had to be increased and those for F^- had to be decreased from the free-ion values. The results are presented in Table XII. On the basis of these, the computed values for B_2^0 and B_2^2 are as given in Table XIII, and those for B_4^0, B_4^2, and B_4^4 are as given in Table XIV.

The increase in the polarizability of the rare-earth ions (with respect to the corresponding free-ion values) is plausible with reference to the discussion of Sec. 4.3, where it was pointed out that such

TABLE XII. Polarizabilities (α_d) for the ions in RF_3 hosts

Host	$R^{3+}(\text{Å}^3)$	$F^-(\times 10^{-2}\ \text{Å}^3)$
La	2.860	1.420
Ce	2.495	1.439
Pr	2.270	1.444
Nd	2.180	1.550

TABLE XIII. Second-order spin-Hamiltonian parameters b_2^m (GHz) for RF_3. Experimental error = ± 0.01 GHz.

Host	Index	Point Charge	Dipole	Total	Experiment	Difference
La	20	0.5460	0.1515	0.6975	0.6930	0.0142
	22	-4.3302	4.2457	-0.0845	-0.0850	0.0005
Ce	20	0.5616	0.1789	0.7405	0.7350	0.0055
	22	-4.4615	4.3776	-0.0839	-0.0840	0.0001
Pr	20	0.5793	0.2012	0.7805	0.7730	0.0075
	22	-4.5770	4.4960	-0.0810	-0.0810	0.0000
Nd	20	0.6321	0.1699	0.8020	0.7950	0.0070
	22	-4.7745	4.6241	-0.1504	-0.1490	-0.0014

TABLE XIV. Fourth-order spin-Hamiltonian values b_4^m (10^{-2} GHz) for RF_3. Experimental error = ± 0.01 GHz.

Host	Index	Point Charge	Dipole	Total	Experiment	Difference
La	40	1.24	0.03	1.27	1.60	- 0.33
	42	-3.80	0.12	-3.68	7.40	-11.10
	44	-8.61	-0.22	-8.83	12.50	-21.30
Ce	40	1.33	0.03	1.36	1.60	- 0.24
	42	-4.00	0.11	-3.89	8.50	-12.40
	44	-8.95	-0.22	-9.17	16.90	-26.10
Pr	40	1.40	0.03	1.43	1.60	- 0.18
	42	-4.15	0.10	-4.05	8.30	-12.30
	44	-9.20	-0.22	-9.42	11.70	-21.10
Nd	40	1.46	0.03	1.49	1.80	- 0.34
	42	-4.23	0.10	-4.13	10.50	-14.60
	44	-9.36	-0.23	-9.59	12.80	-22.40

a result could be produced by an increase in the effective ionic charge that participates in the polarization process. While the mechanisms which would give rise to such an increase are not explicitly known, they presumably relate to distortions in the electron shells caused by the substitution of the Gd^{3+} ion. One would expect that the magnitude of such distortion-related effects would correlate with the difference in ionic radii between the Gd^{3+} ion and the host rare-earth ion, R^{3+}; i.e. with Δr ($\equiv r_R - r_{Gd}$). Fig. 7 shows a plot of the resultant ionic polarizabilities plotted versus Δr. It is seen that, except for Nd, the relations are approximately linear, and that the slope for the positive ions (the R^{3+}) is positive, while that for the negative ions (F^-) is negative. This is the same result as that found for Gd^{3+}: RTH (Sec. 7.2). Of course, the increase in $\alpha(R^{3+})$ with Δr is partially due to the increase in the free-ion values.

The values obtained for the polarizabilities of the F^- ions is small compared to those free-ion values cited in the literature. However, they are plausible in light of Eq. (6.12). This relation may be written, for F^-, approximately as[65]

$$\alpha = \frac{(n_- e + D)^2}{k + S} \tag{7.1}$$

where n_- is the number of outer-shell electrons participating in the polarization process, D is the exchange charge parameter, and k and S are the shell-core and shell-shell force constants, respectively. For F^-, the value of n_- has been reported as low as 0.9 with D/e of the order of[51] - 0.1 . (e is the charge on the electron.) The values for k and S have been given as[51,65] 5110 N/n and 100 N/m, respectively. Employing these values in Eq. (7.1), gives a fluorine polarizability

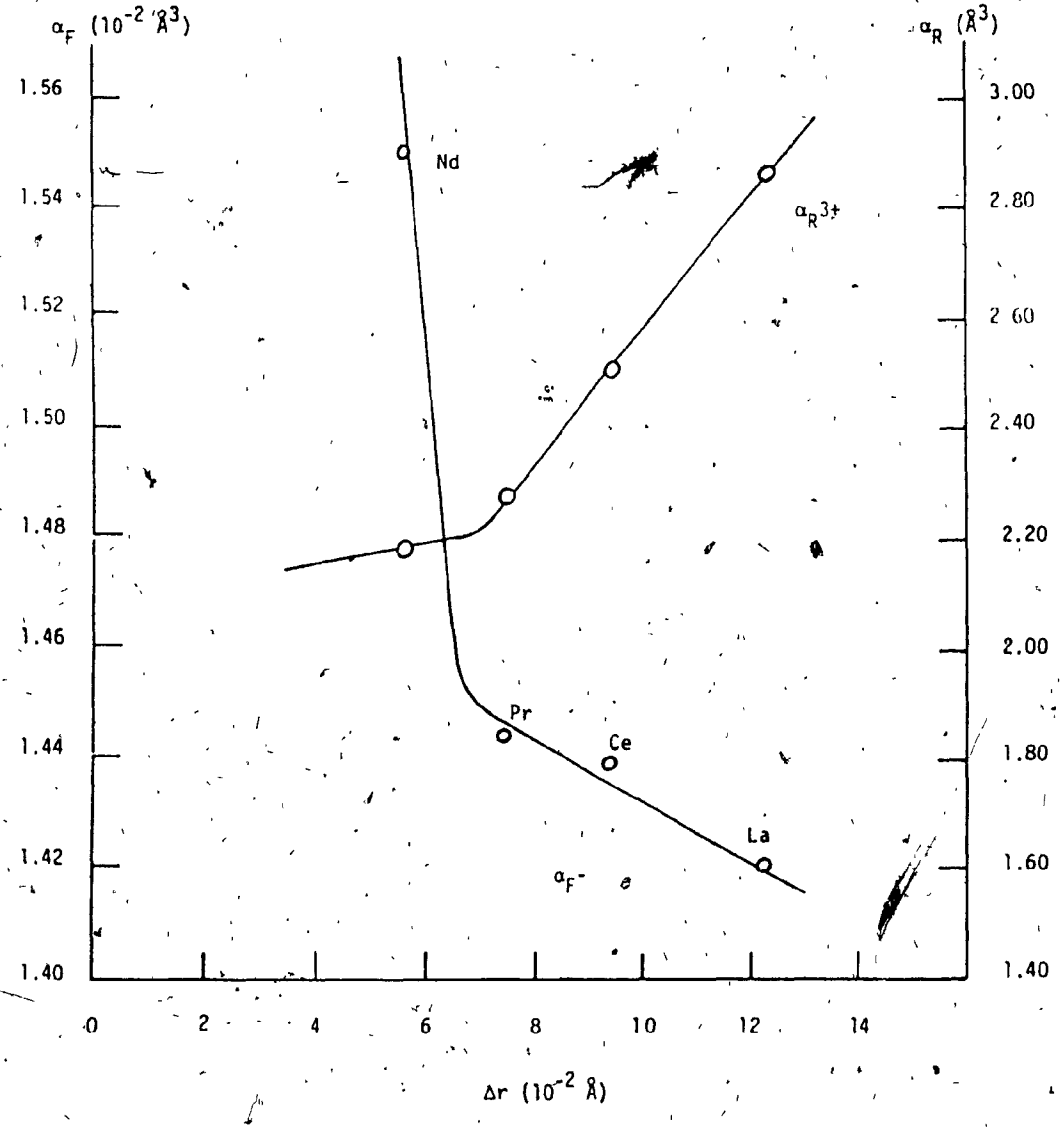

Fig. 7. Graph showing the polarizability α for the various ions in the isostructural series of RF_3 as a function of Δr (10^{-2} Å). The left-hand scale gives the polarizability for the fluorine ions α_F (10^{-2} Å^3). The right-hand scale gives the polarizability for the rare-earth metal ions α_R (Å^3).

value of 0.02 $\AA^3$ which is of the same order of magnitude as that found from the PCID model.

Two observations may now be made regarding the above PCID results. First, the multiplicative factor used for θ_4 (see Sec. (7.1)), in the absence of a theoretical value, was the same for both RTH and RF_3. The fact that good results were achieved for both systems, using this same factor to relate the A_4^m to the B_4^m is a strong indicator that the relation is, in fact, linear and that the model being used is quite general. Second, as seen from Table XIV, the B_2^4 and B_4^4 values do not agree with experiment. However, it is likely, in view of the superposition model results, discussed in Sec. 4.4, that the PCID model predictions for these two parameters would be greatly improved if distortion were taken into account. In other words, distortion aside, it may be said that the two models (SM and PCID) give equally good results.

Chapter 8

CONCLUSIONS

A number of specific conclusions may be drawn from this work. First, the results of both the superposition model and the PCID model support the contention that the relation between the CFPs and the SHPs is linear for the n = 2 and n = 4 parameters, at least for Gd^{3+}. This is evidenced by the fact that the same values for θ_2 and θ_4 were used successfully for both homologous series (RTH and RF_3).

Second, the results of the PCID model support the validity of the conventional crystal-field parameterization scheme. In particular, they support the claim that the scheme is not dependent on the assumption that the crystal field arises solely from the point-charge electrostatic field (see Appendix A). This claim, that the results support the parameterization scheme, is made on purely empirical grounds; namely, that the use of the scheme in the PCID model gives good results. It could be argued that it is the choice of polarizability values which 'forces' the scheme to work. However, as has been mentioned, the polarizability values employed are not arbitrary fitting parameters. They are subject to a number of constraints. Thus, it is the contention here that the basic scheme is validated by the PCID model.

Third, the superposition results demonstrate that, although Newman's model is capable of successfully describing the SHPs, the model may be extended so as to decouple the model parameters, $\bar{b}_n$ and t_n, from metal-ligand distance effects. Also, it appears clear that the superposition model is basically phenomenological in nature in that the physical significance of its parameters is not evident. In addition,

it is not understood how the SM succeeds despite the fact that it considers only the nearest ligands. It is quite possible, in fact, that it does take the rest of the crystal into account by an appropriate scaling of the parameter $\bar{b}_n$. However, more work is needed to fully investigate this.

With regard to the PCID model, per se, there are three points which provide evidence for its claim to be a valid and viable model. First, there is the obvious one; that it provides results within experimental error for those parameters not subject to large distortion effects. This is the first model, free of phenomenological parameters, which can make that claim. It may be contended that this is solely due to one's ability to appropriately adjust the polarizability values. However, there is a limit to this capability in that the α-values must correlate with the free-ion values and with values as predicted by the shell model for ions in situ. In addition, the number of different-ion-type α-values one has for a given host is fewer than the number of data points. Thus, it is argued here that the model does provide a valid description of the crystal field. Second, the trend in the α-values predicted by the model (i.e. α vs Δr) is in accordance with the exchange charge model. This is a cogent point which provides strong evidence for the claim that the α-values predicted actually have something to do with what is going on in the crystal — that they are not of an arbitrary nature. Third, a main advantage of the model is that it provides a guidepost to further research into the basic mechanisms involved in the problem. This is because most previous models have dealt with a myriad of competing and mutually interacting factors which contribute to the ligand field. The PCID model separates out all of

these from point-charge and dipole effects by placing them in the polarizability tensor. That is, it is the claim of the model that the effect of short-range mechanisms such as overlap and covalency is to modify the polarizability values. Thus, the model provides a strong ordering principle by the use of which one can proceed, hopefully, to an ab initio microscopic calculation of the α-values.

The main factor which, at present, prevents such a calculation is the problem of distortion caused by the substitution of the paramagnetic ion. This is because of the fact that such a calculation requires a knowledge of the polarizability values which one is trying to predict. However, this is just where the PCID model could prove to be very valuable since one could take its α-value predictions as trial values in a distortion calculation, get some distortion values (new distorted-ion positions), substitute these back in the PCID model, and then continue this iterative process. The distortion calculation could be based on finding that ion configuration which minimizes the unit-cell (configuration) energy.

From a more general viewpoint, one can conclude from the PCID model that approaches which deal solely with long- or with short-range mechanisms are not providing a true representation of the situation. It seems evident that one must consider both the electrostatic field and near-neighbour phenomena. Although the superposition model may be cited as evidence to the contrary, it is felt that it may yet be shown that this model also depends on long-range effects, although, admittedly there is at present not yet sufficent evidence to state this with certainty.

In summary, it is the claim of this work that the PCID model

provides a valid, effective, and accurate description of spin-Hamiltonian parameters. Also, it is claimed that the model is original in that it is the first polarizable dipole model to employ anisotropic polarizability tensors conforming to the crystal symmetry. In addition, it is claimed that this work demonstrates for the first time the crucial role played by polarizability in the description of the observed parameters.

Appendix A

THE CRYSTAL-FIELD PARAMETERIZATION SCHEME

As was seen in Ch. 3, the conventional method of parameterizing the crystal field implicitly assumes that the crystal field is due solely to the electrostatic point-charge field of the ions. This results in one being able to express the potential energy of the open-shell magnetic electrons in terms of the spherical harmonics Y_n^m (or, equivalently, in terms of the Tesseral harmonics Z_n^m). The purpose of this section is to demonstrate that this result is not dependent on the above-mentioned assumption. That is, it is to be shown that the conventional scheme is adequate, regardless of the specific mechanisms which give rise to the crystal field splittings. The main line of the arguement is due to Newman.[24]

The potential energy of the (magnetic) electrons in a $n'\ell^N$ open-shell paramagnetic ion may be written as

$$V = \sum_i V_i = \sum_i \sum_{n,m} A_n^m t_m^{(n)}(i)$$

$$= \sum_{n,m} A_n^m T_m^{(n)}(i) \qquad (A.1)$$

where

$$T_m^{(n)}(i) = \sum_i t_m^{(n)}(i) \qquad (A.2)$$

Here, i labels the different electrons in the open shell, the A_n^m are expansion coefficents (crystal-field parameters), and $t_m^{(n)}(i)$ is a (Hermitian) tensor operator acting on the coordinates of electron i. With regard to Eq. (A.1), four points may be noted:

(1) the A_n^m are independent of i, (2) all the open-shell electrons are assumed to be equivalent. That is, the contribution of each is taken to be independent of the states of the others in the open shell. This is equivalent to stating that V is a one-particle potential. (3) V is taken to be a function only of the angular coordinates of the electrons. This assumes that all open-shell states have the same radial dependence. (4) As the operators $t_m^{(n)}(i)$ are general tensor operators spanning the irreducible representations of the full rotation group, they can represent the angle dependence of any operator. Hence, the form of V (as in Eq. (A.1)) in no way presupposes it to be purely electrostatic in origin. Other mechanisms, such as covalency, can make a contribution to a potential of this form.

Now, as with any operator in the time-independent Schrodinger equation, V must be Hermitian. The conventional definition of Hermitian tensor operators,

$$T_m^{(n)\dagger} = (-1)^m T_{-m}^{(n)} \qquad (A.3)$$

ensures the Hermiticity of V if one has

$$\left(A_n^m\right)^* = (-1)^m A_n^{-m} . \qquad (A.4)$$

(In these equations, † denotes the complex conjugate transpose of a tensor, while * denotes the complex conjugate.)

Let a one-electron open-shell orbital state be denoted by $|\ell,\alpha\rangle$, where ℓ is the angular momentum quantum number ($\ell = 3$ for a $4f^N$ state), and α denotes all the other quantum numbers required to specify the state. Then the complex conjugate of a tensor operator $t_m^{(n)}$ is defined by

$$\langle \ell,\alpha | t_m^{(n)*} | \ell,\alpha' \rangle = (-1)^{-\alpha'-\alpha} \langle \ell,-\alpha | t_m^{(n)} | \ell,-\alpha' \rangle \qquad (A.5)$$

Note in this regard, that, generally, the wavefunctions, Ψ, between which one calculates the matrix elements of the crystal potential, will be Slater determinants or linear combinations thereof. Each determinant will be of the form $(\chi_1, \ldots, \chi_N, \phi_1, \ldots, \phi_p)$ where the χ's form a set of N one-electron wavefunctions representing the closed shells, this set being the same for all Slater determinants appearing in the expansion of the states Ψ. The remaining set of one-electron wavefunctions (the ϕ's) are those of the magnetic electrons in the unfilled shell. i.e. $\phi \sim |\ell,\alpha>$. In a calculation of $<\Psi|V|\Psi>$, the contribution of the closed shells will be $\sum <\chi_i|V|\chi_i>$. However, if, in the expansion of V (Eq. (A.1)), the n = 0 term is omitted, this closed-shell contribution will be zero. The omission of the n = 0 term is permitted in that the effect of this term is to shift all energies by a constant amount. It thus has no effect on transition energies (energy differences). Hence, one may omit closed shells altogether and write the Slater determinant in the form $(\phi_1, \ldots, \phi_p)$. That this is possible is due to the fact that V is a one-particle operator.[69]

Returning now to Eq. (A.5), the matrix element on the right-hand-side may, according to the Wigner-Eckart theorem be written as[14]

$$\langle \ell,-\alpha | t_m^{(n)} | \ell,-\alpha' \rangle = (-1)^{\ell+\alpha} \begin{pmatrix} \ell & n & \ell \\ \alpha & m & -\alpha' \end{pmatrix} \langle \ell \| t^{(n)} \| \ell \rangle \qquad (A.6)$$

where $\begin{pmatrix} & & \\ & & \end{pmatrix}$ is a Wigner 3j symbol (coupling coefficent) and $< \| \ \| >$ is a so-called reduced matrix element ('reduced' in that it is independent of m). Thus, Eq. (A.5) becomes

$$\langle \ell,\alpha | t_m^{(n)*} | \ell,\alpha' \rangle = (-1)^{\ell-\alpha'} \begin{pmatrix} \ell & n & \ell \\ \alpha & m & -\alpha' \end{pmatrix} \langle \ell \| t^{(n)} \| \ell \rangle \quad \text{(A.7)}$$

Also (analagous to Eq. (A.6)), one has

$$\langle \ell,\alpha | t_{-m}^{(n)} | \ell,\alpha' \rangle = (-1)^{\ell-\alpha} \begin{pmatrix} \ell & n & \ell \\ -\alpha & -m & \alpha' \end{pmatrix} \langle \ell \| t^{(n)} \| \ell \rangle \quad \text{(A.8)}$$

However, there exists the relation[70]

$$\begin{pmatrix} \ell & n & \ell \\ -\alpha & -m & \alpha' \end{pmatrix} = (-1)^{2\ell+n} \begin{pmatrix} \ell & n & \ell \\ \alpha & m & -\alpha' \end{pmatrix} \quad \text{(A.9)}$$

Thus, Eq. (A.8) becomes

$$\langle \ell,\alpha | t_{-m}^{(n)} | \ell,\alpha' \rangle = (-1)^{(\ell-\alpha)+(2\ell+n)} \begin{pmatrix} \ell & n & \ell \\ \alpha & m & -\alpha' \end{pmatrix} \langle \ell \| t^{(n)} \| \ell \rangle \quad \text{(A.10)}$$

It is well known that, in order for the coupling coefficent in Eq. (A.10) not to vanish, one must have $\alpha = \alpha' - m$ ('triangle condition'). Thus substituting for α in the exponent in Eq. (A.10) gives

$$\langle \ell,\alpha | t_{-m}^{(n)} | \ell,\alpha' \rangle = (-1)^{\ell-\alpha'} (-1)^{2\ell} (-1)^{m+n} \begin{pmatrix} \ell & n & \ell \\ \alpha & m & -\alpha' \end{pmatrix} \langle \ell \| t^{(n)} \| \ell \rangle \quad \text{(A.11)}$$

Clearly $(-1)^{2\ell} = 1$. Then comparing Eq. (A.11) with Eq. (A.7) gives

$$\langle \ell,\alpha | t_{-m}^{(n)} | \ell,\alpha' \rangle = (-1)^{m+n} \langle \ell,\alpha | t_m^{(n)*} | \ell,\alpha' \rangle \quad \text{(A.12)}$$

Thus, for all states constructed from states of the form $|\ell,\alpha\rangle$, one must have

$$t_m^{(n)*} = (-1)^{m+n} t_{-m}^{(n)} \quad \text{(A.13)}$$

Now V, in addition to being Hermitian, must also be time-reversal invar-

iant. This implies that V must be real.[71] This condition, coupled with Eq. (A.13), requires that one also have

$$\left(A_n^m\right)^* = (-1)^{m+n} A_n^{-m} \qquad \text{(A.14)}$$

Comparing Eq. (A.14) with Eq. (A.4) shows that n must be even. It is important to note that this restriction follows from the general constraints of Hermiticity and time-reversal invariance which must hold for any operator. In the conventional parameterization scheme, the restriction to even n is derived by noting that the odd n spherical harmonics have odd parity and hence give vanishing matrix elements between states of a given ℓ. But, such an arguement depends on having previously assumed that V may be expressed in terms of the spherical harmonics, Y_n^m, as would be the case if the crystal field were purely electrostatic in origin. However, having shown, from very general considerations, that n must be even, no generality is lost by taking

$$t_m^{(n)}(i) = Y_n^m(\theta_i, \phi_i) \qquad \text{(A.15)}$$

(apart from fixing the value of $\langle \ell || t^{(n)} || \ell \rangle$). Hence, the conventional parameterization scheme, which is equivalent to Eq. (A.15), is adequate in all circumstances.

The number of parameters, A_n^m, which occur is also constrained by the fact that, in Eq. (A.6), the matrix elememts will vanish unless $n \leq 2\ell$. For the rare-earth metals (4f shell), since one has $\ell = 3$, n is thus restricted to the values 2, 4, 6 (the constant A_0^0 is omitted, as mentioned above). In specific cases, the number of parameters may be further reduced by the symmetry of the crystal enviornment.

Appendix B

UNIT CELL STRUCTURE FOR RF_3 AND RTH

This section collates the information required for calculations involving the two homologous series RF_3 and RTH. The theory relating to lattice vectors is presented, and the specific cell data are given.

B.1 Direct Lattice Vectors

The unit cell structure for a given crystal will correspond to one of the 230 space groups. For each space group there will be a number of subgroups corresponding to sublattices. Given the position of an ion in a specific sublattice, the positions of the others (the so-called equivalent positions) can be generated by symmetry operations. Usually one knows from the literature which ion type corresponds to a given sublattice. Then, using published tables,[49] one can calculate the coordinates for all of the ions in the cell. The procedure will be described specifically for RF_3, as an example. Later, the corresponding data will also be given for RTH.

Table XV shows the coordinates of the equivalent positions for a cell with the RF_3 structure. The structure is trigonal with $D_{3d}^4(P\bar{3}c1)$ symmetry.[31,33,35] The numerical values or unit cell parameters (x, y, z) to be assigned to a given sublattice are given in Table XV to the right of the listing of the positions for that sublattice. These are the same for all crystals with the RF_3 structure. For a specific crystal, one gets the actual coordinate values by multiplying by the lattice constants (cell edge lengths) a, b, c. For example, a given coordinate (p, q, r) would become (pa, qb, rc). The lattice constants for RF_3 are given in

TABLE XV. Positional parameters for RF_3. (See Ref.35)

Number of positions, Wyckoff notation, point symmetry, and atom type	Coordinates			Unit cell parameters
12 g 1 F(I)	x,y,z;	$\bar{y},x-y,z$;	$y-x,\bar{x},z$;	$x = 0.312$
	$\bar{x},\bar{y},\bar{z}$;	$y,y-x,\bar{z}$;	$x-y,x,\bar{z}$;	$y = -0.005$
	$\bar{y},\bar{x},{}^1/_2+z$;	$x,x-y,{}^1/_2+z$;	$y-x,y,{}^1/_2+z$;	$z = 0.581$
	$y,x,{}^1/_2-z$;	$\bar{x},y-x,{}^1/_2-z$;	$x-y,\bar{y},{}^1/_2-z$.	
4 d 3 F(II)	${}^1/_3,{}^2/_3,z$;	${}^2/_3,{}^1/_3,\bar{z}$;	${}^1/_3,{}^2/_3,{}^1/_2+z$;	$z = 0.313$
	${}^2/_3,{}^1/_3,{}^1/_2-z$.			
2 a 32 F(III)	$0,0,{}^1/_4$;	$0,0,{}^3/_4$.		
6 f 2 R	$x,0,{}^1/_4$;	$0,x,{}^1/_4$;	$\bar{x},\bar{x},{}^1/_4$;	$x = 0.340$
	$\bar{x},0,{}^3/_4$;	$0,\bar{x},{}^3/_4$;	$x,x,{}^3/_4$.	

Table XVI. In practice, one is interested in the position of a given ion, $\vec{r}(x, y, z)$, relative to the position, $\vec{r}\ (x_o, y_o, z_o)$, of the substituted paramagnetic ion (say Gd^{3+}). i.e. one form the vector, $\vec{r} - \vec{r}_o$. The position of any other ion outside the unit cell which is a member of the sublattice including the ion whose position is given by $\vec{r}$ may be generated by $\vec{r} + \vec{\ell}$ where

$$\vec{\ell} = \ell_1 \vec{a} + \ell_2 \vec{b} + \ell_3 \vec{c} \qquad (B.1)$$

where ℓ_1, ℓ_2, ℓ_3 are integers. The position relative to Gd^{3+} is then

$$\vec{R} = \vec{\ell} + \vec{r} - \vec{r}_o \qquad (B.2)$$

All of the above is with respect to the crystal frame of reference. In general, the cell edges $\vec{a}$, $\vec{b}$, $\vec{c}$ will not be mutually orthogonal, so one must transform to the laboratory frame of reference. For RF_3, $\vec{b}$ is at an angle of 120° with respect to $\vec{a}$, while $\vec{c}$ is perpendicular to both $\vec{a}$ and $\vec{b}$. Making the appropriate transformation, Eq. (B.2) becomes, in componeht form,

$$X = \{\ell_1 + (x - x_o)\}a + \{\ell_2 + (y - y_o)\}b \cos 60^\circ \qquad (B.3a)$$

$$Y = \{\ell_2 + (y - y_o)\}b \sin 60^\circ \qquad (B.3b)$$

$$Z = \{\ell_3 + (z - z_o)\}c \qquad (B.3c)$$

For RF_3, there is one set of (x, y, z) values for each of the 24 ions in the unit cell.

TABLE XVI. Lattice constants (in angstrom units) for RF_3. (See Ref. 64)

Host	a,b	c
LaF_3	7.186	7.352
CeF_3	7.112	7.279
PrF_3	7.061	7.218
NdF_3	7.030	7.119

In the EPR measurements[33] for the spin-Hamiltonian parameters discussed in this work, the z and y axes were coincident with the $\vec{a}$ and $\vec{c}$ axes, respectively. Thus, in an actual calculation, one must relabel the expressions in Eq. (B.3). (i.e. $X \rightarrow Z$, $Y \rightarrow X$, $Z \rightarrow Y$)

The equivalent positions and lattice constants for RTH are given, respectively, in Tables XVII and XVIII. The crystal structure is[36] monoclinic with C_{2h}^4 (P2/c) symmetry. In this system, the angle between $\vec{a}$ and $\vec{c}$ is $\beta = 93.65°$ and the zx plane is coincident with the ac plane, the z axis making an angle χ with $\vec{a}$. This angle (χ) is different for different hosts (the values are included in Table XVIII). The relations, for RTH, analagous to Eq. (B.3) are

$$X = \{\ell_1 + (x - x_0)\} a \cos\chi + \{\ell_2 + (y - y_0)\} b \cos(\beta - \chi) \quad \text{(B.4a)}$$

$$Y = -\{\ell_1 + (x - x_0)\} a \sin\chi + \{\ell_2 + (y - y_0)\} b \sin(\beta - \chi) \quad \text{(B.4b)}$$

$$Z = \{\ell_3 + (z - z_0)\} c \quad \text{(B.4c)}$$

B.2 Reciprocal Lattice Vectors

To employ Ewald's method (see Appendix C), one requires reciprocal lattice vectors in addition to the direct lattice vectors defined in the previous section. Given a direct lattice vector, $\vec{\ell}$, as defined by Eq. (B.1), the corresponding reciprocal lattice vector, $\vec{g}$, is defined by

$$\vec{g} = k_1 \vec{\alpha} + k_2 \vec{\beta} + k_3 \vec{\gamma} \quad \text{(B.5)}$$

TABLE XVII. Positional parameters for RTH. (See Ref. 72)

Number of positions, Wyckoff notation, point symmetry, and atom type				Coordinates			Unit cell parameters x	y	z
4	g	1	Cl(II)	x,y,z;	$\bar{x},\bar{y},\bar{z}$;		0.0587	0.8370	0.2601
				$\bar{x}$,y,$^1/_2$-z;	x,$\bar{y}$,$^1/_2$+z.				
			O(I)				0.2813	0.0471	0.5432
			O(II)				0.1423	0.4254	0.0888
			O(III)				0.4406	0.2088	0.1058
			H(I)				0.272	0.920	0.605
			H(II)				0.364	0.082	0.608
			H(III)				0.174	0.484	0.987
			H(IV)				0.117	0.548	0.140
			H(V)				0.534	0.322	0.149
			H(VI)				0.476	0.258	0.002
2	f	2	Cl(I)	$^1/_2$,y,$^1/_4$;	$^1/_2$,$\bar{y}$,$^3/_4$.			0.3769	
2	e	2	R	0,y,$^1/_4$;	0,$\bar{y}$,$^3/_4$.			0.1521	

TABLE XVIII. Lattice constants for RTH. (See Refs. 36, 37)

The lengths a, b, c are in angstrom units and the angle χ is in degrees.

Host	a	b	c	χ
Nd	9.72	6.60	7.90	58.5
Sm	9.67	6.55	7.96	63.0
Eu	9.68	6.53	7.96	62.5
Tb	9.63	6.51	7.89	61.0
Dy	9.61	6.49	7.87	62.0
Ho	9.58	6.47	7.84	63.0
Er	9.57	6.47	7.84	60.5
Tm	9.55	6.45	7.82	64.5

where

$$k_i = \frac{2\pi}{V} n_i \quad (i = 1, 2, 3) \tag{B.6}$$

and

$$\vec{\alpha} = \vec{b} \times \vec{c} \;, \quad \vec{\beta} = \vec{c} \times \vec{a} \;, \quad \vec{\gamma} = \vec{a} \times \vec{b} \tag{B.7}$$

Here, the n_i are integers and $V = \vec{a} \cdot (\vec{b} \times \vec{c})$ is the volume of the unit cell.

For RF_3, the components of $\vec{g}$ are given by

$$g_x = \frac{2\pi n_1}{a} \tag{B.8a}$$

$$g_y = \frac{2\pi n_1 \cos\beta}{a \sin\beta} + \frac{2\pi n_2}{b \sin\beta} \tag{B.8b}$$

$$g_z = \frac{2\pi n_3}{c} \tag{B.8c}$$

For RTH, they are

$$g_x = \frac{2\pi n_1 \sin(\beta - \gamma)}{a \sin\beta} + \frac{2\pi n_2 \sin\gamma}{b \sin\beta} \tag{B.9a}$$

$$g_y = -\frac{2\pi n_1 \cos(\beta - \gamma)}{a \sin\beta} + \frac{2\pi n_2 \cos\gamma}{b \sin\beta} \tag{B.9b}$$

$$g_z = \frac{2\pi n_3}{c} \tag{B.9c}$$

Appendix C

EWALD'S METHOD

This appendix discusses the theory and application of Ewald's method.[39] Sec. (C.1) develops and explains the basic equations for sums of the form $\sum (1/R)$, where R is an ionic distance. The treatment up to the end of Eq. (C.23) follows that of Ziman.[66] Expressions for the Tesseral harmonics (which occur in the crystal-field parameters), or for the electric field, all involve derivatives of sums of this sort. Sec. (C.2) treats the first and second derivatives, while Sec. (C.3) deals with those of higher order.

C.1 Derivation

The lattice structure is invariant under any translation represented by the sum of integral multiples of the unit-cell vectors $\vec{a}_1$, $\vec{a}_2$, $\vec{a}_3$. That is, any lattice point can be reached by the translation

$$\vec{\ell} = \ell_1 \vec{a}_1 + \ell_2 \vec{a}_2 + \ell_3 \vec{a}_3 \qquad (C.1)$$

where ℓ_1, ℓ_2, ℓ_3 are integers. These vectors, $\vec{\ell}$, will be called direct (lattice) vectors, and they span a direct (lattice) space. Similarly, one can define reciprocal (lattice) vectors, $\vec{g}$, spanning a reciprocal (lattice) space, through

$$\vec{g} = 2\pi n_1 \vec{b}_1 + 2\pi n_2 \vec{b}_2 + 2\pi n_3 \vec{b}_3 \qquad (C.2)$$

where n_1, n_2, n_3 are integers and

$$\vec{b}_i = \frac{\vec{a}_j \times \vec{a}_k}{\vec{a}_i \cdot (\vec{a}_j \times \vec{a}_k)} \qquad (C.3)$$

Clearly,

$$\vec{g}\cdot\vec{\ell} = 2\pi \qquad (C.4)$$

where n is an integer. Now consider a function $f(\vec{r})$ which is periodic in $\vec{\ell}$. (i.e. $f(\vec{r}+\vec{\ell}) = f(\vec{r})$) This may be written as

$$f(\vec{r}) = \sum_{\vec{g}} A_{\vec{g}}\, e \qquad (C.5)$$

where $A_{\vec{g}}$, the Fourier transform of $f(\vec{r})$, is (V_c is the crystal volume)

$$A_{\vec{g}} = \frac{1}{V_c}\int_c f(\vec{r})\, e^{-i\vec{g}\cdot\vec{r}}\, d\vec{r} \qquad (C.6)$$

Note that the periodicity of $f(\vec{r})$ is guaranteed by Eq. (C.4). A more appropriate way of expressing Eq. (C.4) is to observe that it is equivalent to

$$e^{i\vec{g}\cdot\vec{r}} = 1 \qquad (C.7)$$

Now consider the function

$$F(\vec{r},\rho) \equiv \frac{2}{\sqrt{\pi}}\sum_{\vec{\ell}} e^{-|\vec{\ell}-\vec{r}|^2\rho^2} \qquad (C.8)$$

where ρ is an arbitrary parameter. Because of the sum over $\vec{\ell}$, $F(\vec{r},\rho)$ is periodic in $\vec{\ell}$. Via Eqs. (C.5) and (C.6), this periodicity means that $F(\vec{r},\rho)$ may be expressed as

$$F(\vec{r},\rho) = \sum_{\vec{g}} F_{\vec{g}}\, e^{i\vec{g}\cdot\vec{r}} \qquad (C.9)$$

where

$$F_{\vec{g}} = \frac{1}{V_c}\int_c \frac{2}{\sqrt{\pi}}\sum_{\vec{\ell}} e^{-|\vec{\ell}-\vec{r}|^2\rho^2 - i\vec{g}\cdot\vec{r}}\, d\vec{r}$$

$$= \frac{2}{\sqrt{\pi}V_c}\sum_{\vec{\ell}}\int_c \exp\left\{-\vec{\ell}\cdot(\vec{\ell}-2\vec{r}) - r^2\rho^2 - i\vec{g}\cdot\vec{r}\right\} d\vec{r} \qquad (C.10)$$

However, since $F(\vec{r},\rho)$ is periodic in $\vec{\ell}$, each term in Eq. (C.10) will give the same result as at $\vec{\ell}=0$. The number of terms in the sum equals the number of atoms in the crystal, N, say. Hence

$$F_{\vec{g}} = \frac{2}{\sqrt{\pi}}\frac{N}{V_c}\int_c \exp\left\{-r^2\rho^2 - i\vec{g}\cdot\vec{r}\right\} d\vec{r} \qquad (C.11)$$

where V_c is the volume of the crystal. Thus V_c/N is the volume of the

unit cell (V) and[66]

$$\frac{1}{\sqrt{\pi}}\int \exp\left\{-r^2\rho^2 - i\vec{g}\cdot\vec{r}\right\} d\vec{r} = \frac{\pi}{\rho^3} e^{-g^2/4\rho^2} \tag{C.12}$$

Thus, Eq. (C.11) becomes

$$F_{\vec{g}} = \frac{2\pi}{V}\frac{1}{\rho^3} e^{-g^2/4\rho^2} \tag{C.13}$$

Thus, from Eq. (C.9), one has

$$F(\vec{r},\rho) = \sum_{\vec{g}} \frac{2\pi}{V}\frac{1}{\rho^3} e^{-g^2/4\rho^2} e^{i\vec{g}\cdot\vec{r}} \tag{C.14}$$

Equating Eq. (C.14) with Eq. (C.8), gives

$$\frac{2}{\sqrt{\pi}}\sum_{\vec{\ell}} e^{-|\vec{\ell}-\vec{r}|^2\rho^2} = \frac{2\pi}{V}\sum_{\vec{g}}\frac{1}{\rho^3} e^{-g^2/4\rho^2} e^{i\vec{g}\cdot\vec{r}} \tag{C.15}$$

However, there exists the identity

$$\frac{2}{\sqrt{\pi}}\int_0^\infty e^{-z^2\rho^2} d\rho = \frac{1}{|z|} \tag{C.16}$$

Thus the left-hand side (L.H.S.) of Eq. (C.15) becomes, on integrating and using Eq. (C.16),

$$\text{L.H.S.} = \frac{2}{\sqrt{\pi}}\sum_{\vec{\ell}}\int_0^\infty e^{-|\vec{\ell}-\vec{r}|^2\rho^2} d\rho = \sum_{\vec{\ell}} \frac{1}{|\vec{\ell}-\vec{r}|} \tag{C.17}$$

Similarly, the right-hand side (R.H.S.) of Eq. (C.15) is

$$\begin{aligned}\text{R.H.S.} &= \frac{2\pi}{V}\int_0^\infty \sum_{\vec{g}}\frac{1}{\rho^3} e^{-g^2/4\rho^2} e^{i\vec{g}\cdot\vec{r}} d\rho \\ &= \frac{2\pi}{V}\int_0^G \sum_{\vec{g}}\frac{1}{\rho^3} e^{-g^2/4\rho^2} e^{i\vec{g}\cdot\vec{r}} d\rho \\ &\quad + \frac{2\pi}{V}\int_G^\infty \sum_{\vec{g}}\frac{1}{\rho^3} e^{-g^2/4\rho^2} e^{i\vec{g}\cdot\vec{r}} d\rho\end{aligned} \tag{C.18}$$

In the second integral (G to ∞), one can substitute from Eq. (C.15) so that Eq. (C.18) becomes

$$\begin{aligned}\text{R.H.S.} &= \frac{2\pi}{V}\int_0^G \sum_{\vec{g}}\frac{1}{\rho^3} e^{-g^2/4\rho^2} e^{i\vec{g}\cdot\vec{r}} d\rho \\ &\quad + \frac{2}{\sqrt{\pi}}\int_G^\infty \sum_{\vec{\ell}} e^{-|\vec{\ell}-\vec{r}|^2\rho^2} d\rho\end{aligned} \tag{C.19}$$

Now, the first integral in Eq. (C.19) can be evaluated as

$$\int_0^G \frac{1}{\rho^3} e^{-G^2/4\rho^2} e^{-i\vec{g}\cdot\vec{r}}\, d\rho = \frac{1}{2G^2} e^{-i\vec{g}\cdot\vec{r}} \frac{e^{-g^2/4G^2}}{g^2/4G^2} \qquad (C.20)$$

and the second integral in Eq. (C.14) can be written as

$$\frac{2}{\sqrt{\pi}} \int_G^\infty e^{-|\vec{\ell}-\vec{r}|^2\rho^2}\, d\rho = \frac{\mathrm{erfc}\{G|\vec{\ell}-\vec{r}|\}}{|\vec{\ell}-\vec{r}|} \qquad (C.21)$$

where erfc is the complementary error function defined by

$$\mathrm{erfc}(z) = \frac{2}{\sqrt{\pi}} \int_z^\infty e^{-t^2} dt = 1 - \mathrm{erf}(z) \qquad (C.22)$$

Combining Eqs. (C.17), (C.20), and (C.21) gives Ewald's result:

$$\sum_{\vec{\ell}} \frac{1}{|\vec{\ell}-\vec{r}|} = \frac{\pi}{V} \sum_{\vec{g}} \frac{e^{i\vec{g}\cdot\vec{r}} e^{-g^2/4G^2}}{g^2/4} + \sum_{\vec{\ell}} \frac{\mathrm{erfc}\{G|\vec{\ell}-\vec{r}|\}}{|\vec{\ell}-\vec{r}|} \qquad (C.23)$$

In the following, one uses the notation

$$\vec{R} \equiv \vec{\ell} - \vec{r}\,, \quad R = |\vec{R}| \qquad (C.24)$$

Thus, sums over $\vec{\ell}$ can be replaced by sums over $\vec{R}$. Also note that

$$\sum_{\vec{g}} e^{i\vec{g}\cdot\vec{r}} = \sum_{\vec{g}} e^{-i\vec{g}\cdot\vec{r}} = \sum_{\vec{g}} e^{-i\vec{g}\cdot\vec{R}} \qquad (C.25)$$

Thus, Eq. (C.23) may be written as

$$\sum_{\vec{R}} \frac{1}{R} = \frac{\pi}{V} \sum_{\vec{g}} \frac{e^{i\vec{g}\cdot\vec{r}} e^{-g^2/4G^2}}{g^2/4} + \sum_{\vec{R}} \frac{\mathrm{erfc}(GR)}{R} \qquad (C.26)$$

Note that in using Eq. (C.26), or any of its derivatives, one takes only the real part of the expression.[67] It is normally not necessary to specify this, because in a sum over all $\vec{g}$-values the imaginary parts will cancel. However, there would still remain a discontinuity along the imaginary axis in the case of $\vec{g} \to 0$. Dealing only with the real part of the expression removes this problem. (Full consideration will be given later to the cases of $\vec{R} \to 0$ and $\vec{g} \to 0$.)

Before proceeding further, it is illustrative to consider the physical basis for the Ewald expression (Eq. (C.26)). The method works by considering each point-charge sublattice (Bravais lattice) to be neutralized by a uniform charge distribution, in order to avoid a divergence in its potential. (If one sums over all the lattices in the crystal, these neutralizing distributions will cancel. This is as in the original method. If one does not sum over all the lattices, then correction terms will arise, as will be discussed later.) This distribution (point charges plus neutralizing charge) is then split into separate parts. To the neutralizing charge is added a lattice of Gaussian functions normalized to unity. The neutralizing charge plus the Gaussian functions will be called the first Ewald component. The second Ewald component consists of the point charges, neutralized by the Gaussian functions. In the final expression for the required potential, the Fourier representation of the potential represented by the first component is combined with the potential of the second component. An appropriate value for the half-width of the Gaussian is chosen so that both series converge rapidly. The details are as follows. First, consider a one-dimensional probability space, x, described by the Gaussian f(x):

$$f(x) = \frac{1}{\sqrt{2\pi}} \frac{1}{\sigma} e^{-\frac{(x-\mu)^2}{2\sigma^2}} \qquad (C.27)$$

where σ and μ are the standard deviation and mean, respectively. Associated with this is the distribution function, F(x), which gives the probability that a given result X is between - x and x.

$$F(x) \equiv Pr(|X| < x) = 2\int_0^x f(x)\, dx$$

$$= \sqrt{\frac{2}{\pi}} \frac{1}{\sigma} \int_0^x \exp\left\{ - \frac{(t-\mu)^2}{2\sigma^2} \right\} dt$$

$$= \sqrt{\frac{2}{\pi}} \frac{1}{\sigma} \int_0^x \exp\left\{ - \left(\frac{t-\mu}{\sqrt{2}\sigma} \right)^2 \right\} d\left(\frac{t}{\sqrt{2}\sigma} \right) \cdot \sqrt{2}\sigma$$

$$= \frac{2}{\sqrt{\pi}} \int_0^{\frac{x-\mu}{\sqrt{2}\sigma}} e^{-t^2} dt$$

$$= \operatorname{erf}\left(\frac{x-\mu}{\sqrt{2}\sigma} \right) \qquad \text{(C.28)}$$

But the half-width, η, for which $f(\pm\eta) = f(0)/e$, is $\eta \sqrt{2}\sigma$. Defining the reciprocal half-width, $G \equiv 1/\eta$, gives $F(x) = \operatorname{erf}\{G(x - \mu)\}$ and $f(x)$ can be re-expressed as

$$f(x) = \frac{G}{\sqrt{\pi}} e^{-G^2(x-\mu)^2} \qquad \text{(C.29)}$$

In a three-dimensional probability space, these results would become

$$f(\vec{r}) = \frac{G^3}{\pi^{3/2}} e^{-G^2(\vec{r}-\vec{\mu})^2} \qquad \text{(C.30)}$$

where $f(\vec{r})$ now represents a probability density and

$$F(\vec{r}) = \operatorname{erf}\{ G(\vec{r}-\vec{\mu}) \} \qquad \text{(C.31)}$$

Now, instead of thinking of a probability density, one can think in terms of the charge density, $\rho(\vec{r})$, at the point $\vec{r}$ due to a spherical charge distribution centered at $\vec{r}_\ell$, still with Gaussian reciprocal half-width G (in each of three dimensions). Thus, one has, analogous to Eq. (C.30)

$$\rho(\vec{r}) = \frac{G^3}{\pi^{3/2}} e^{-G^2(\vec{r}-\vec{r}_\ell)^2} \qquad \text{(C.32)}$$

This represents the Gaussian charge distribution which is to be added to the neutralizing charge distribution to form the above-mentioned first Ewald component. Thus, summing over ℓ, the first Ewald

component is

$$\rho_1(\vec{r}) = \frac{G^3}{\pi^{3/2}} \sum_{\vec{\ell}} e^{-G^2(\vec{r}-\vec{r}_\ell)^2} - \frac{1}{V} \qquad (C.33)$$

where V is the volume of the unit cell. Now, in line with the procedure described by Eqs. (C.9) - (C.15), this may be expanded in a Fourier series to give

$$\rho_1(\vec{r}) = \frac{1}{V} \sum_{\vec{g}} \exp\{-g^2/4G^2 + i\vec{g}\cdot\vec{r}\} - \frac{1}{V} \qquad (C.34)$$

To find the corresponding electrostatic potential $\Phi_1(\vec{r})$ at $\vec{r}$ due to $\rho_1(\vec{r})$, one notes that these are related by Poisson's equation.

i.e. $$\nabla^2 \Phi_1(\vec{r}) = -4\pi \rho_1(\vec{r}) \qquad (C.35)$$

Thus, integrating this ('i' occurs twice, which cancels the minus sign in Eq. (C.35)), one obtains

$$\Phi_1(\vec{r}) = \frac{\pi}{V} \sum_{\vec{g}} \frac{e^{-g^2/4G^2} e^{i\vec{g}\cdot\vec{r}}}{g^2/4} \qquad (C.36)$$

This is identical with the first term on the R.H.S. of Eq. (C.23).

Now consider $\rho_2(\vec{r})$ defined by

$$\rho_2(\vec{r}) = \sum_{\vec{\ell}} \left\{ \delta(\vec{r}-\vec{r}_\ell) - \frac{G^3}{\pi^{3/2}} e^{-G^2(\vec{r}-\vec{r}_\ell)^2} \right\} \qquad (C.37)$$

where the point-charge densities are represented by delta functions. This is the second Ewald component. This may be integrated to give

$$\Phi_2(\vec{r}) = \sum_{\vec{\ell}} \frac{\operatorname{erfc}\{G|\vec{r}-\vec{r}_\ell|\}}{|\vec{r}-\vec{r}_\ell|} \qquad (C.38)$$

which is seen to be identical with the second term on the R.H.S. of Eq. (C.23).

Now $\Phi_2(\vec{r})$ vanishes in the limit $G \to \infty$ and converges rapidly for

large G, whereas $\Phi_2(\vec{r})$ vanishes in the limit $G \to 0$ and converges rapidly for small G. Thus a proper choice of G ensures rapid convergence for both sums.

In practice, it is of little difficulty to find the appropriate G-value, as one can do sums in $\vec{R}$- and in $\vec{g}$-space over a few ions and simply adjust ('tune') G so that the sums are of opposite sign and of roughly equal magnitude. (A typical G-value is 0.5 $\mathring{A}^{-1}$.) Once this has been done, any sum can be made to converge by summing over a maximum of the equivalent of sixty-four unit cells. (4 ℓ-shells) (i.e. In Eq. (C.1) the maximum value for any ℓ_i would be $|\ell_i| = 4$.) This corresponds to a total of about 700 terms to be summed in each space ($\vec{R}$- and $\vec{g}$-). Conversely, a 'brute-force' sum, to get the same accuracy, would have to sum over roughly 2.4 million terms (corresponding to a sphere of radius 400 Å). Thus one has a saving in computer time by a factor of about 1700 using this method. It is also found in actual calculations that, if a given Ewald series converges for a given value of G, then the various expressions for the derivatives of that series will also converge for the same value of G.

Note that, despite the lack of difficulty in determining an appropriate G-value, as described above, some authors have given various prescriptions or recipes for G. For example, Weenk and Harwig[67] claim repeated success by taking $G = V^{-\frac{1}{3}}$, where V is the volume of the unit cell under consideration. For a typical V, this gives G of the order of 0.2 $\mathring{A}^{-1}$. Another method, reported by the same authors, is to take G as being the inverse of the minimum distance between the ions in the lattice. This gives $G = 0.5\ \mathring{A}^{-1}$, which is the same as the value found above by comparing the leading terms in the R- and g-space expansions.

C.2 Derivatives and Correction Terms

In most applications, including the present study, Eq. (C.26), per se, is not used because one is interested in such quantities as the electric field strength, which involve the derivative(s) of Eq. (C.26). This is significant in that Eq. (C.26), as is, has singularities in the limits $\vec{R} \to 0$ and $\vec{g} \to 0$. In cases where one sums over all the sublattices of a crystal, these singularities will cancel, due to the (electrical) neutrality of the crystal. However, there are some cases where there are quantities (e.g. electric dipole moments) where it is known a priori, from symmetry considerations, that, for a given sublattice, the quantity in question vanishes. It would therefore save computation time if one could sum only over the remaining lattices from which it is known there is a non-zero contribution. However, one can do this only if one knows how to deal with the singularities that would otherwise have been cancelled.

The method of dealing with this will be illustrated for the case of Eq. (C.26) and its first and second derivatives. For the work described here, one needs derivatives up to and including the fifth order. As the results for orders 3 to 5 are rather lengthy, they are given separately in Sec. (C.3).

First, considering that it is sufficient to deal only with the real part of (eq. (C.26), that equation may be written as

$$\sum_{\vec{R}} \frac{1}{R} = \frac{\pi}{V} \sum_{\vec{g}} \frac{e^{-g^2/4G^2} \cos(\vec{g}\cdot\vec{r})}{g^2/4} + \sum_{\vec{R}} \frac{\mathrm{erfc}(GR)}{R} \qquad (C.39)$$

If the sums are limited to $\vec{R} \neq 0$, $\vec{g} \neq 0$, one has

$$\sum_{\vec{R}\neq 0} \frac{1}{R} = \frac{\pi}{V} \sum_{\vec{g}\neq 0} \frac{e^{-g^2/4G^2} \cos(\vec{g}\cdot\vec{r})}{g^2/4} + \sum_{\vec{R}\neq 0} \frac{\mathrm{erfc}(GR)}{R} + \lim_{\vec{R}\to 0} \left\{ \frac{\mathrm{erfc}(GR)}{R} - \frac{1}{R} \right\} + \lim_{\vec{g}\to 0} \left\{ \frac{4\pi}{V} \left(\frac{1}{g^2} \right) \right\} \qquad (C.40)$$

where in the last term the limits for the exponential and cosine factors have been taken. Clearly, the limit $\vec{g} \to 0$ is discontinuous. This is why Eq. (C.40) can only be used in the case where one sums over a neutral crystal. If one is using Eq. (C.40) in a sum over a neutral crystal, the $\vec{R} \to 0$ limit will also cancel. Despite this, it is illustrative to evaluate this limit anyway since it does in fact converge, and because the method of calculating it is similar to that for derivatives where the corresponding $\vec{g} \to 0$ limit is continuous, thus allowing a sum over only some of the sublattices, if so desired. The technique is based on Eq. (C.22) and the fact that

$$\lim_{\vec{R}\to 0} \left\{ \operatorname{erf}(GR) \right\} = \lim_{\vec{R}\to 0} \left\{ \frac{2}{\sqrt{\pi}} GR\, e^{-G^2R^2} \right\} \qquad \text{(C.41)}$$

Thus, evaluating the $\vec{R} \to 0$ term in Eq. (C.40), one has

$$\lim_{\vec{R}\to 0} \left\{ \frac{\operatorname{erfc}(GR)}{R} - \frac{1}{R} \right\} = \lim_{\vec{R}\to 0} \left\{ -\frac{\operatorname{erf}(GR)}{R} \right\} = -\frac{2G}{\sqrt{\pi}} \qquad \text{(C.42)}$$

Now consider the case of the first derivative, $\frac{\partial}{\partial R_\alpha}$, of Eq. (C.39), where R_α, $\alpha = 1, 2, 3$ are the Cartesian components of the vector $\vec{R}$. To evaluate this, one uses the relation

$$\frac{\partial}{\partial R_\alpha} \left\{ \operatorname{erfc}(GR) \right\} = -\frac{2G}{\sqrt{\pi}} e^{-G^2R^2} \frac{\partial R}{\partial R_\alpha} \qquad \text{(C.43)}$$

The result is

$$\frac{\partial}{\partial R_\alpha} \left\{ \sum_{\vec{R}} \left(\frac{1}{R} \right) \right\} = -\frac{\pi}{V} \sum_{\vec{g}} \frac{e^{-g^2/4G^2}}{g^2/4} g_\alpha \sin(\vec{g}\cdot\vec{r}) - \sum_{\vec{R}} \frac{R_\alpha}{R^3} \left\{ \operatorname{erfc}(GR) + \frac{2}{\sqrt{\pi}} (GR) e^{-G^2R^2} \right\} \qquad \text{(C.44)}$$

Noting that $\lim_{\vec{g}\to 0} \sin(\vec{g}\cdot\vec{r}) = \lim_{\vec{g}\to 0} (\vec{g}\cdot\vec{r})$, $\lim_{\vec{g}\to 0} (\exp(-g^2/4G^2)) = 1$, and $\frac{\partial}{\partial R_\alpha}(1/R) = -R_\alpha/R^3$, this may be written as

$$\sum_{\vec{R}\neq 0}\left\{\frac{\partial}{\partial R_\alpha}\left(\frac{1}{R}\right)\right\} = -\frac{\pi}{V}\sum_{\vec{g}\neq 0}\frac{e^{-g^2/4G^2}}{g^2/4}\, g_\alpha \sin(\vec{g}\cdot\vec{r})$$
$$\rightarrow \sum_{\vec{R}\neq 0}\frac{R_\alpha}{R^3}\left\{\operatorname{erfc}(GR)+\frac{2}{\sqrt{\pi}}(GR)\,e^{-G^2R^2}\right\}$$
$$+\lim_{\vec{R}\to 0}\frac{R_\alpha}{R^3}\left\{[1-\operatorname{erfc}(GR)]-\frac{2}{\sqrt{\pi}}(GR)\,e^{-G^2R^2}\right\}$$
$$-\lim_{\vec{g}\to 0}\left\{\frac{4\pi}{V}\,\frac{g_\alpha(\vec{g}\cdot\vec{r})}{g^2}\right\}. \qquad (C.45)$$

From the use of Eqs. (C.22) and (C.41), it is seen that the $\vec{R}$-space limit is identically zero. As to the $\vec{g}$-space limit, it is of the form

$$\mathcal{L}im(\vec{g}) = \lim_{g\to 0}\left\{\frac{g_\alpha g_\beta r_\beta}{g^2}\right\}. \qquad (C.46)$$

Thus, in effect, one requires the value of $\lim_{g\to 0}(g_\alpha g_\beta/g^2)$. To determine this, realizing that its value depends on the direction in which the limit is approached, one may take the average value evaluated over all possible directions. That is, one can integrate the expression over a sphere of unit radius, and then get the average by dividing by 4π. (This procedure has been described by Misra and Lewis.[68]) Thus using $g_x = g\sin\theta\cos\phi$, $g_y = g\sin\theta\sin\phi$, $g_z = g\cos\theta$, one has

$$\lim_{\vec{g}\to 0}\left(\frac{g_\alpha g_\beta}{g^2}\right) = \frac{1}{4\pi}\int_{\theta=0}^{\pi}\int_{\phi=0}^{2\pi}\frac{g_\alpha g_\beta}{g^2}\sin\theta\, d\theta\, d\phi. \qquad (C.47)$$

Now if $\alpha \neq \beta$, the integrand will be an odd function and the result will be zero. If $\alpha = \beta$, the result will be 1/3, independent of α. Hence one can write

$$\lim_{\vec{g}\to 0}\left(\frac{g_\alpha g_\beta}{g^2}\right) = \frac{\delta_{\alpha\beta}}{3} \qquad (C.48)$$

where $\delta_{\alpha\beta}$ is the Kronecker delta function. Returning to Eq. (C.46), one has $\mathcal{L}im(\vec{g}) = r_\alpha/3$. Thus the final form for the first derivative, Eq. (C.45), is

$$\sum_{\vec{R}\neq 0}\left\{\frac{\partial}{\partial R_\alpha}\left(\frac{1}{R}\right)\right\} = -\frac{\pi}{V}\sum_{\vec{g}}\frac{e^{-g^2/4G^2}}{g^2/4}\, g_\alpha \sin(\vec{g}\cdot\vec{r})$$
$$-\sum_{\vec{R}\neq 0}\frac{R_\alpha}{R^3}\left\{\operatorname{erfc}(GR)+\frac{2}{\sqrt{\pi}}GR\,e^{-G^2R^2}\right\}-\frac{4\pi}{3V}r_\alpha \qquad (C.49)$$

Thus, in this form, Eq. (C.49) may be used for sums in which not all of the sublattices of a given crystal are involved, contrary to the situation with Eq. (C.40).

One may proceed in a similar fashion for the second derivative. Noting that

$$\frac{\partial^2}{\partial R_\alpha \partial R_\beta}\left(\frac{1}{R}\right) = \frac{3R_\alpha R_\beta - R^2\delta_{\alpha\beta}}{R^5} \qquad \text{(C.50)}$$

gives

$$\begin{aligned}\sum_{\vec{R}\neq 0}\left\{\frac{\partial^2}{\partial R_\alpha \partial R_\beta}\left(\frac{1}{R}\right)\right\} &= -\frac{\pi}{V}\sum_{\vec{g}\neq 0}\frac{e^{-g^2/4G^2}}{g^2/4}\, g_\alpha g_\beta \cos(\vec{g}\cdot\vec{r}) \\ &+ \sum_{\vec{R}\neq 0}\left[\frac{2G}{\sqrt{\pi}R^4}\left\{2(GR)^2 R_\alpha R_\beta + 3R_\alpha R_\beta - 2R^2\delta_{\alpha\beta}\right\}\right. \\ &\left. + \frac{\operatorname{erfc}(GR)}{R^5}\left\{3R_\alpha R_\beta - R^2\delta_{\alpha\beta}\right\}\right] - \frac{4\pi}{V}\lim_{\vec{g}\to 0}\left\{\frac{g_\alpha g_\beta}{g^2}\right\} \\ &+ \lim_{\vec{R}\to 0}\left[\frac{2G}{\sqrt{\pi}R^4}e^{-G^2R^2}\left\{2(GR)^2 R_\alpha R_\beta + 3R_\alpha R_\beta - 2R^2\delta_{\alpha\beta}\right\}\right. \\ &\left. - \operatorname{erf}(GR)\left\{3R_\alpha R_\beta - R^2\delta_{\alpha\beta}\right\}\cdot\frac{1}{R^5}\right] \qquad \text{(C.51)}\end{aligned}$$

where Eq. (C.22) has been used. Clearly, from Eq. (C.48), the $\vec{g}$-limit is $-\frac{4\pi}{3V}\delta_{\alpha\beta}$. Using Eq. (C.41), the $\vec{R}$-limit may be evaluated to give

$$\lim(\vec{R}) = \lim_{\vec{R}\to 0}\left\{\frac{4G^3}{\sqrt{\pi}}\frac{R_\alpha R_\beta}{R^2}\right\}. \qquad \text{(C.52)}$$

However, this is of the same form as Eq. (C.48), giving

$$\lim(\vec{R}) = \frac{4G^3}{3\sqrt{\pi}}\delta_{\alpha\beta}. \qquad \text{(C.53)}$$

Hence the final expression for the second derivative is

$$\begin{aligned}\sum_{\vec{R}\neq 0}\left\{\frac{\partial^2}{\partial R_\alpha \partial R_\beta}\left(\frac{1}{R}\right)\right\} &= -\frac{\pi}{V}\sum_{\vec{g}\neq 0}\frac{e^{-g^2/4G^2}}{g^2/4}\, g_\alpha g_\beta \cos(\vec{g}\cdot\vec{r}) \\ &+ \sum_{\vec{R}\neq 0}\left[\frac{2G}{\sqrt{\pi}R^4}e^{-G^2R^2}\left\{2(GR)^2 R_\alpha R_\beta + 3R_\alpha R_\beta - 2R^2\delta_{\alpha\beta}\right\}\right. \\ &\left. + \frac{\operatorname{erfc}(GR)}{R^5}\left\{3R_\alpha R_\beta - R^2\delta_{\alpha\beta}\right\}\right] + \frac{4\delta_{\alpha\beta}}{3}\left\{\frac{G^3}{\sqrt{\pi}} - \frac{\pi}{V}\right\}. \qquad \text{(C.54)}\end{aligned}$$

For the third- and higher-order derivatives, the procedure is now straight forward. First, no more $\vec{g}$-limit problems will be encountered, since the g-dimension of the numerator will be greater than that of the denominator, thus giving a $\vec{g}$-limit identically zero. Second, for the $\vec{R}$-limits, those of odd-order derivatives will also be identically zero

as was the case with the R-limit for the first derivative. The R-limits for even orders may be derived in a fashion similar to that used to obtain Eq. (C.48). This is done in Sec. C.3 .

C.3 Evaluation of Higher-Order Derivatives

C.3.1 Third Order

In the following, for convenience, one defines

$$\phi = GR \tag{C.55}$$

$$\{\vec{g}\} = \frac{\pi}{V} \sum_{\vec{g}} \frac{e^{-g^2/4G^2}}{g^2/4} \cos(\vec{g}\cdot\vec{r}) \tag{C.56}$$

$$\{\vec{R}\} = \sum_{\vec{R}} \frac{\operatorname{erfc}(\phi)}{R} \tag{C.57}$$

The symbolic notation, $D^3 \equiv \dfrac{\partial^3}{\partial R_\alpha \partial R_\beta \partial R_\gamma}$, is also used. Then the third-order derivatives become

$$D^3\{\vec{g}\} = \frac{\pi}{V} \sum \frac{e^{-g^2/4G^2}}{g^2/4} g_\alpha g_\beta g_\gamma \sin(\vec{g}\cdot\vec{r}) \tag{C.58}$$

where

$$\lim_{\vec{g}\to 0} D^3\{\vec{g}\} = 0 \tag{C.59}$$

and

$$D^3\{\vec{R}\} = \sum_{\vec{R}} \Big[-\frac{2}{\sqrt{\pi}} \frac{\phi}{R^7} e^{-\phi^2} \{15 + 10\phi^3 + 4\phi^5\} R_\alpha R_\beta R_\gamma + \frac{1}{R^5}\Big\{\frac{2}{\sqrt{\pi}} \phi e^{-\phi^2}(3+2\phi^3) + 3\operatorname{erfc}(\phi)\Big\}\{R_\alpha \delta_{\beta\gamma} + R_\beta \delta_{\alpha\gamma} + R_\gamma \delta_{\alpha\beta}\} - 15 \frac{R_\alpha R_\beta R_\gamma}{R^7} \operatorname{erfc}(\phi)\Big]. \tag{C.60}$$

The limit to be evaluated in this case is $\lim_{\vec{R}\to 0} [D^3\{\vec{R}\}]$, which, using

$$D^3\Big(\frac{1}{R}\Big) = \frac{3}{R^5}\left(R_\alpha \delta_{\beta\gamma} + R_\beta \delta_{\alpha\gamma} + R_\gamma \delta_{\alpha\beta}\right) - 15 \frac{R_\alpha R_\beta R_\gamma}{R^7} \tag{C.61}$$

is given by

$$\lim_{\vec{R}\to 0}\left[D^3\{\vec{R}\}\right] = \lim_{\vec{R}\to 0}\Big[-\frac{2}{\sqrt{\pi}} \frac{\phi}{R^7} e^{-\phi^2}\{15 + 10\phi^3 + 4\phi^5\} R_\alpha R_\beta R_\gamma + \frac{1}{R^5}\Big\{\frac{2}{\sqrt{\pi}} \phi e^{-\phi^2}(3+2\phi^3) + 3\operatorname{erfc}(\phi)\Big\}\{R_\alpha \delta_{\beta\gamma} + R_\beta \delta_{\alpha\gamma} + R_\gamma \delta_{\alpha\beta}\} - 15 \frac{R_\alpha R_\beta R_\gamma}{R^7} \operatorname{erfc}(\phi) + 15 \frac{R_\alpha R_\beta R_\gamma}{R^7} - \frac{3}{R^5}\{R_\alpha \delta_{\beta\gamma} + \cdots\}. \tag{C.62}$$

Using $\lim_{R\to 0} \operatorname{erf}(\phi) = \frac{2}{\sqrt{\pi}}\phi\, e^{-\phi^2}$ and $\operatorname{erfc}(\phi) = 1 - \operatorname{erf}(\phi)$, gives

$$\lim_{\vec{R}\to 0}\left[D^3\{\vec{R}\}\right] = \lim_{\vec{R}\to 0}\Big[-\frac{2}{\sqrt{\pi}}\frac{\phi e^{-\phi^2}}{R^7}\{15+10\phi^2+4\phi^4\}R_\alpha R_\beta R_\gamma$$
$$+\frac{1}{R^5}\Big\{\frac{2}{\sqrt{\pi}}\phi e^{-\phi^2}(3+2\phi^2)\Big\}\{R_\alpha\delta_{\beta\gamma}+\cdots\} - \frac{6}{\sqrt{\pi}}\frac{\phi e^{-\phi^2}}{R^5}\{R_\alpha\delta_{\beta\gamma}+\cdots\}$$
$$+\frac{30}{\sqrt{\pi}}\frac{\phi e^{-\phi^2}}{R^7}R_\alpha R_\beta R_\gamma\Big]$$
$$= \lim_{R\to 0}\Big[-\frac{2}{\sqrt{\pi}}e^{-\phi^2}\Big\{10G^4\left(\frac{R_\alpha R_\beta R_\gamma}{R^3}\right)+4G^5 R_\alpha\left(\frac{R_\beta R_\gamma}{R^2}\right)$$
$$+G^4\Big\{\left(\frac{R_\alpha}{R}\right)\delta_{\beta\gamma}+\left(\frac{R_\beta}{R}\right)\delta_{\alpha\gamma}+\left(\frac{R_\gamma}{R}\right)\delta_{\alpha\beta}\Big\}\Big] \qquad (C.63)$$

However, $\lim_{\vec{R}\to 0}(R_\alpha R_\beta R_\gamma/R^3) = 0$, since it is an odd function as explained in Sec. C.2 . The same is true for $\lim_{\vec{R}\to 0}(R_\alpha/R)$. The value of $\lim_{\vec{R}\to 0}(R_\beta R_\gamma/R^2)$ is finite, but it is multiplied by R_α, which is zero in the limit. Thus there are no correction terms whatever for the third derivative.

C.3.2 Fourth Order

In analogy to the previous notation, one has

$$D^4\{\vec{g}\} = \frac{\pi}{V}\sum_{\vec{g}}\frac{e^{-g^2/4G^2}}{g^2/4}g_\alpha g_\beta g_\gamma g_\epsilon \cos(\vec{g}\cdot\vec{r}) \qquad (C.64)$$

and

$$\lim_{\vec{g}\to 0}\left[D^4\{\vec{g}\}\right] = 0. \qquad (C.65)$$

Also

$$D^4\{\vec{R}\} = \sum_{\vec{R}}\Big[\Big\{\frac{2}{\sqrt{\pi}}\phi e^{-\phi^2}(105+70\phi^2+28\phi^4+8\phi^6)+105\operatorname{erfc}(\phi)\Big\}\frac{R_\alpha R_\beta R_\gamma R_\epsilon}{R^9}$$
$$-\Big\{\frac{2}{\sqrt{\pi}}\phi e^{-\phi^2}(15+10\phi^2+4\phi^4)+15\operatorname{erfc}(\phi)\Big\}\times$$
$$\{R_\alpha R_\beta\delta_{\gamma\epsilon}+R_\alpha R_\gamma\delta_{\beta\epsilon}+R_\alpha R_\epsilon\delta_{\beta\gamma}+R_\beta R_\gamma\delta_{\alpha\epsilon}+R_\beta R_\epsilon\delta_{\alpha\gamma}+R_\gamma R_\epsilon\delta_{\alpha\beta}\}\cdot\frac{1}{R^7}$$
$$+\Big\{\frac{2}{\sqrt{\pi}}\phi e^{-\phi^2}(3+2\phi^2)+3\operatorname{erfc}(\phi)\Big\}\{\delta_{\alpha\beta}\delta_{\gamma\epsilon}+\delta_{\alpha\gamma}\delta_{\beta\epsilon}+\delta_{\alpha\epsilon}\delta_{\beta\gamma}\}\cdot\frac{1}{R^5} \qquad (C.66)$$

Note that in the limit one has $e^{-\phi^2}\to 1$, and that the term involving ϕ^6 goes to zero. Also, one has

$$D^4\left(\frac{1}{R}\right) = \frac{3}{R^5}\left(\delta_{\alpha\beta}\delta_{\gamma\epsilon}+\delta_{\alpha\gamma}\delta_{\beta\epsilon}+\delta_{\alpha\epsilon}\delta_{\beta\gamma}\right)$$
$$-\frac{15}{R^7}\left(R_\alpha R_\beta\delta_{\gamma\epsilon}+\cdots\right)+\frac{105}{R^9}R_\alpha R_\beta R_\gamma R_\epsilon \qquad (C.67)$$

Hence

$$\lim_{\vec{R}\to 0}\left[\mathcal{D}^4\{\vec{R}\}\right] = \left\{\frac{2}{\sqrt{\pi}}\phi\left(105+70\phi^2+28\phi^4\right)+105\,\mathrm{erfc}(\phi)\right\}\frac{R_\alpha R_\beta R_\gamma R_\epsilon}{R^9}$$
$$-\left\{\frac{2}{\sqrt{\pi}}\phi\left(15+10\phi^2+4\phi^4\right)+15\,\mathrm{erfc}(\phi)\right\}\left\{R_\alpha R_\beta\delta_{\gamma\epsilon}+\cdots\right\}\cdot\frac{1}{R^7}$$
$$+\left\{\frac{2}{\sqrt{\pi}}\phi\left(3+2\phi^2\right)+3\,\mathrm{erfc}(\phi)\right\}\left\{R_\alpha R_\beta\delta_{\gamma\epsilon}+\cdots\right\}\cdot\frac{1}{R^5}$$
$$-\frac{3}{R^5}\left(\delta_{\alpha\beta}\delta_{\gamma\epsilon}+\cdots\right)+\frac{15}{R^7}\left(R_\alpha R_\beta\delta_{\gamma\epsilon}+\cdots\right)-\frac{105}{R^9}R_\alpha R_\beta R_\gamma R_\epsilon$$
$$=\frac{2}{\sqrt{\pi}}\frac{\phi^3}{R^5}\left\{\left(70+28\phi^2\right)\left(\frac{R_\alpha R_\beta R_\gamma R_\epsilon}{R^4}\right)-\left(10+4\phi^2\right)\left(\frac{R_\alpha R_\beta\delta_{\gamma\epsilon}+\cdots}{R^2}\right)\right.$$
$$\left.+\;2\left(\delta_{\alpha\beta}\delta_{\gamma\epsilon}+\cdots\right)\right. . \qquad \text{(C.68)}$$

However, using the methods of Sec. C.2, it is not difficult to show that

$$\lim_{\vec{R}\to 0}\left(\frac{R_\alpha R_\beta R_\gamma R_\epsilon}{R^4}\right)=\frac{1}{15}\left(\delta_{\alpha\beta}\delta_{\delta\epsilon}+\delta_{\alpha\gamma}\delta_{\beta\epsilon}+\delta_{\alpha\epsilon}\delta_{\beta\gamma}\right) \qquad \text{(C.69)}$$

and

$$\lim_{\vec{R}\to 0}\left(\frac{R_\alpha R_\beta\delta_{\gamma\epsilon}+R_\alpha R_\gamma\delta_{\beta\epsilon}+R_\alpha R_\epsilon\delta_{\beta\gamma}+R_\beta R_\gamma\delta_{\alpha\epsilon}+R_\beta R_\epsilon\delta_{\alpha\gamma}+R_\gamma R_\epsilon\delta_{\alpha\beta}}{R^2}\right)$$
$$=\frac{2}{3}\left(\delta_{\alpha\beta}\delta_{\gamma\epsilon}+\delta_{\alpha\gamma}\delta_{\beta\epsilon}+\delta_{\alpha\epsilon}\delta_{\beta\gamma}\right). \qquad \text{(C.70)}$$

Thus,

$$\lim_{\vec{R}\to 0}\left[\mathcal{D}^4\{\vec{R}\}\right]=\frac{2}{\sqrt{\pi}}\frac{\phi^3}{R^5}\left\{\left(\frac{70+28\phi^2}{15}\right)-\frac{2}{3}\left(10+4\phi^2\right)+2\right\}\times$$
$$\left\{\delta_{\alpha\beta}\delta_{\gamma\epsilon}+\cdots\right\}. \qquad \text{(C.71)}$$

The terms in ϕ^3 cancel and one is left with (recall $\phi \equiv GR$)

$$\lim_{\vec{R}\to 0}\left[\mathcal{D}^4\{\vec{R}\}\right]=-\frac{8G^5}{5\sqrt{\pi}}\left(\delta_{\alpha\beta}\delta_{\gamma\epsilon}+\delta_{\alpha\gamma}\delta_{\beta\epsilon}+\delta_{\alpha\epsilon}\delta_{\beta\gamma}\right). \qquad \text{(C.72)}$$

C.3.3 Fifth Order

One has

$$\mathcal{D}^5\{\vec{g}\}=\frac{\pi}{V}\sum_{\vec{g}\neq 0}\frac{e^{-g^2/4G^2}}{g^2/4}\,g_\alpha g_\beta g_\gamma g_\epsilon g_\eta\,\sin(\vec{g}\cdot\vec{r}) \qquad \text{(C.73)}$$

and

$$\lim_{\vec{g}\to 0}\left[\mathcal{D}^5\{\vec{g}\}\right]=0. \qquad \text{(C.74)}$$

Also

$$\lim_{\vec{R}\to 0}\left[\mathcal{D}^5\{\vec{R}\}\right]=0. \qquad \text{(C.75)}$$

The expression for $D^5\{\vec{R}\}$ is

$$
\begin{aligned}
D^5\{\vec{R}\} = &\left[-\frac{2}{\sqrt{\pi}}\phi e^{-\phi^2}\{16\phi^8 + 72\phi^6 + 252\phi^4 + 560\phi^2 + 945\}\right. \\
&\left. - 945\,\mathrm{erfc}(\phi)\right]\frac{R_\alpha R_\beta R_\gamma R_\epsilon R_\eta}{R^{11}} \\
&+\left[\frac{2}{\sqrt{\pi}}\phi e^{-\phi^2}\{8\phi^6 + 28\phi^4 + 70\phi^2 + 105\} + 105\,\mathrm{erfc}(\phi)\right]\times \\
&\left(R_\beta R_\gamma R_\epsilon \delta_{\alpha\eta} + R_\alpha R_\gamma R_\epsilon \delta_{\beta\eta} + R_\alpha R_\beta R_\epsilon \delta_{\gamma\eta} + R_\alpha R_\beta R_\gamma \delta_{\epsilon\eta}\right)\cdot\frac{1}{R^9} \\
&+\left[\frac{2}{\sqrt{\pi}}\phi e^{-\phi^2}\{8\phi^6 + 28\phi^4 + 70\phi^2 + 105\} + 105\,\mathrm{erfc}(\phi)\right]\times \\
&\left(R_\alpha R_\beta \delta_{\gamma\epsilon} + R_\alpha R_\gamma \delta_{\beta\epsilon} + R_\alpha R_\epsilon \delta_{\beta\gamma} + R_\beta R_\gamma \delta_{\alpha\epsilon} + R_\beta R_\epsilon \delta_{\alpha\gamma} + R_\gamma R_\epsilon \delta_{\alpha\beta}\right)\cdot\frac{R_\eta}{R^9} \\
&-\left[\frac{2}{\sqrt{\pi}}\phi e^{-\phi^2}(4\phi^4 + 10\phi^2 + 15) + 15\,\mathrm{erfc}(\phi)\right]\times \\
&\left(R_\beta \delta_{\alpha\eta}\delta_{\gamma\epsilon} + R_\alpha \delta_{\beta\eta}\delta_{\gamma\epsilon} + R_\gamma \delta_{\alpha\eta}\delta_{\beta\epsilon} + R_\alpha \delta_{\gamma\eta}\delta_{\beta\gamma} + R_\epsilon \delta_{\alpha\eta}\delta_{\beta\gamma} + R_\alpha \delta_{\epsilon\eta}\delta_{\beta\gamma}\right. \\
&\left. + R_\gamma \delta_{\beta\eta}\delta_{\alpha\epsilon} + R_\beta \delta_{\gamma\eta}\delta_{\alpha\epsilon} + R_\epsilon \delta_{\beta\eta}\delta_{\alpha\gamma} + R_\beta \delta_{\epsilon\eta}\delta_{\alpha\gamma} + R_\epsilon \delta_{\gamma\epsilon}\delta_{\alpha\beta} + R_\gamma \delta_{\epsilon\eta}\delta_{\alpha\beta}\right)\cdot\frac{1}{R^7} \\
&-\left[\frac{2}{\sqrt{\pi}}\phi e^{-\phi^2}\{4\phi^4 + 10\phi^2 + 15\} + 15\,\mathrm{erfc}(\phi)\right]\times \\
&\left(\delta_{\alpha\beta}\delta_{\gamma\epsilon} + \delta_{\alpha\gamma}\delta_{\beta\epsilon} + \delta_{\alpha\epsilon}\delta_{\beta\gamma}\right)\cdot\frac{R_\eta}{R^7}\,. \qquad \text{(C.76)}
\end{aligned}
$$

The use of all of the equations related to Ewald's method is based on the fact that the parameters A_n^m can be expressed in terms of derivatives of 1/r. Expressions giving these parameters in derivative form are provided in Table XIX.

TABLE XIX. Derivative expressions for the parameters A_n^m.

n	m	A_n^m
2	0	$\frac{1}{4}\ \frac{\partial^2}{\partial z^2}\left(\frac{1}{r}\right)$
2	2	$\frac{1}{4}\left(2\frac{\partial^2}{\partial x^2}+\frac{\partial^2}{\partial z^2}\right)\left(\frac{1}{r}\right)$
4	0	$\frac{1}{192}\ \frac{\partial^4}{\partial z^4}\left(\frac{1}{r}\right)$
4	2	$\frac{1}{48}\left(\frac{\partial^4}{\partial x^4}-\frac{\partial^4}{\partial y^4}\right)\left(\frac{1}{r}\right)$
4	4	$\frac{1}{48}\left(\frac{\partial^4}{\partial x^4}+\frac{\partial^4}{\partial y^4}-\frac{3}{4}\ \frac{\partial^4}{\partial z^4}\right)\left(\frac{1}{r}\right)$

Appendix D

DIPOLE MOMENTS FOR CeF_3 AND $NdCl_3.6H_2O$

The dipole moments as predicted by the PCID model (using Eq. (5.14)) are provided for a representative host from each of the series considered in this work. The results are given in Table XX for CeF_3 and in Table XXI for $NdCl_3.6H_2O$.

TABLE XX. Dipole moments (Å/e) for CeF_3 as predicted by the PCID model. The ions are numbered in the same order as they appear in Table XV. The three data columns give the x, y, z components, respectively, of the induced dipole moment vector.

A computer printout of the tabular data is given on the following page.

ION NO.	P(X)	P(Y)	P(Z)
1	.9280E-02	.2315E-03	.5513E-02
2	-.3768E-02	.2315E-03	-.9280E-02
3	-.5513E-02	.2315E-03	.3768E-02
4	-.9280E-02	-.2315E-03	-.5513E-02
5	.3768E-02	-.2315E-03	.9280E-02
6	.5513E-02	-.2315E-03	-.3768E-02
7	-.5513E-02	.2315E-03	-.9280E-02
8	-.3768E-02	.2315E-03	.5513E-02
9	.9280E-02	.2315E-03	.3768E-02
10	.5513E-02	-.2315E-03	.9280E-02
11	.3768E-02	-.2315E-03	-.5513E-02
12	-.9280E-02	-.2315E-03	-.3768E-02
13	0.	-.2315E-02	0.
14	0.	.2315E-02	0.
15	0.	-.2315E-02	0.
16	0.	.2315E-02	0.
17	0.	0.	0.
18	0.	0.	0.
19	0.	0.	.1623E+00
20	.1623E+00	0.	0.
21	-.1623E+00	0.	-.1623E+00
22	0.	0.	-.1623E+00
23	-.1623E+00	0.	0.
24	.1623E+00	0.	.1623E+00

TABLE XXI. Dipole moments (Å/e) for $NdCl_3.6H_2O$ as predicted by the PCID model. With reference to Table XVII, the ions are numbered according to the following ordering of sublattices: R, Cl(I), Cl(II), then the oxygens, followed by the hydrogens. The three data columns give the x, y, z components, respectively, of the induced dipole moment vector.

A computer printout of the tabular data is given on the following page.

ION NO.	P(X)	P(Y)	P(Z)
1	.1213E-04	.2431E-04	.9003E-01
2	-.1213E-04	-.2431E-04	-.9003E-01
3	-.3399E-02	-.3759E-02	.4279E-02
4	-.3553E-02	-.6617E-02	-.2449E-02
5	.1413E+00	-.3841E+00	.5306E+00
6	-.1413E+00	.3841E+00	-.5306E+00
7	-.1413E+00	.3841E+00	.5306E+00
8	.1413E+00	-.3841E+00	-.5306E+00
9	-.7643E-01	.1414E+00	.9495E-01
10	.7643E-01	-.1414E+00	-.9495E-01
11	.7643E-01	-.1414E+00	.9495E-01
12	-.7643E-01	.1414E+00	-.9495E-01
13	-.1110E+00	.8465E-01	-.1080E+00
14	.1110E+00	-.8465E-01	.1080E+00
15	.1110E+00	-.8465E-01	-.1080E+00
16	-.1110E+00	.8465E-01	.1080E+00
17	-.6708E-01	.7910E-01	.2335E+00
18	.6708E-01	-.7910E-01	-.2335E+00
19	.6708E-01	-.7910E-01	.2335E+00
20	-.6708E-01	.7910E-01	-.2335E+00
21	.4319E-01	-.7461E-01	-.1289E-01
22	-.4319E-01	.7461E-01	.1289E-01
23	-.4319E-01	.7461E-01	-.1289E-01
24	.4319E-01	-.7461E-01	.1289E-01
25	-.3856E-01	-.4793E-01	-.3468E-01
26	.3856E-01	.4793E-01	.3468E-01
27	.3856E-01	.4793E-01	-.3468E-01
28	-.3856E-01	-.4793E-01	.3468E-01
29	.5781E-01	-.3961E-01	.4874E-01
30	-.5781E-01	.3961E-01	-.4874E-01
31	-.5781E-01	.3961E-01	.4874E-01
32	.5781E-01	-.3961E-01	-.4874E-01
33	.6738E-01	-.4197E-01	.1284E-01
34	-.6738E-01	.4197E-01	-.1284E-01
35	-.6738E-01	.4197E-01	.1284E-01
36	.6738E-01	-.4197E-01	-.1284E-01
37	-.8102E-02	-.6915E-02	-.1088E+00
38	.8102E-02	.6915E-02	.1088E+00
39	.8102E-02	.6915E-02	-.1088E+00
40	-.8102E-02	-.6915E-02	.1088E+00
41	.2130E-01	-.1328E-01	-.9082E-01
42	-.2130E-01	.1328E-01	.9082E-01
43	-.2130E-01	.1328E-01	-.9082E-01
44	.2130E-01	-.1328E-01	.9082E-01

Appendix E

LISTING OF COMPUTER PROGRAMS

The computer programs used for the PCID model calculations for the two series (RF_3 and RTH) are given. Although the programs are not documented, an explanatory note is provided with each. This, plus an understanding of Appendix C (Ewald's method) should make them usable.

Program Index

Program FL01 calculates all quantities for the series RF_3 which do not depend on polarizability values. Initial data is read from a file which contains the information given in Table XV. The output is stored on a tape which is to be read by FL02. Both FL01 and FL02 deal only with second-order ($n = 2$) parameters.

```
      PROGRAM FLO1(INPUT,OUTPUT,TAPE15)
      DIMENSION R(3),G(3),XO(24),YO(24),ZO(24),P(24,3),
     1AN(4,3),ANAME(4),DIRQM(3,3),RECQM(3,3),QMAT1(24,3,3),
     2 QMAT3(24,3,3),DIREL(3),RECEL(3),DIRPO(3,3),
     3 TEMSEL(24,3),PNM(3,24,3),E(24,3),TR(3),TG(3),
     4 QMAT2(24,3,3),IESS(24,3,3),RECPO(3,3)
      COMMON/ONE/G,R,PROD
      COMMON/REPLY/ANS1,ANS2
      COMMON/ADD/QMAT3
      COMMON/CHADD/ISITE,TEMSEL
      COMMON/FIELD/E
      COMMON/OLLA/FACMOD
      COMMON/VOL/V,INUC
      DATA PIE/3.14159/
      DATA (AN(1,I),I=1,3)/7.186,7.186,7.352/
      DATA (AN(2,I),I=1,3)/7.112,7.112,7.279/
      DATA (AN(3,I),I=1,3)/7.061,7.061,7.218/
      DATA (AN(4,I),I=1,3)/7.030,7.030,7.119/
      DATA BET/60./
      DATA GEE,ILIM,INUC/0.5,4,2/
      DATA IPRIN/1/
C
C
C     1 = LA  2 = CE  3 = PR  4 = ND
C
C
C
      ANAME(1) = 2HLA
      ANAME(2) = 2HCE
      ANAME(3) = 2HPR
      ANAME(4) = 2HND
C
      ANUC = ANAME(INUC)
C
C
      BET = BET*(PIE/180.)
C
      DO 210 I = 1,24
      READ 215,(P(I,J),J=1,3)
  215 FORMAT(3(F7.4))
  210 CONTINUE
C
      DO 230 I = 1,24
      DO 229 J = 1,3
      READ228,(IESS(I,J,K),K=1,3)
  228 FORMAT(3(I2))
  229 CONTINUE
  230 CONTINUE
C
      NTB1 = 1
      NTB2 = 3
      C = AN(INUC,1)
      A = AN(INUC,2)
      B = AN(INUC,3)
```

```
      V = A*B*C*SIN(BET)
C
C
      DO 9999 ITRIP = 1,3
      IF(ITRIP.EQ.1) ISITE = 1
      IF(ITRIP.EQ.2) ISITE = 13
      IF(ITRIP.EQ.3) ISITE = 19
C
C
      AAN = P(ISITE,1)
      BBN = P(ISITE,2)
      CCN = P(ISITE,3)
      DO 999 I9 = 1,24
      ZO(I9) = P(I9,1) - AAN
      XO(I9) = P(I9,2) - BBN
      YO(I9) = P(I9,3) - CCN
C
      DO 510 L = 1,3
      DIREL(L) = 0.
      RECEL(L) = 0.
      DO 500 M = 1,3
      DIRPO(L,M) = 0.
      RECPO(L,M) = 0.
      DIRQM(L,M) = 0.
      RECQM(L,M) = 0.
  500 CONTINUE
  510 CONTINUE
C
      DO 100 I = 1,ILIM
      AL = FLOAT(I) - 1.
 2000 CONTINUE
      DO 95 J = 1,ILIM
      AM = FLOAT(J) - 1.
 1000 CONTINUE
      DO 90 K = 1,ILIM
      ANN = FLOAT(K) - 1.
      TL = 2.*PIE*AL
      TM = 2.*PIE*AM
      TN = 2.*PIE*ANN
   20 R(1) = (AL + XO(I9))*A - (AM + YO(I9))*B*COS(BET)
      R(2) = (AM + YO(I9))*B*SIN(BET)
      R(3) = (ANN + ZO(I9))*C
      G(1) = TL/A
      G(2) = TL*COS(BET)/(A*SIN(BET)) + TM/(B*SIN(BET))
      G(3) = TN/C
C
      TR(1) = R(1)
      TR(2) = R(2)
      TR(3) = R(3)
      TG(1) = G(1)
      TG(2) = G(2)
      TG(3) = G(3)
C
      RV = SQRT(R(1)**2 + R(2)**2 + R(3)**2)
```

```
      IF((ITRIP.EQ.3).AND.(RV.LE.3.0)) PRINT 2222,I9,AL,
     1AM,ANN,RV,(R(KK),KK=1,3)
 2222 FORMAT(1X,I2,2X,3(F3.0,1X),F10.5,1X,3(F10.5,1X))
      GV = SQRT(G(1)**2 + G(2)**2 + G(3)**2)
C
C
      SQP = SQRT(PIE)
      R2P = (RV**2)*SQP
      R4P = (RV**4)*SQP
      R5 = RV**5
      R6P = (RV**6)*SQP
      R7 = RV**7
      G2 = GV**2
      G3 = GEE**3
      G5 = GV**5
C
C
      GRV = GEE*RV
      GR2 = (GEE*RV)**2
      IF(GR2.GT.100.) GO TO 888
      EXPD = EXP(-GR2)
      GO TO 889
  888 EXPD = 0.
  889 CONTINUE
C
      CALL ERFN(GRV,ERROR)
C
      DO 776 L = 1,3
C
      IF(RV.EQ.0.) GO TO 80
      DIREL(L) = DIREL(L) + R(L)*ERROR/(RV**3) + 2.*GEE
     1 *R(L)*EXPD/R2P
      IF(ISITE.NE.19) GO TO 80
      DO 801 M = 1,3,2
      IF(L.EQ.M) DEL1 = 1.
      IF(L.NE.M) DEL1 = 0.
      DIRPO(M,L) = DIRPO(M,L) - ((30.*GEE)/R6P + 20.*G3/
     1 R4P + (8.*G5/R2P))*(TR(L)*(TR(M)**2))*EXPD + (((6.*
     2 GEE)/R4P)*EXPD + ((4.*G3)/R2P)*EXPD + (3.*ERROR)/
     3 R5)*(2.*TR(M)*DEL1 + TR(L)) - (15.*TR(L)*(TR(M)
     4**2)*ERROR)/R7
  801 CONTINUE
   80 CONTINUE
C
      DO 775 M = 1,3
      IF(L.EQ.M) DELTA = 1.
      IF(L.NE.M) DELTA = 0.
C
      IF(RV.EQ.0.) GO TO 81
      DIRQM(L,M) = DIRQM(L,M) + 4.*(GEE**3)*R(L)*R(M)*
     1EXPD/((RV**2)*SQRT(PIE)) + 6.*GEE*R(L)*R(M)*EXPD/
     2((RV**4)* - 2.*GEE*EXPD*DELTA/((RV**2)*SQRT(PIE))
     3SQRT(PIE)) + (3.*R(L)*R(M)/(RV**2) - DELTA)*
     4(ERROR/(RV**3))
```

```
      GO TO 777
   81 DIRQM(L,M) = DIRQM(L,M) + 4.*(GEE**3)*DELTA/(3.*
     1SQRT(PIE))
  777 CONTINUE
  775 CONTINUE
  776 CONTINUE
C
C
      IF((AL.EQ.0.).AND.(AM.EQ.0.).AND.(ANN.EQ.0.))GGG = 0.
      IF(GGG.EQ.0.) GO TO 745
      GRAT = (GV/(2.*GEE))**2
      IF(GRAT.GT.100.)GO TO 788
      EXPG = EXP(-GRAT)
      GO TO 789
  788 EXPG = 0.
  789 CONTINUE
C
      CALL DOTPC(PROPC)
      CALL DOTEL(PROEL)
C
  745 CONTINUE
C
      DO 760 L = 1,3
      IF(GGG.EQ.0.) GO TO 755
      RECEL(L) = RECEL(L) + (PIE/V)*4.*G(L)*PROEL*EXPG/G2
      IF(ISITE.NE.19) GO TO 755
C
      DO 754 M = 1,3,2
      RECPO(M,L) = RECPO(M,L) + (4.*PIE/V)*TG(L)*(TG(M)
     1.**2)*PROEL*EXPG/G2
  754 CONTINUE
  755 CONTINUE
C
      DO 750 M = 1,3
      IF(L.EQ.M) DELTA = 1.
      IF(L.NE.M) DELTA = 0.
      IF(GGG.EQ.0.) GO TO 54
      RECQM(L,M) = RECQM(L,M) - (PIE/V)*4.*G(L)*G(M)*PROPC
     1*EXPG/(GV**2)
      GO TO 778
   54 RECQM(L,M) = RECQM(L,M) - 4.*PIE*DELTA/(3.*V)
  778 CONTINUE
  750 CONTINUE
  760 CONTINUE
C
C
C
      GGG = 1.
      IF(ANN.LE.0.) GO TO 90
      ANN = - ANN
      TN = - TN
      GO TO 20
   90 CONTINUE
      IF(AM.LE.0.) GO TO 95
```

```
      AM = - AM
      TM = - TM
      GO TO 1000
   95 CONTINUE
      IF(AL.LE.0.) GO TO 100
      AL = - AL
      TL = - TL
      GO TO 2000
  100 CONTINUE
C
C
      DO 340 L = 1,3
      TEMSEL(I9,L) = DIREL(L) + RECEL(L)
      IF(ITRIP.NE.3) GO TO 349
      PNM(1,I9,L) = DIRPO(1,L) + RECPO(1,L)
      PNM(3,I9,L) = DIRPO(3,L) + RECPO(3,L)
  349 CONTINUE
      DO 330 M = 1,3
      IF(ITRIP.EQ.2) GO TO 350
      IF(ITRIP.EQ.3) GO TO 360
      QMAT1(I9,L,M) = DIRQM(L,M) + RECQM(L,M)
      GO TO 370
  350 QMAT2(I9,L,M) = DIRQM(L,M) + RECQM(L,M)
      GO TO 370
  360 QMAT3(I9,L,M) = DIRQM(L,M) + RECQM(L,M)
  370 CONTINUE
  330 CONTINUE
  340 CONTINUE
C
C
  999 CONTINUE
C
      IF(ITRIP.EQ.3) CALL CHARE
      CALL CHAEL
C
 9999 CONTINUE
C
      DO 3200 I = 1,24
      DO 3190 J = 1,3
      WRITE(15,3180)(QMAT1(I,J,K),K=1,3)
      WRITE(15,3180)(QMAT2(I,J,K),K=1,3)
      WRITE(15,3180)(QMAT3(I,J,K),K=1,3)
 3190 CONTINUE
 3200 CONTINUE
 3180 FORMAT(3(F15.8))
      WRITE(15,3180)(E(1,I),I=1,3)
      WRITE(15,3180)(E(13,I),I=1,3)
      WRITE(15,3180)(E(19,I),I=1,3)
C
      IF(IPRIN.EQ.0) GO TO 3111
C
      DO 3170 I = 1,24
      WRITE(15,3180)(PNM(1,I,J),J=1,3)
      WRITE(15,3180)(PNM(3,I,J),J=1,3)
```

```
 3170 CONTINUE
      WRITE(15,3160)FACMOD,V,INUC,ANS1,ANS2
 3160 FORMAT(2(F15.8),I1,2(F10.4))
C
 3111 CONTINUE
C
      DO 3120 I = 1,24
      DO 3119 J = 1,3
      WRITE(15,3118)(IESS(I,J,K),K=1,3)
 3119 CONTINUE
 3120 CONTINUE
 3118 FORMAT(3(I2))
C
C
C
      STOP
      END
      SUBROUTINE CHARE
      DIMENSION QMAT3(24,3,3),TE(2,2)
      COMMON/ADD/QMAT3
      COMMON/OLLA/FACMOD
      COMMON/REPLY/ANS1,ANS2
C
      TE(1,1) = 0.
      TE(1,2) = 0.
      TE(2,1) = 0.
      TE(2,2) = 0.
C
      DO 10 I = 1,18
      TE(1,1) = TE(1,1) + QMAT3(I,3,3)
      TE(2,1) = TE(2,1) + QMAT3(I,3,3) + 2.*QMAT3(I,1,1)
   10 CONTINUE
C
      DO 15 I = 19,24
      TE(1,2) = TE(1,2) + QMAT3(I,3,3)
      TE(2,2) = TE(2,2) + QMAT3(I,3,3) + 2.*QMAT3(I,1,1)
   15 CONTINUE
C
      E1 = TE(1,1)*(-1.) + TE(1,2)*(+3.)
      E2 = TE(2,1)*(-1.) + TE(2,2)*(+3.)
C
      AK1 = -12.*(1534.**3)/(5.*(32200.**2)*40000.)
      AK2 = 16.*1534./(245.*32200.)
      RCAP2 = -0.07*(0.529**2)
      R2 = 0.785*(0.529**2)
      AKAY = AK1*R2 + AK2*RCAP2
      GAM = 0.33
      CONV = 116195.62
      FACMOD = CONV*AKAY*GAM*29.9
      ANS1 = - 0.25*FACMOD*E1
      ANS2 = - 0.25*FACMOD*E2
C
      RETURN
      END
```

```
      SUBROUTINE CHAEL
      DIMENSION TE(2,3),E(24,3),TEMSEL(24,3)
      COMMON/CHADD/ISITE,TEMSEL
      COMMON/FIELD/E
C
      DO 5 I = 1,2
      DO 4 J = 1,3
      TE(I,J) = 0.
    4 CONTINUE
    5 CONTINUE
C
      DO 10 I = 1,18
      DO  8 J = 1,3
      TE(1,J) = TE(1,J) + TEMSEL(I,J)
    8 CONTINUE
   10 CONTINUE
C
      DO 15 I = 19,24
      DO 14 J = 1,3
      TE(2,J) = TE(2,J) + TEMSEL(I,J)
   14 CONTINUE
   15 CONTINUE
C
      DO 20 I = 1,3
      E(ISITE,I) = TE(1,I)*(-1.) + TE(2,I)*(+3.)
   20 CONTINUE
C
C
      RETURN
      END
      SUBROUTINE ERFN(GRV,ERROR)
      DATA  P/0.3275911/
      DATA A1/0.254829592/
      DATA A2/-0.284496736/
      DATA A3/1.421413741/
      DATA A4/-1.453152027/
      DATA A5/1.061405429/
C
      T = 1./(1. + P*GRV)
      IF ( GRV.GT.10. ) GO TO 50
      EX = EXP(-(GRV**2))
      GO TO 60
   50 EX = 0.
   60 CONTINUE
      SUM = A1*T + A2*T**2 + A3*T**3 + A4*T**4 + A5*T**5
      ERROR = 1. - SUM*EX
      ERROR = 1. - ERROR
      RETURN
      END
      SUBROUTINE DOTPC(PROPC)
      DIMENSION R(3),G(3),PRO(3)
      COMMON/ONE/G,R,PROD
C
      SPRO = 0.
```

```
      DO 10 I = 1,3
      PRO(I) = G(I)*R(I)
      SPRO = SPRO + PRO(I)
   10 CONTINUE
      PROPC = COS(SPRO)
      RETURN
      END
      SUBROUTINE DOTEL(PROEL)
      DIMENSION R(3),G(3),PRO(3)
      COMMON/ONE/G,R,PROD
C
      SPRO = 0.
      DO 10 I = 1,3
      PRO(I) = G(I)*R(I)
      SPRO = SPRO + PRO(I)
   10 CONTINUE
      PROEL = SIN(SPRO)
      RETURN
      END
```

Program FL02 reads the output from FL01 and proceeds to calculate the induced dipole moments at the various ion sites. The external library subroutine LEQT2F solves the required set of simultaneous linear equations. The spin-Hamiltonian parameters are then calculated.

The reason for splitting up FL01 and FL02 is that the former may be run once and the data stored permanently, while FL02 requires numerous runs in order to obtain the appropriate polarizability values.

```
      PROGRAM FLO2(INPUT,OUTPUT,TAPE15,TAPE19)
      DIMENSION WK(40),IESS(24,3,3),ALIV(24,3,3),
     1 QMAT2(24,3,3),QMAT3(24,3,3),QMDEL1(24,3,3),
     2 QMDEL3(24,3,3),PROD1(24,3,3),PROD2(24,3,3),
     3 ESS(24,3,3),QUPE(5,5),DIMO(24,3),ELF(5),E(24,3),
     4 DEL(24,3),B20EXP(4),B22EXP(4),QMAT1(24,3,3),
     5 REDO(3,3),QMDEL2(24,3,3),PROD3(24,3,3),
     6 PNM(3,24,3)
      EXTERNAL LEQT2F
      DATA (B20EXP(I),I=1,4)/0.693,0.735,0.773,0.795/
      DATA (B22EXP(I),I=1,4)/-0.085,-0.084,-0.081,-0.149/
C
      DO 3200 I = 1,24
      DO 3190 J = 1,3
      READ(15,3180)(QMAT1(I,J,K),K=1,3)
      READ(15,3180)(QMAT2(I,J,K),K=1,3)
      READ(15,3180)(QMAT3(I,J,K),K=1,3)
 3190 CONTINUE
 3200 CONTINUE
 3180 FORMAT(3(F15.8))
      READ(15,3180)(E(1,I),I=1,3)
      READ(15,3180)(E(13,I),I=1,3)
      READ(15,3180)(E(19,I),I=1,3)
      DO 3170 I = 1,24
      READ(15,3180)(PNM(1,I,J),J=1,3)
      READ(15,3180)(PNM(3,I,J),J=1,3)
 3170 CONTINUE
      READ(15,3160)FACMOD,V,INUC,ANS1,ANS2
 3160 FORMAT(2(F15.8),I1,2(F10.4))
C
      WRITE(19,3305)INUC
 3305 FORMAT(1X,*TRIFLUORIDE RESULTS  INUC = *,I1,//)
      DO 810 I = 1,24
      DO 800 J = 1,3
      DEL(I,J) = 0.
  800 CONTINUE
  810 CONTINUE
      DEL(1,1) = 1.
      DEL(13,2) = 1.
      DEL(19,3) = 1.
C
C
C
      DO 5 I = 1,24
      DO 4 J = 1,3
      READ (15,6)(IESS(I,J,K),K=1,3)
    6 FORMAT(3(I2))
    4 CONTINUE
    5 CONTINUE
C
      DO 9 I = 1,24
      ESS(I,1,1) = FLOAT(IESS(I,2,2))
      ESS(I,1,2) = FLOAT(IESS(I,2,3))
      ESS(I,1,3) = FLOAT(IESS(I,2,1))
```

```
      ESS(I,2,1) = FLOAT(IESS(I,3,2))
      ESS(I,2,2) = FLOAT(IESS(I,3,3))
      ESS(I,2,3) = FLOAT(IESS(I,3,1))
      ESS(I,3,1) = FLOAT(IESS(I,1,2))
      ESS(I,3,2) = FLOAT(IESS(I,1,3))
      ESS(I,3,3) = FLOAT(IESS(I,1,1))
    9 CONTINUE
C
C
C
      DO 294 IGR = 1,1
      ALFL1 = 0.01438 + 0.00001*FLOAT(IGR)
      ALFL2 = ALFL1 + 0.0000
      ALFL3 = ALFL1
      DO 293 IFR = 1,1
      ALLA1 = 2.493 + 0.002*FLOAT(IFR)
      ALLA2 = ALLA1
      ALLA3 = ALLA1
C
      ELF(1) = E(1,1)
      ELF(2) = E(1,2)
      ELF(3) = E(1,3)
      ELF(4) = E(13,2)
      ELF(5) = E(19,3)
C
      DO 19 I = 1,24
      DO 18 J = 1,3
      DO 17 K = 1,3
      ALIV(I,J,K) = 0.
   17 CONTINUE
   18 CONTINUE
   19 CONTINUE
C
      DO 20 I = 1,18
      ALIV(I,1,1) = 1./ALFL1
      ALIV(I,2,2) = 1./ALFL2
      ALIV(I,3,3) = 1./ALFL3
   20 CONTINUE
      DO 15 I = 19,24
      ALIV(I,1,1) = 1./ALLA1
      ALIV(I,2,2) = 1./ALLA2
      ALIV(I,3,3) = 1./ALLA3
   15 CONTINUE
C
      DO 35 I = 1,3
      DO 30 J = 1,3
      DO 25 K = 1,24
      QMDEL1(K,I,J) = ALIV(K,I,J)*DEL(K,1) - QMAT1(K,I,J)
      QMDEL2(K,I,J) = ALIV(K,I,J)*DEL(K,2) - QMAT2(K,I,J)
      QMDEL3(K,I,J) = ALIV(K,I,J)*DEL(K,3) - QMAT3(K,I,J)
   25 CONTINUE
   30 CONTINUE
   35 CONTINUE
C
```

```
C
      DO 500 I = 1,24
      DO 495 J = 1,3
      DO 490 K = 1,3
      PROD1(I,J,K) = 0.
      PROD2(I,J,K) = 0.
      PROD3(I,J,K) = 0.
  490 CONTINUE
  495 CONTINUE
  500 CONTINUE
C
      DO 485 I = 1,5
      DO 480 J = 1,5
      QUPE(I,J) = 0.
  480 CONTINUE
  485 CONTINUE
C
C
      DO 55 I = 1,24
      DO 50 J = 1,3
      DO 45 K = 1,3
      DO 40 L = 1,3
      PROD1(I,J,K) = PROD1(I,J,K) + QMDEL1(I,J,L)*ESS(I,L,K)
      PROD2(I,J,K) = PROD2(I,J,K) + QMDEL2(I,J,L)*ESS(I,L,K)
      PROD3(I,J,K) = PROD3(I,J,K) + QMDEL3(I,J,L)*ESS(I,L,K)
   40 CONTINUE
   45 CONTINUE
   50 CONTINUE
   55 CONTINUE
C
C
      DO 70 I = 1,12
      DO 65 J = 1,3
      QUPE(4,J) = QUPE(4,J) + PROD2(I,2,J)
      QUPE(5,J) = QUPE(5,J) + PROD3(I,3,J)
      DO 60 K = 1,3
      QUPE(J,K) = QUPE(J,K) + PROD1(I,J,K)
   60 CONTINUE
   65 CONTINUE
   70 CONTINUE
C
      DO 85 I = 13,16
      QUPE(4,4) = QUPE(4,4) + PROD2(I,2,2)
      QUPE(5,4) = QUPE(5,4) + PROD3(I,3,2)
      DO 80 J = 1,3
      QUPE(J,4) = QUPE(J,4) + PROD1(I,J,2)
   80 CONTINUE
   85 CONTINUE
C
      DO 95 I = 19,24
      QUPE(4,5) = QUPE(4,5) + PROD2(I,2,3)
      QUPE(5,5) = QUPE(5,5) + PROD3(I,3,3)
      DO 90 J = 1,3
      QUPE(J,5) = QUPE(J,5) + PROD1(I,J,3)
```

```
   90 CONTINUE
   95 CONTINUE
C
      IDGT = 0
C
      CALL LEQT2F(QUPE,1,5,5,ELF,IDGT,WK,IER)
C
      DO 200 I = 1,24
      DO 195 J = 1,3
      DIMO(I,J) = 0.
  195 CONTINUE
  200 CONTINUE
C
      DO 110 I = 1,12
      DO 105 J = 1,3
      DO 100 K = 1,3
      DIMO(I,J) = DIMO(I,J) + ESS(I,J,K)*ELF(K)
  100 CONTINUE
  105 CONTINUE
  110 CONTINUE
C
      ELF(1) = 0.
      ELF(2) = ELF(4)
      ELF(3) = 0.
C
C
      DO 125 I = 13,16
      DO 120 J = 1,3
      DO 115 K = 1,3
      DIMO(I,J) = DIMO(I,J) + ESS(I,J,K)*ELF(K)
  115 CONTINUE
  120 CONTINUE
  125 CONTINUE
C
      ELF(1) = 0.
      ELF(2) = 0.
      ELF(3) = ELF(5)
C
      DO 140 I = 19,24
      DO 135 J = 1,3
      DO 130 K = 1,3
      DIMO(I,J) = DIMO(I,J) + ESS(I,J,K)*ELF(K)
  130 CONTINUE
  135 CONTINUE
  140 CONTINUE
C
C
      DO 2222 I = 1,24
      WRITE(19,2223)(DIMO(I,J),J=1,3)
 2223 FORMAT(1X,3(E10.3,3X))
 2222 CONTINUE
C
C
C
```

```
      EPO1 = 0.
      EPO2 = 0.
      DO 160 I = 1,24
      DO 155 J = 1,3
      EPO1 = EPO1 + DIMO(I,J)*PNM(3,I,J)
      EPO2 = EPO2 + DIMO(I,J)*(2.*PNM(1,I,J) + PNM(3,I,J))
  155 CONTINUE
  160 CONTINUE
C
      ANS21 = - 0.25*FACMOD*EPO1
      ANS22 = - 0.25*FACMOD*EPO2
C
      BTOTO = ANS1 + ANS21
      BTOT2 = ANS2 + ANS22
      DIFFO = BTOTO - B20EXP(INUC)
      DIFF2 = BTOT2 - B22EXP(INUC)
C
      BOEX = B20EXP(INUC)
      B2EX = B22EXP(INUC)
      FAC11 = (BTOTO - BOEX)**2
      FAC21 = (BTOT2 - B2EX)**2
      FACDE = BOEX**2 + B2EX**2
      FUNC = (FAC11*(B2EX**2) + FAC21*(BOEX**2))/FACDE
C
C
      IF(FUNC.GT.0.00005) GO TO 293
      WRITE(19,3311) ALLA1,ALLA2,ALLA3,ALFL1,ALFL2,ALFL3
 3311 FORMAT(1X,3(F6.3,2X),3(F11.7,2X))
      WRITE(19,3322) ANS1,ANS21,BTOTO,BOEX,DIFFO
      WRITE(19,3333) ANS2,ANS22,BTOT2,B2EX,DIFF2,FUNC
 3322 FORMAT(1X,5(F9.4,2X))
 3333 FORMAT(1X,5(F9.4,2X),E10.3,/)
C
C
  293 CONTINUE
  294 CONTINUE
  295 CONTINUE
C
      STOP
      END
```

Program FL014 is similar to FL01 except that it deals with fourth-order parameters.

```
      PROGRAM FLO14(INPUT,OUTPUT,TAPE16)
      DIMENSION R(3),G(3),XO(24),YO(24),ZO(24),P(24,3),
     1AN(4,3),ANAME(4),DIRQM(3,3),RECQM(3,3),QMAT1(24,3,3),
     2 QMAT3(24,3,3),DIREL(3),RECEL(3),DIRPO(3,3),
     3 PNM(3,24,3),E(24,3),TR(3),TG(3),QMNEW(24,3),
     4 QMAT2(24,3,3),IESS(24,3,3),RECPO(3,3)
      COMMON/ONE/G,R,PROD
      COMMON/REPLY/ANS1,ANS2,ANS3
      COMMON/ADD/QMNEW
      COMMON/QLLA/FACMOD
      COMMON/VOL/V,INUC
      DATA PIE/3.14159/
      DATA (AN(1,I),I=1,3)/7.186,7.186,7.352/
      DATA (AN(2,I),I=1,3)/7.112,7.112,7.279/
      DATA (AN(3,I),I=1,3)/7.061,7.061,7.218/
      DATA (AN(4,I),I=1,3)/7.030,7.030,7.119/
      DATA BET/60./
      DATA GEE,ILIM,INUC/0.5,4,4/
C
C
C     1 = LA  2 = CE  3 = PR  4 = ND
C
C
C
      ANAME(1) = 2HLA
      ANAME(2) = 2HCE
      ANAME(3) = 2HPR
      ANAME(4) = 2HND
C
      ANUC = ANAME(INUC)
C
C
      BET = BET*(PIE/180.)
C
      DO 210 I = 1,24
      READ 215,(P(I,J),J=1,3)
  215 FORMAT(3(F7.4))
  210 CONTINUE
C
      DO 230 I = 1,24
      DO 229 J = 1,3
      READ228,(IESS(I,J,K),K=1,3)
  228 FORMAT(3(I2))
  229 CONTINUE
  230 CONTINUE
C
      NTB1 = 1
      NTB2 = 3
      C = AN(INUC,1)
      A = AN(INUC,2)
      B = AN(INUC,3)
      V = A*B*C*SIN(BET)
C
C
```

```
      DO 9999 ITRIP = 1,3
      IF(ITRIP.EQ.1) ISITE = 1
      IF(ITRIP.EQ.2) ISITE = 13
      IF(ITRIP.EQ.3) ISITE = 19
C
C
      AAN = P(ISITE,1)
      BBN = P(ISITE,2)
      CCN = P(ISITE,3)
      DO 999 I9 = 1,24
      ZO(I9) = P(I9,1) - AAN
      XO(I9) = P(I9,2) - BBN
      YO(I9) = P(I9,3) - CCN
C
      DO 510 L = 1,3
      DIRQM(L) = 0.
      RECQM(L) = 0.
      DO 500 M = 1,3
      DIRPO(L,M) = 0.
      RECPO(L,M) = 0.
  500 CONTINUE
  510 CONTINUE
C
      DO 100 I = 1,ILIM
      AL = FLOAT(I) - 1.
 2000 CONTINUE
      DO 95 J = 1,ILIM
      AM = FLOAT(J) - 1.
 1000 CONTINUE
      DO 90 K = 1,ILIM
      ANN = FLOAT(K) - 1.
      TL = 2.*PIE*AL
      TM = 2.*PIE*AM
      TN = 2.*PIE*ANN
   20 R(1) = (AL + XO(I9))*A - (AM + YO(I9))*B*COS(BET)
      R(2) = (AM + YO(I9))*B*SIN(BET)
      R(3) = (ANN + ZO(I9))*C
      G(1) = TL/A
      G(2) = TL*COS(BET)/(A*SIN(BET)) + TM/(B*SIN(BET))
      G(3) = TN/C
C
      TR(1) = R(1)
      TR(2) =  R(2)
      TR(3) = R(3)
      TG(1) = G(1)
      TG(2) =  G(2)
      TG(3) = G(3)
C
      RV = SQRT(R(1)**2 + R(2)**2 + R(3)**2)
      GV = SQRT(G(1)**2 + G(2)**2 + G(3)**2)
C
C
      SQP = SQRT(PIE)
      R5 = RV**5
```

```
      R7 = RV**7
      R9 = RV**9
      R11 = RV**11
      G2 = GV**2
      G3 = GEE**3
      G5 = GV**5
C
C
      GRV = GEE*RV
      GR2 = (GEE*RV)**2
      GR4 = GR2**2
      GR6 = GR2**3
      GR8 = GR2**4
      IF(GR2.GT.100.) GO TO 888
      EXPD = EXP(-GR2)
      GO TO 889
  888 EXPD = 0.
  889 CONTINUE
C
      CALL ERFN(GRV,ERROR)
C
      FRONT = 2.*GRV*EXPD/SQP
C
      DO 776 L = 1,3
C
      IF(RV.EQ.0.) GO TO 80
      IF(ISITE.NE.19) GO TO 80
      DO 801 M = 1,3
      IF(L.EQ.M) DEL1 = 1.
      IF(L.NE.M) DEL1 = 0.
      FAC11 = (16.*GR8+72.*GR6+252.*GR4+560.*GR2+945.)
     1 *FRONT + 945.*ERROR
      FAC12 = R(L)*(R(M)**4)/R11
      FAC21 = FRONT*(8.*GR6 + 28.*GR4 + 70.*GR2 + 105.) +
     1 105.*ERROR
      FAC22 = (4.*R(M)*DEL1 + 6.*R(L))*(R(M)**2)/R9
      FAC31 = FRONT*(4.*GR4 + 10.*GR2 + 15.) + 15.*ERROR
      FAC32 = (12.*R(M)*DEL1 + 3.*R(L))/R7
      DIRPO(L,M) = DIRPO(L,M) - FAC11*FAC12 + FAC21*FAC22 -
     1 FAC31*FAC32
  801 CONTINUE
   80 CONTINUE
C
C
      IF(RV.EQ.0.) GO TO 776
      TERM1 = (FRONT*(105. + 70.*GR2 + 28.*GR4 + 8.*GR6) +
     1 105.*ERROR)*(R(L)**4)/R9
      TERM2 = (FRONT*(15. + 10.*GR2 + 4.*GR4) + 15.*ERROR)*
     1 6.*(R(L)**2)/R7
      TERM3 = (FRONT*(3. + 2.*GR2) + 3.*ERROR)*3./R5
      DIRQM(L) = DIRQM(L) + TERM1 - TERM2 + TERM3
  776 CONTINUE
C
C
```

```
      IF((AL.EQ.0.).AND.(AM.EQ.0.).AND.(ANN.EQ.0.))GGG = 0.
      IF(GGG.EQ.0.) GO TO 745
      GRAT = (GV/(2.*GEE))**2
      IF(GRAT.GT.100.)GO TO 788
      EXPG = EXP(-GRAT)
      GO TO 789
  788 EXPG = 0.
  789 CONTINUE
C
      CALL DOTPC(PROPC)
      CALL DOTEL(PROEL)
C
  745 CONTINUE
C
      DO 760 L = 1,3
      IF(GGG.EQ.0.) GO TO 755
      IF(ISITE.NE.19) GO TO 755
C
      DO 754 M = 1,3
      RECPO(L,M)=RECPO(L,M)+(4.*PIE/V)*TG(L)*(TG(M)**4)*
     1 PROEL*EXPG/G2
  754 CONTINUE
  755 CONTINUE
C
      IF(GGG.EQ.0.) GO TO 54
      RECQM(L)=RECQM(L)+(PIE/V)*4.*(G(L)**4)*PROPC*EXPG/G2
   54 CONTINUE
  760 CONTINUE
C
C
C
      GGG = 1.
      IF(ANN.LE.0.) GO TO 90
      ANN = - ANN
      TN = - TN
      GO TO 20
   90 CONTINUE
      IF(AM.LE.0.) GO TO 95
      AM = - AM
      TM = - TM
      GO TO 1000
   95 CONTINUE
      IF(AL.LE.0.) GO TO 100
      AL = - AL
      TL = - TL
      GO TO 2000
  100 CONTINUE
C
C
      DO 340 L = 1,3
      DO 330 M = 1,3
      PNM(L,I9,M) = DIRPO(L,M) + RECPO(L,M)
  330 CONTINUE
      QMNEW(I9,L) = DIRQM(L) + RECQM(L)
```

```
  340 CONTINUE
C
C
  999 CONTINUE
C
      IF(ITRIP.EQ.3) CALL CHARE
C
 9999 CONTINUE
C
      DO 3170 I = 1,24
      WRITE(16,3180)(PNM(1,I,J),J=1,3)
      WRITE(16,3180)(PNM(2,I,J),J=1,3)
      WRITE(16,3180)(PNM(3,I,J),J=1,3)
 3170 CONTINUE
C
      DO 3120 I = 1,24
      WRITE(16,3180)(QMNEW(I,J),J=1,3)
 3120 CONTINUE
 3180 FORMAT(3(F15.8))
      WRITE(16,3160)FACMOD,V,INUC,ANS1,ANS2,ANS3
 3160 FORMAT(2(F15.8),I1,3(F10.4))
C
C
C
      STOP
      END
      SUBROUTINE CHARE
      DIMENSION QMNEW(24,3);TE(3,2)
      COMMON/ADD/QMNEW
      COMMON/OLLA/FACMOD
      COMMON/REPLY/ANS1,ANS2,ANS3
C
      TE(1,1) = 0.
      TE(1,2) = 0.
      TE(3,1) = 0.
      TE(3,2) = 0.
      TE(2,1) = 0.
      TE(2,2) = 0.
C
      DO 10 I = 1,18
      TE(1,1) = TE(1,1) + QMNEW(I,3)/192.
      TE(2,1) = TE(2,1) + (QMNEW(I,2) - QMNEW(I,1))/48.
      TE(3,1) = TE(3,1) + (QMNEW(I,1) + QMNEW(I,2) -
     1 0.75*QMNEW(I,3))/48.
   10 CONTINUE
C
      DO 15 I = 19,24
      TE(1,2) = TE(1,2) + QMNEW(I,3)/192.
      TE(2,2) = TE(2,2) + (QMNEW(I,2) - QMNEW(I,1))/48.
      TE(3,2) = TE(3,2) + (QMNEW(I,1) + QMNEW(I,2) -
     1 0.75*QMNEW(I,3))/48.
   15 CONTINUE
C
      E1 = TE(1,1)*(-1.) + TE(1,2)*(+3.)
```

```
      E2 = TE (2,1)*(-1.) + TE(2,2)*(+3.)
      E3 = TE(3,1)*(-1.) + TE(3,2)*(+3.)
C
      R2 = 1.515*(0.529**4)
      CONV = 116195.62
      FACMOD = (CONV*29.9*R2/60.)*0.33/169.
      ANS1 =  - 0.25*FACMOD*E1
      ANS2 =  - 0.25*FACMOD*E2
      ANS3 = - 0.25*FACMOD*E3
C
      RETURN
      END
      SUBROUTINE ERFN(GRV,ERROR)
      DATA P/0.3275911/
      DATA A1/0.254829592/
      DATA A2/-0.284496736/
      DATA A3/1.421413741/
      DATA A4/-1.453152027/
      DATA A5/1.061405429/
C
      T = 1./(1. + P*GRV)
      IF ( GRV.GT.10. ) GO TO 50
      EX = EXP(-(GRV**2))
      GO TO 60
   50 EX = 0.
   60 CONTINUE
      SUM = A1*T + A2*T**2 + A3*T**3 + A4*T**4 + A5*T**5
      ERROR = 1. - SUM*EX
      ERROR = 1. - ERROR
      RETURN
      END
      SUBROUTINE DOTPC(PROPC)
      DIMENSION R(3),G(3),PRO(3)
      COMMON/ONE/G,R,PROD
C
      SPRO = 0.
      DO 10 I = 1,3
      PRO(I) = G(I)*R(I)
      SPRO = SPRO + PRO(I)
   10 CONTINUE
      PROPC = COS(SPRO)
      RETURN
      END
      SUBROUTINE DOTEL(PROEL)
      DIMENSION R(3),G(3),PRO(3)
      COMMON/ONE/G,R,PROD
C
      SPRO = 0.
      DO 10 I = 1,3
      PRO(I) = G(I)*R(I)
      SPRO = SPRO + PRO(I)
   10 CONTINUE
      PROEL = SIN(SPRO)
      RETURN
```

END

Program FLO24 is similar to FLO2 except that it deals with fourth-order parameters. Also, it takes as input the dipole moments as already determined by FLO2.

```
      PROGRAM FLO24(INPUT,OUTPUT,TAPE15,TAPE19)
      DIMENSION WK(40),IESS(24,3,3),ALIV(24,3,3),
     1 QMAT2(24,3,3),QMAT3(24,3,3),QMDEL1(24,3,3),
     2 QMDEL3(24,3,3),PROD1(24,3,3),PROD2(24,3,3),
     3 ESS(24,3,3),QUPE(5,5),DIMO(24,3),ELF(5),E(24,3),
     4 REDO(3,3),DEL(24,3),B40EXP(4),B42EXP(4),B44EXP(4),
     5 QMAT1(24,3,3),QMDEL2(24,3,3),PROD3(24,3,3),
     6 PNMNEW(3,24,3),QMNEW(24,3)
      EXTERNAL LEQT2F
      DATA (B40EXP(I),I=1,4)/0.016,0.016,0.016,0.018/
      DATA (B42EXP(I),I=1,4)/+0.074,+0.085,+0.083,+0.105/
      DATA (B44EXP(I),I=1,4)/0.125,0.169,0.117,0.128/
C
      DO 3200 I = 1,24
      DO 3190 J = 1,3
      READ(15,3180)(QMAT1(I,J,K),K=1,3)
      READ(15,3180)(QMAT2(I,J,K),K=1,3)
      READ(15,3180)(QMAT3(I,J,K),K=1,3)
 3190 CONTINUE
 3200 CONTINUE
 3180 FORMAT(3(F15.8))
      READ(15,3180)(E(1,I),I=1,3)
      READ(15,3180)(E(13,I),I=1,3)
      READ(15,3180)(E(19,I),I=1,3)
      DO 5 I = 1,24
      DO 4 J = 1,3
      READ (15,6)(IESS(I,J,K),K=1,3)
    6 FORMAT(3(I2))
    4 CONTINUE
    5 CONTINUE
C
 3160 FORMAT(2(F15.8),I1,3(F10.4))
C
      DO 810 I = 1,24
      DO 800 J = 1,3
      DEL(I,J) = 0.
  800 CONTINUE
  810 CONTINUE
      DEL(1,1) = 1.
      DEL(13,2) = 1.
      DEL(19,3) = 1.
C
C
      DO 3120 I = 1,24
      DO 3119 L = 1,3
      READ(15,3180)(PNMNEW(L,I,J),J=1,3)
 3119 CONTINUE
 3120 CONTINUE
C
C
      DO 3118 I = 1,24
      READ(15,3180)(QMNEW(I,J),J=1,3)
 3118 CONTINUE
C
```

```
      READ(15,3160)FACMOD,V,INUC,ANS1,ANS2,ANS3
C
C
C
      DO 9 I = 1,24
      ESS(I,1,1) = FLOAT(IESS(I,2,2))
      ESS(I,1,2) = FLOAT(IESS(I,2,3))
      ESS(I,1,3) = FLOAT(IESS(I,2,1))
      ESS(I,2,1) = FLOAT(IESS(I,3,2))
      ESS(I,2,2) = FLOAT(IESS(I,3,3))
      ESS(I,2,3) = FLOAT(IESS(I,3,1))
      ESS(I,3,1) = FLOAT(IESS(I,1,2))
      ESS(I,3,2) = FLOAT(IESS(I,1,3))
      ESS(I,3,3) = FLOAT(IESS(I,1,1))
    9 CONTINUE
C
C
C
      ALFL1 = 0.01551
      ALFL2 = ALFL1 + 0.0000
      ALFL3 = ALFL1
      ALLA1 = 2.18
      ALLA2 = ALLA1
      ALLA3 = ALLA1
C
      ELF(1) = E(1,1)
      ELF(2) = E(1,2)
      ELF(3) = E(1,3)
      ELF(4) = E(13,2)
      ELF(5) = E(19,3)
C
      DO 19 I = 1,24
      DO 18 J = 1,3
      DO 17 K = 1,3
      ALIV(I,J,K) = 0.
   17 CONTINUE
   18 CONTINUE
   19 CONTINUE
C
      DO 20 I = 1,18
      ALIV(I,1,1) = 1./ALFL1
      ALIV(I,2,2) = 1./ALFL2
      ALIV(I,3,3) = 1./ALFL3
   20 CONTINUE
      DO 15 I = 19,24
      ALIV(I,1,1) = 1./ALLA1
      ALIV(I,2,2) = 1./ALLA2
      ALIV(I,3,3) = 1./ALLA3
   15 CONTINUE
C
      DO 35 I = 1,3
      DO 30 J = 1,3
      DO 25 K = 1,24
      QMDEL1(K,I,J) = ALIV(K,I,J)*DEL(K,1) - QMAT1(K,I,J)
```

```
      QMDEL2(K,I,J) = ALIV(K,I,J)*DEL(K,2) - QMAT2(K,I,J)
      QMDEL3(K,I,J) = ALIV(K,I,J)*DEL(K,3) - QMAT3(K,I,J)
   25 CONTINUE
   30 CONTINUE
   35 CONTINUE
C
C
      DO 500 I = 1,24
      DO 495 J = 1,3
      DO 490 K = 1,3
      PROD1(I,J,K) = 0.
      PROD2(I,J,K) = 0.
      PROD3(I,J,K) = 0.
  490 CONTINUE
  495 CONTINUE
  500 CONTINUE
C
      DO 485 I = 1,5
      DO 480 J = 1,5
      QUPE(I,J) = 0.
  480 CONTINUE
  485 CONTINUE
C
C
      DO 55 I = 1,24
      DO 50 J = 1,3
      DO 45 K = 1,3
      DO 40 L = 1,3
      PROD1(I,J,K) = PROD1(I,J,K) + QMDEL1(I,J,L)*ESS(I,L,K)
      PROD2(I,J,K) = PROD2(I,J,K) + QMDEL2(I,J,L)*ESS(I,L,K)
      PROD3(I,J,K) = PROD3(I,J,K) + QMDEL3(I,J,L)*ESS(I,L,K)
   40 CONTINUE
   45 CONTINUE
   50 CONTINUE
   55 CONTINUE
C
C
      DO 70 I = 1,12
      DO 65 J = 1,3
      QUPE(4,J) = QUPE(4,J) + PROD2(I,2,J)
      QUPE(5,J) = QUPE(5,J) + PROD3(I,3,J)
      DO 60 K = 1,3
      QUPE(J,K) = QUPE(J,K) + PROD1(I,J,K)
   60 CONTINUE
   65 CONTINUE
   70 CONTINUE
C
      DO 85 I = 13,16
      QUPE(4,4) = QUPE(4,4) + PROD2(I,2,2)
      QUPE(5,4) = QUPE(5,4) + PROD3(I,3,2)
      DO 80 J = 1,3
      QUPE(J,4) = QUPE(J,4) + PROD1(I,J,2)
   80 CONTINUE
   85 CONTINUE
```

```
C
      DO 95 I = 19,24
      QUPE(4,5) = QUPE(4,5) + PROD2(I,2,3)
      QUPE(5,5) = QUPE(5,5) + PROD3(I,3,3)
      DO 90 J = 1,3
      QUPE(J,5) = QUPE(J,5) + PROD1(I,J,3)
   90 CONTINUE
   95 CONTINUE
C
      IDGT = 0
C
      CALL LEQT2F(QUPE,1,5,5,ELF,IDGT,WK,IER)
C
      DO 200 I = 1,24
      DO 195 J = 1,3
      DIMO(I,J) = 0.
  195 CONTINUE
  200 CONTINUE
C
      DO 110 I = 1,12
      DO 105 J = 1,3
      DO 100 K = 1,3
      DIMO(I,J) = DIMO(I,J) + ESS(I,J,K)*ELF(K)
  100 CONTINUE
  105 CONTINUE
  110 CONTINUE
C
      ELF(1) = 0.
      ELF(2) = ELF(4)
      ELF(3) = 0.
C
C
      DO 125 I = 13,16
      DO 120 J = 1,3
      DO 115 K = 1,3
      DIMO(I,J) = DIMO(I,J) + ESS(I,J,K)*ELF(K)
  115 CONTINUE
  120 CONTINUE
  125 CONTINUE
C
      ELF(1) = 0.
      ELF(2) = 0.
      ELF(3) = ELF(5)
C
      DO 140 I = 19,24
      DO 135 J = 1,3
      DO 130 K = 1,3
      DIMO(I,J) = DIMO(I,J) + ESS(I,J,K)*ELF(K)
  130 CONTINUE
  135 CONTINUE
  140 CONTINUE
C
C
C
```

```
C
  150 CONTINUE
C
      EPO1 = 0.
      EPO2 = 0.
      EPO3 = 0.
      DO 160 I = 1,24
      DO 155 J = 1,3
      EPO1 = EPO1 + DIMO(I,J)*PNMNEW(J,I,3)
      EPO2 = EPO2 + DIMO(I,J)*(PNMNEW(J,I,2) - PNMNEW(J,I,1))
      EPO3 = EPO3 + DIMO(I,J)*(PNMNEW(J,I,1) + PNMNEW(J,I,2)
     1 - 0.75*PNMNEW(J,I,3))
  155 CONTINUE
  160 CONTINUE
C
      ANS21 =  - 0.25*FACMOD*EPO1/192.
      ANS22 = - 0.25*FACMOD*EPO2/48.
      ANS23 = - 0.25*FACMOD*EPO3/48.
C
      BTOT0 = ANS1 + ANS21
      BTOT2 = ANS2 + ANS22
      BTOT4 = ANS3 + ANS23
      DIFF0 = BTOT0 - B40EXP(INUC)
      DIFF2 = BTOT2 - B42EXP(INUC)
      DIFF4 = BTOT4 - B44EXP(INUC)
C
      PRINT(19,170)INUC,ANS1,ANS21,BTOT0,B40EXP(INUC),DIFF0
      PRINT(19,170)INUC,ANS2,ANS22,BTOT2,B42EXP(INUC),DIFF2
      PRINT(19,170)INUC,ANS3,ANS23,BTOT4,B44EXP(INUC),DIFF4
  170 FORMAT(1X,I1,5(E10.3,1X))
  294 CONTINUE
  295 CONTINUE
C
      STOP
      END
```

Program TRY calculates the second-order data for RTH which is not dependent on polarizability values. It is similar to FL01 except that the charge parameter η is required for dealing with the water molecules. Also, because there are 32 unknowns (as compared to 5 for RF_3), the programming structure is somewhat more complicated. The output of program TRY is stored on a tape which is to be read by CL3HX2.

```
      PROGRAM TRY(INPUT,OUTPUT,TAPE13)
      DIMENSION R(3),G(3),XO(44),YO(44),ZO(44),P(44,3),
     1ANAME(9),DIRQM(3,3),RECQM(3,3),UCP(36),QMAT(12,44,9),
     2 CC(9),SC(9),CD(9),SD(9),TEEL3(44,3),TEEL4(44,3),
     3 DIREL(3),RECEL(3),DIRPO(3,3),RECPO(3,3),
     3 TEMSEL(44,3),PNM(3,44,3),E(44,3),TR(3),TG(3),
     4 TA(9),TB(9),TC(9),TCHI(9)
      COMMON/ONE/G,R,PROD
      COMMON/ADD/QMAT
      COMMON/CHADD/ISITE,TEMSEL
      COMMON/FIELD/E,TEEL3,TEEL4
      COMMON/POT/PNM
      COMMON/OLLA/FACMOD
      COMMON/VOL/V,NHST
      DATA PIE/3.14159/
      DATA GEE,NIONS,ILIM,NHST/0.5,44,4,2/
      DATA (TCHI(I),I=1,9)/58.5,62.25,64.,62.,60.75,61.5,62.,
     1 63.,64./
      DATA BETA/93.65/
      DATA (ANAME(I),I=1,9)/2HND,2HSM,2HEU,2HGD,2HTB,2HDY,
     1 2HHO,2HER,2HTM/
      DATA(TA(I),I=1,9)/9.72,9.67,9.68,9.65,9.63,9.61,9.58,
     1 9.57,9.55/
      DATA(TB(I),I=1,9)/6.60,6.55,6.53,6.53,6.51,6.49,6.47,
     1 6.47,6.45/
      DATA(TC(I),I=1,9)/7.90,7.96,7.96,7.92,7.89,7.87,7.84,
     1 7.84,7.82/
      DATA (UCP(I),I=1,36)/.25,.1521,.25,.75,.3769,.25,
     1 .0587,.837,.2601,.2813,.0471,.5432,.1423,.4254,.0888,
     1 .4406,.2988,.1058,.272,.92,.605,.364,.082,.608,
     3 .174,.484,.987,.117,.548,.14,.534,.322,.149,.476,
     4 .258,.002/
C
      CONV = PIE/180.
      BET = BETA*CONV
C
      I = NHST
      A = TA(I)
      C = TB(I)
      B = TC(I)
      CHI = TCHI(I)*CONV
      SB = SIN(BET)
      CC = COS(CHI)
      SC = SIN(CHI)
      CD = COS(BET - CHI)
      SD = SIN(BET - CHI)
      V = A*B*C*SB
C
      DO 217 I = 1,3
      J = I + 3
      P(1,I) = UCP(I)
      P(3,I) = UCP(J)
      P(2,I) = 1. - P(1,I)
      P(4,I) = 1. - P(3,I)
```

```
  217 CONTINUE
      J = 1
      DO 15 I = 5,41,4
      J = J + 1
      I61 = 8*J + 1
      I62 = I61 + 1
      I63 = I61 + 2
      P(I,1) = UCP(I61)
      P(I,2) = UCP(I62)
      P(I,3) = UCP(I63)
C
      K = I + 1
      P(K,1) = 1. - P(I,1)
      P(K,2) = 1. - P(I,2)
      P(K,3) = 1. - P(I,3)
      L = I + 2
      P(L,1) = 0.5 - P(I,1)
      P(L,2) = P(I,2)
      P(L,3) = 0.5 - P(I,3)
C
      M = I + 3
      P(M,1) = 0.5 + P(I,1)
      P(M,2) = 1.0 - P(I,2)
      P(M,3) = 0.5 + P(I,3)
   15 CONTINUE
C
      DO 9999 ITRIP = 1, 12
      IF(ITRIP.EQ.1) ISITE = 1
      IF(ITRIP.EQ.2) ISITE = 3
      IF(ITRIP.EQ.3) ISITE = 5
      IF(ITRIP.GT.3) ISITE = ISITE + 4
C
      AAN = P(ISITE,1)
      BBN = P(ISITE,2)
      CCN = P(ISITE,3)
      DO 999 I9 = 1,44
      XO(I9) = P(I9,1) - AAN
      ZO(I9) = P(I9,2) - BBN
      YO(I9) = P(I9,3) - CCN
C
C
      DO 510 L = 1,3
      DIREL(L) = 0.
      RECEL(L) = 0.
      DO 500 M = 1,3
      DIRPO(L,M) = 0.
      RECPO(L,M) = 0.
      DIRQM(L,M) = 0.
      RECQM(L,M) = 0.
  500 CONTINUE
  510 CONTINUE
C
      DO 100 I = 1,ILIM
      AL = FLOAT(I) - 1.
```

```
 2000 CONTINUE
      DO 95 J = 1,ILIM
      AM = FLOAT(J) - 1.
 1000 CONTINUE
      DO 90 K = 1,ILIM
      ANN = FLOAT(K) - 1.
      TL = 2.*PIE*AL
      TM = 2.*PIE*AM
      TN = 2.*PIE*ANN
   20 R(1) = (AL + XO(I9))*A*CC + (AM + YO(I9))*B*CD
      R(2) = - (AL + XO(I9))*A*SC + (AM + YO(I9))*B*SD
      R(3) = (ANN + ZO(I9))*C
      G(1) = (TL*SD)/(A*SB) + (TM*SC)/(B*SB)
      G(2) = - (TL*CD)/(A*SB) + (TM*CC)/(B*SB)
      G(3) = TN/C
C
      TR(1) = R(1)
      TR(2) = R(2)
      TR(3) = R(3)
      TG(1) = G(1)
      TG(2) = G(2)
      TG(3) = G(3)
C
      RV = SQRT(R(1)**2 + R(2)**2 + R(3)**2)
      GV = SQRT(G(1)**2 + G(2)**2 + G(3)**2)
C
C
      SQP = SQRT(PIE)
      R2P = (RV**2)*SQP
      R4P = (RV**4)*SQP
      R5 = RV**5
      R6P = (RV**6)*SQP
      R7 = RV**7
      G2 = GV**2
      G3 = GEE**3
      G5 = GV**5
C
C
      GRV = GEE*RV
      GR2 = (GEE*RV)**2
      IF(GR2.GT.100.) GO TO 888
      EXPD = EXP(-GR2)
      GO TO 889
  888 EXPD = 0.
  889 CONTINUE
C
      CALL ERFN(GRV,ERROR)
C
      DO 776 L = 1,3
C
      IF(RV.EQ.0.) GO TO 80
      DIREL(L)=DIREL(L)+R(L)*ERROR/(RV**3)+2.*GEE*R(L)*
     1 EXPD/R2P
      IF(ISITE.NE.1) GO TO 80
```

```
      DO 801 M = 1,3,2
      IF(L.EQ.M) DEL1 = 1.
      IF(L.NE.M) DEL1 = 0.
      DIRPO(M,L)=DIRPO(M,L)-((30.*GEE)/R6P+20.*G3/R4P+
     1(8.*G5/R2P))*(TR(L)*(TR(M)**2))*EXPD+(((6.*GEE)/R4P)*
     2EXPD+((4.*G3)/R2P)*EXPD+(3.*ERROR)/R5)*(2.*TR(M)*DEL1+
     3 TR(L)) - (15.*TR(L)*(TR(M)**2)*ERROR)/R7
  801 CONTINUE
   80 CONTINUE
C
      DO 775 M = 1,3
      IF(L.EQ.M) DELTA = 1.
      IF(L.NE.M) DELTA = 0.
C
      IF(RV.EQ.0.) GO TO 81
      DIRQM(L,M)=DIRQM(L,M)+4.*(GEE**3)*R(L)*R(M)*EXPD/
     1((RV**2)*SQRT(PIE)) + 6.*GEE*R(L)*R(M)*EXPD/
     2((RV**4)* - 2.*GEE*EXPD*DELTA/((RV**2)*SQRT(PIE))
     3SQRT(PIE))+(3.*R(L)*R(M)/(RV**2)-DELTA)*(ERROR/
     4 (RV**3))
      GO TO 777
   81 DIRQM(L,M) = DIRQM(L,M) + 4.*(GEE**3)*DELTA/(3.*
     1 SQRT(PIE))
  777 CONTINUE
  775 CONTINUE
  776 CONTINUE
C
C
      IF((AL.EQ.0.).AND.(AM.EQ.0.).AND.(ANN.EQ.0.))GGG=0.
      IF(GGG.EQ.0.) GO TO 745
      GRAT = (GV/(2.*GEE))**2
      IF(GRAT.GT.100.)GO TO 788
      EXPG = EXP(-GRAT)
      GO TO 789
  788 EXPG = 0.
  789 CONTINUE
C
      CALL DOTPC(PROPC)
      CALL DOTEL(PROEL)
C
  745 CONTINUE
C
      DO 760 L = 1,3
      IF(GGG.EQ.0.) GO TO 755
      RECEL(L)=RECEL(L)+(PIE/V)*4.*G(L)*PROEL*EXPG/G2
      IF(ISITE.NE.1) GO TO 755
C
      DO 754 M = 1,3,2
      RECPO(M,L)=RECPO(M,L)+(4.*PIE/V)*TG(L)*(TG(M)**2)*
     1 PROEL*EXPG/G2
  754 CONTINUE
  755 CONTINUE
C
      DO 750 M = 1,3
```

```
      IF(L.EQ.M)  DELTA = 1.
      IF(L.NE.M)  DELTA = 0.
      IF(GGG.EQ.0.) GO TO 54
      RECQM(L,M)=RECQM(L,M)-(PIE/V)*4.*G(L)*G(M)*PROPC*EXPG/
     1(GV**2)
      GO TO 778
   54 RECQM(L,M) = RECQM(L,M) - 4.*PIE*DELTA/(3.*V)
  778 CONTINUE
  750 CONTINUE
  760 CONTINUE
C
C
C
      GGG = 1.
      IF(ANN.LE.0.) GO TO 90
      ANN = - ANN
      TN = - TN
      GO TO 20
   90 CONTINUE
      IF(AM.LE.0.) GO TO 95
      AM = - AM
      TM = - TM
      GO TO 1000
   95 CONTINUE
      IF(AL.LE.0.) GO TO 100
      AL = - AL
      TL = - TL
      GO TO 2000
  100 CONTINUE
C
C
      J = 0
      DO 340 L = 1,3
      TEMSEL(I9,L) = DIREL(L) + RECEL(L)
      IF(ITRIP.NE.1) GO TO 349
      PNM(1,I9,L) = DIRPO(1,L) + RECPO(1,L)
      PNM(3,I9,L) = DIRPO(3,L) + RECPO(3,L)
  349 CONTINUE
      DO 330 M = 1,3
      J = J + 1
      QMAT(ITRIP,I9,J) = DIRQM(L,M) + RECQM(L,M)
  330 CONTINUE
  340 CONTINUE
C
C
C
C
  999 CONTINUE
C
      CALL CHAEL'
C
 9999 CONTINUE
C
      DO 820 ITRIP = 1,12
```

```
      DO 819 I9 = 1,44
      WRITE(13,810)(QMAT(ITRIP,I9,J),J=1,5)
      WRITE(13,811)(QMAT(ITRIP,I9,K),K=6,9)
  819 CONTINUE
  820 CONTINUE
C
      DO 830 ITRIP = 1,12
      IF(ITRIP.EQ.1) ISITE = 1
      IF(ITRIP.EQ.2) ISITE = 3
      IF(ITRIP.EQ.3) ISITE = 5
      IF(ITRIP.GT.3) ISITE = ISITE + 4
      WRITE(13,812)(E(ISITE,J),J=1,3)
      WRITE(13,812)(TEEL3(ISITE,J),J=1,3)
      WRITE(13,812)(TEEL4(ISITE,J),J=1,3)
  830 CONTINUE
      DO 840 I9 = 1,44
      WRITE(13,813)(PNM(1,I9,J),J=1,3)
      WRITE(13,813)(PNM(3,I9,J),J=1,3)
  840 CONTINUE
  810 FORMAT(5(F13.8))
  811 FORMAT(4(F13.8))
  812 FORMAT(3(F13.8))
  813 FORMAT(3(F13.8))
C
C
C
      STOP
      END
      SUBROUTINE CHAEL
      DIMENSION TE(4,3),E(44,3),TEMSEL(44,3),TEEL3(44,3),
     1 TEEL4(44,3)
      COMMON/CHADD/ISITE,TEMSEL
      COMMON/FIELD/E,TEEL3,TEEL4
C
      DO 5 I = 1,4
      DO 4 J = 1,3
      TE(I,J) = 0.
    4 CONTINUE
    5 CONTINUE
C
      DO 10 I = 1,2
      DO  8 J = 1,3
      TE(1,J) = TE(1,J) + TEMSEL(I,J)
    8 CONTINUE
   10 CONTINUE
C
      DO 15 I = 3,8
      DO 14 J = 1,3
      TE(2,J) = TE(2,J) + TEMSEL(I,J)
   14 CONTINUE
   15 CONTINUE
C
      DO 17 I = 9,20
      DO 16 J = 1,3
```

```
      TE(3,J) = TE(3,J) + TEMSEL(I,J)
   16 CONTINUE
   17 CONTINUE
C
      DO 19 I = 21,44
      DO 18 J = 1,3
      TE(4,J) = TE(4,J) + TEMSEL(I,J)
   18 CONTINUE
   19 CONTINUE
C
      DO 20 I = 1,3
      E(ISITE,I) = TE(1,I)*(+3.) + TE(2,I)*(-1.)
      TEEL3(ISITE,I) = TE(3,I)
      TEEL4(ISITE,I) = TE(4,I)
   20 CONTINUE
C
C
      RETURN
      END
      SUBROUTINE ERFN(GRV,ERROR)
      DATA P/0.3275911/
      DATA A1/0.254829592/
      DATA A2/-0.284496736/
      DATA A3/1.421413741/
      DATA A4/-1.453152027/
      DATA A5/1.061405429/
C
      T = 1./(1. + P*GRV)
      IF ( GRV.GT.10. ) GO TO 50
      EX = EXP(-(GRV**2))
      GO TO 60
   50 EX = 0.
   60 CONTINUE
      SUM = A1*T + A2*T**2 + A3*T**3 + A4*T**4 + A5*T**5
      ERROR = 1. - SUM*EX
      ERROR = 1. - ERROR
      RETURN
      END
      SUBROUTINE DOTPC(PROPC)
      DIMENSION R(3),G(3),PRO(3)
      COMMON/ONE/G,R,PROD
C
      SPRO = 0.
      DO 10 I = 1,3
      PRO(I) = G(I)*R(I)
      SPRO = SPRO + PRO(I)
   10 CONTINUE
      PROPC = COS(SPRO)
      RETURN
      END
      SUBROUTINE DOTEL(PROEL)
      DIMENSION R(3),G(3),PRO(3)
      COMMON/ONE/G,R,PROD
C
```

```
      SPRO = 0.
      DO 10 I = 1,3
      PRO(I) = G(I)*R(I)
      SPRO = SPRO + PRO(I)
   10 CONTINUE
      PROEL = SIN(SPRO)
      RETURN
      END
```

Program CL3HX2 is the RTH analogue of FL02.

```
      PROGRAM CL3HX2(INPUT,OUTPUT,TAPE13,TAPE6)
      REAL WK(1450),ALIV(44,9),QMAT(12,44,9),NEWPR(12,12,9),
     1 QMDEL(12,44,9),PROD(12,44,9),ATEM(3,3),BTEM(3,3),
     3 ESS(44,3,3),QUPE(36,36),DIMO(44,3),ELF(36),E(44,3),
     4 AMXTEM(44,3,3),OFFDIA(4),EPS(4,3,3),ALTEM(4,3),
     5 B22EXP(9),DIA(4),DEL(12,44),ELPRO(44,3),TEEL3(44,3),
     6 ALRE(9),PNM(3,44,3),B20EXP(9),TEEL4(44,3)
      DIMENSION DELPOL(4)
      EXTERNAL LEQT2F
      COMMON/FIELD/E,ELPRO,TEEL3,TEEL4
      COMMON/CHARGE/ETA
      COMMON/POINT/QMAT,FACMOD,ANS1,ANS2
      DATA (ALRE(I),I=1,9)/1.23,1.11,1.06,1.01,0.97,0.94,
C     ALRE(1) = 1.23  (EXPL FREE ION VALUE)
C     ALRE(3) = 1.06 (EXXPL FREE ION VALUE)
     1 0.90,0.86,0.83/
      DATA (OFFDIA(I),I=1,4)/0.0,0.0,0.00,0.00/
      DATA (B20EXP(I),I=1,9)/1.855,1.864,1.854,0.0000,1.882,
     1 1.883,1.890 ,1.843,1.880/
      DATA (B22EXP(I),I=1,9)/-1.065,-1.112,-1.150,-0.0000,
     1 -1.191,-1.228,-1.241,-1.276,-1.311/
      DATA ETA,ALCL,ALOX,ALHY/0.4,1.40,3.10,0.6/
      DATA NHST/9/
C
      DO 869 I = 1,12
      DO 868 J = 1,44
      DEL(I,J) = 0.
  868 CONTINUE
  869 CONTINUE
      DEL(1,1) = 1.
      DEL(2,3) = 1.
      J = 1
      DO 870 I = 3,12
      J = J + 4
      DEL(I,J) = 1.
  870 CONTINUE
C
      DO 820 ITRIP = 1,12
      DO 819 I9 = 1,44
      READ(13,810)(QMAT(ITRIP,I9,J),J=1,5)
      READ(13,811)(QMAT(ITRIP,I9,K),K=6,9)
  819 CONTINUE
  820 CONTINUE
      DO 830 ITRIP = 1,12
      IF(ITRIP.EQ.1) ISITE = 1
      IF(ITRIP.EQ.2) ISITE = 3
      IF(ITRIP.EQ.3) ISITE =5
      IF(ITRIP.GT.3) ISITE = ISITE + 4
      READ(13,812)(ELPRO(ISITE,J),J=1,3)
      READ(13,812)(TEEL3(ISITE,J),J=1,3)
      READ(13,812)(TEEL4(ISITE,J),J=1,3)
  830 CONTINUE
      DO 840 I9 = 1,44
      READ(13,813)(PNM(1,I9,J),J=1,3)
```

```
      READ(13,813)(PNM(3,I9,J),J=1,3)
  840 CONTINUE
C
  810 FORMAT(5(F13.8))
  811 FORMAT(4(F13.8))
  812 FORMAT(3(F13.8))
  813 FORMAT(3(F13.8))
C
C
C
C
      DO 510 I = 1,44
      DO 505 J = 1,3
      DO 501 K = 1,3
      ESS(I,J,K) = 0.
  501 CONTINUE
  505 CONTINUE
  510 CONTINUE
      DO 515 I = 1,3,2
      DO 514 J = 1,3
      ESS(I,J,J) = 1.
  514 CONTINUE
  515 CONTINUE
      DO 520 I = 5,41,4
      DO 519 J = 1,3
      ESS(I,J,J) = 1.
  519 CONTINUE
  520 CONTINUE
      DO 525 I = 2,4,2
      DO 524 J = 1,3
      ESS(I,J,J) = -1.
  524 CONTINUE
  525 CONTINUE
      DO 530 I = 6,42,4
      DO 529 J = 1,3
      ESS(I,J,J) = -1.
  529 CONTINUE
  530 CONTINUE
      DO 535 I = 7,43,4
      DO 534 J = 1,2
      ESS(I,J,J) = -1.
  534 CONTINUE
      ESS(I,3,3) = 1.
  535 CONTINUE
      DO 540 I = 8,44,4
      DO 539 J = 1,2
      ESS(I,J,J) = 1.
  539 CONTINUE
      ESS(I,3,3) = -1.
  540 CONTINUE
C
C
  400 CONTINUE
C
```

```
      DO 8040 IJ0 = 1,1
      ETA = 0.471 - 0.001*FLOAT(IJ0)
      CALL CHARE
      CALL CHAEL
      DO 8035 IJ1 = 1,5
      ALTEM(1,2) = +0.58 - 0.01*FLOAT(IJ1)
      ALTEM(1,1) = ALTEM(1,2)
      ALTEM(1,3) = ALTEM(1,2)
      DO 8030 IJ2 = 1,1
      ALTEM(2,2) = 2.86 - 0.02*FLOAT(IJ2)
      ALTEM(2,1) = ALTEM(2,2)
      ALTEM(2,3) = ALTEM(2,2)
      DO 8025 IJ3 = 1,1
      ALTEM(3,2) = 6.80 + 0.02*FLOAT(IJ3)
      ALTEM(3,1) = ALTEM(3,2)
      ALTEM(3,3) = ALTEM(3,2)
      DO 8024 IJ4 = 1,1
      ALTEM(4,2) =    0.396 - 0.001*FLOAT(IJ4)
      ALTEM(4,1) = ALTEM(4,2)
      ALTEM(4,3) = ALTEM(4,2)
C
      DO 8020 IK1 = 1,1
      OFFDIA(1) = -1.00 + 1.00*FLOAT(IK1)
      DO 8019 IK2 = 1,1
      OFFDIA(2) = + 0.32 + 0.02*FLOAT(IK2)
      DO 8018 IK3 = 1,1
      OFFDIA(3) = 2.42 - 0.2*FLOAT(IK3)
      DO 8017 IK4 = 1,1
      OFFDIA(4) = + 0.029  + 0.002*FLOAT(IK4)
C
C
      ELF(1) = E(1,1)
      ELF(2) = E(1,2)
      ELF(3) = E(1,3)
      ELF(4) = E(3,1)
      ELF(5) = E(3,2)
      ELF(6) = E(3,3)
      I = 6
      DO 3 J = 5,41,4
      DO 2 K = 1,3
      I = I + 1
      ELF(I) = E(J,K)
    2 CONTINUE
    3 CONTINUE
C
      DO 270 I = 1,4
      DO 269 J = 1,3
      DO 268 K = 1,3
      EPS(I,J,K) = 0.
  268 CONTINUE
  269 CONTINUE
  270 CONTINUE
C
      DO 2000 KK = 1,4
```

```
      DIA(KK) = ALTEM(KK,1)*ALTEM(KK,3) - OFFDIA(KK)**2
      IF(DIA(KK).EQ.0.) DIA(KK) = DIA(KK) + 0.001
      EPS(KK,1,1) = ALTEM(KK,3)/DIA(KK)
      EPS(KK,2,2) = 1./ALTEM(KK,2)
      EPS(KK,3,3) = ALTEM(KK,1)/DIA(KK)
      EPS(KK,1,3) = - OFFDIA(KK)/DIA(KK)
      EPS(KK,3,1) = EPS(KK,1,3)
 2000 CONTINUE
C
C
      DO 220 I = 1,44
      IF(I.LE.2) ISUB = 1
      IF((I.GT.2).AND.(I.LE.8)) ISUB = 2
      IF((I.GT.8).AND.(I.LE.20)) ISUB = 3
      IF((I.GT.20).AND.(I.LE.44)) ISUB = 4
      DO 230   J = 1,3
      DO 240 K = 1,3
      AMXTEM(I,J,K) = EPS(ISUB,J,K)
  240 CONTINUE
  230 CONTINUE
  220 CONTINUE
C
      DO 215 I = 1,44
      L = 0
      DO 213 J = 1,3
      DO 211 K = 1,3
      L = L + 1
      ALIV(I,L) = AMXTEM(I,J,K)
  211 CONTINUE
  213 CONTINUE
  215 CONTINUE
C
      DO 40 L = 1,12
      DO 35 I = 1,9
      DO 25 K = 1,44
      QMDEL(L,K,I) = ALIV(K,I)*DEL(L,K) - QMAT(L,K,I)
   25 CONTINUE
   35 CONTINUE
   40 CONTINUE
C
C
      DO 500 I = 1,12
      DO 495 J = 1,44
      DO 490 K = 1,9
      PROD(I,J,K) = 0.
  490 CONTINUE
  495 CONTINUE
  500 CONTINUE
C
      DO 485 I = 1,36
      DO 480 J = 1,36
      QUPE(I,J) = 0.
  480 CONTINUE
  485 CONTINUE
```

```
C
C
C
      DO 58 I = 1,12
      DO 56 J = 1,44
      K = 0
      DO 54 L = 1,3
      DO 53 M = 1,3
      K = K + 1
      ATEM(L,M) = QMDEL(I,J,K)
   53 CONTINUE
   54 CONTINUE
      DO 52 L = 1,3
      DO 51 M = 1,3
      BTEM(L,M) = 0.
   51 CONTINUE
   52 CONTINUE
      DO 50 L = 1,3
      DO 49 M = 1,3
      DO 48 N = 1,3
      BTEM(L,M) = BTEM(L,M) + ATEM(L,N)*ESS(J,N,M)
   48 CONTINUE
   49 CONTINUE
   50 CONTINUE
      KK = 0
      DO 47 L = 1,3
      DO 46 M = 1,3
      KK = KK + 1
      PROD(I,J,KK) = BTEM(L,M)
   46 CONTINUE
   47 CONTINUE
   56 CONTINUE
   58 CONTINUE
C
C
      DO 70 I = 1,12
      DO 65 J = 1,12
      DO 60 K = 1,9
      NEWPR(I,J,K) = 0.
   60 CONTINUE
   65 CONTINUE
   70 CONTINUE
      DO 75 I = 1,12
      DO 74 J = 1,9
      DO 73 K = 1,2
      NEWPR(I,1,J) = NEWPR(I,1,J) + PROD(I,K,J)
   73 CONTINUE
      DO 72 K = 3,4
      NEWPR(I,2,J) = NEWPR(I,2,J) + PROD(I,K,J)
   72 CONTINUE
      K = 1
      DO 771 L = 3,12
      K = K + 4
      M = K + 3
```

```
      DO 770 N = K,M
      NEWPR(I,L,J) = NEWPR(I,L,J) + PROD(I,N,J)
  770 CONTINUE
  771 CONTINUE
   74 CONTINUE
   75 CONTINUE
      DO 95 I = 1,12
      DO 93 J = 1,12
      DO 89 K = 1,3
      DO 87 L = 1,3
      II = 3*(I - 1) + K
      JJ = 3*(J - 1) + L
      M = L + 3*(K - 1)
      QUPE(II,JJ) = NEWPR(I,J,M)
   87 CONTINUE
   89 CONTINUE
   93 CONTINUE
   95 CONTINUE
C
C
      IDGT = 0
C
      CALL LEQT2F(QUPE,1,36,36,ELF,IDGT,WK,IER)
C
      DO 200 I = 1,44
      DO 195 J = 1,3
      DIMO(I,J) = 0.
  195 CONTINUE
  200 CONTINUE
C
      DO 110 I = 1,2
      DO 105 J = 1,3
      DO 100 K = 1,3
      DIMO(I,J) = DIMO(I,J) + ESS(I,J,K)*ELF(K)
  100 CONTINUE
  105 CONTINUE
  110 CONTINUE
C
C
C
      DO 125 I = 3,4
      DO 120 J = 1,3
      DO 115 K = 1,3
      L = K + 3
      DIMO(I,J) = DIMO(I,J) + ESS(I,J,L)*ELF(K)
  115 CONTINUE
  120 CONTINUE
  125 CONTINUE
C
      K = 1
      DO 140 I = 3,12
      K = K + 4
      M = K + 3
      DO 137 J = K,M
```

```
      DO 134 L = 1,3
      DO 131 N = 1,3
      K2 = 3*(I - 1) + N
      DIMO(J,L) = DIMO(J,L) + ESS(J,L,N)*ELF(K2)
  131 CONTINUE
  134 CONTINUE
  137 CONTINUE
  140 CONTINUE
C
C
C
  150 CONTINUE
C
C
      EPO1 = 0.
      EPO2 = 0.
      IF(ETA.EQ.1.) IDO = 20
      IF(ETA.LT.1.) IDO = 44
      DO 160 I = 1,IDO
      DO 155 J = 1,3
      EPO1 = EPO1 + DIMO(I,J)*PNM(3,I,J)
      EPO2 = EPO2 + DIMO(I,J)*(2.*PNM(1,I,J) + PNM(3,I,J))
  155 CONTINUE
  160 CONTINUE
C
      ANS21 = - 0.25*FACMOD*EPO1
      ANS22 = - 0.25*FACMOD*EPO2
C
      BTOT0 = ANS1 + ANS21
      BTOT2 = ANS2 + ANS22
      DIFF0 = BTOT0 - B20EXP(NHST)
      DIFF2 = BTOT2 - B22EXP(NHST)
C
      B0EX = B20EXP(NHST)
      B2EX = B22EXP(NHST)
      FAC11 = (BTOT0 - B0EX)**2
      FAC21 = (BTOT2 - B2EX)**2
      FACDE = B0EX**2 + B2EX**2
      FUNC = (FAC11*(B2EX**2) + FAC21*(B0EX**2))/FACDE
C
C
      WRITE(6,1170)NHST,ETA,(ALTEM(KL),KL=1,4),(OFFDIA(I),
     1 I=1,4)
 1170 FORMAT(1X,I1,2X,9(F8.3,1X),/)
      WRITE(6,170)ANS1,ANS21,BTOT0,B20EXP(NHST),DIFF0
      WRITE(6,171)ANS2,ANS22,BTOT2,B22EXP(NHST),DIFF2,FUNC
  170 FORMAT(1X,5(F9.4,2X))
  171 FORMAT(1X,5(F9.4,2X),E10.3,//)
C
C
 8017 CONTINUE
 8018 CONTINUE
 8019 CONTINUE
 8020 CONTINUE
```

```
 8024 CONTINUE
 8025 CONTINUE
 8030 CONTINUE
 8035 CONTINUE
 8040 CONTINUE
 8021 CONTINUE
C
      STOP
      END
      SUBROUTINE CHARE
      DIMENSION QMAT(12,44,9),TE(4,2)
      COMMON/POINT/QMAT,FACMOD,ANS1,ANS2
      COMMON/CHARGE/ETA
C
      DO 5 I = 1,4
      DO 4 J = 1,2
      TE(I,J) = 0.
    4 CONTINUE
    5 CONTINUE
C
      DO 10 I = 1,2
      TE(1,1) = TE(1,1) + QMAT(1,I,9)
      TE(1,2) = TE(1,2) + QMAT(1,I,9) + 2.*QMAT(1,I,1)
   10 CONTINUE
C
      DO 15 I = 3,8
      TE(2,1) = TE(2,1) + QMAT(1,I,9)
      TE(2,2) = TE(2,2) + QMAT(1,I,9) + 2.*QMAT(1,I,1)
   15 CONTINUE
C
      DO 20 I = 9,20
      TE(3,1) = TE(3,1) + QMAT(1,I,9)
      TE(3,2) = TE(3,2) + QMAT(1,I,9) + 2.*QMAT(1,I,1)
   20 CONTINUE
C
      DO 25 I = 21,44
      TE(4,1) = TE(4,1) + QMAT(1,I,9)
      TE(4,2) = TE(4,2) + QMAT(1,I,9) + 2.*QMAT(1,I,1)
   25 CONTINUE
C
      E1 = TE(1,1)*(+3.) + TE(2,1)*(-1.) +
     1 (-2.*ETA)*TE(3,1) + ETA*TE(4,1)
      E2 = TE(1,2)*(+3.) + TE(2,2)*(-1.) +
     1 (-2.*ETA)*TE(3,2) + ETA*TE(4,2)
C
      AK1 = -12.*(1534.**3)/(5.*(32200.**2)*40000.)
      AK2 = 16.*1534./(245.*32200.)
      RCAP2 = - 0.07*(0.529**2)
      R2 = 0.785*(0.529**2)
      AKAY = AK1*R2 + AK2*RCAP2
      GAM = 0.33
      CONV = 116195.62
      FACMOD = CONV*AKAY*GAM*29.9
      ANS1 = - 0.25*FACMOD*E1
```

```
      ANS2 = - 0.25*FACM06*E2
C
      WRITE(6,40)E1,E2
   40 FORMAT(1X,*A VALUES*,2X,2(F10.4,2X))
C
      RETURN
      END
      SUBROUTINE CHAEL
      DIMENSION E(44,3),ELPRO(44,3),TEEL3(44,3),TEEL4(44,3)
      COMMON/FIELD/E,ELPRO,TEEL3,TEEL4
      COMMON/CHARGE/ETA
C
C
      DO 20 I = 1,12
      IF(I.EQ.1) ISITE = 1
      IF(I.EQ.2) ISITE = 3
      IF(I.EQ.3) ISITE = 5
      IF(I.GE.4) ISITE = ISITE + 4
      DO 15 J = 1,3
      E(ISITE,J) = ELPRO(ISITE,J) - 2.*ETA*TEEL3(ISITE,J) +
     1 ETA*TEEL4(ISITE,J)
   15 CONTINUE
   20 CONTINUE
C
      RETURN
      END
```

Program TRY4 is the RTH analogue of FL014.

```
      PROGRAM TRY4(INPUT,OUTPUT,TAPE18)
      DIMENSION R(3),G(3),XO(44),YO(44),ZO(44),P(44,3),
     1ANAME(9),DIRQM(3),RECQM(3),UCP(36),QMNEW(44,3),
     2 CC(9),SC(9),CD(9),SD(9),
     3 DIRPO(3,3),RECPO(3,3),
     3 PNM(3,44,3),TR(3),TG(3),
     4 TA(9),TB(9),TC(9),TCHI(9)
      COMMON/ONE/G,R,PROD
      COMMON/ADD/QMAT
      COMMON/CHADD/ISITE,TEMSEL
      COMMON/FIELD/E,TEEL3,TEEL4
      COMMON/POT/PNM
      COMMON/OLLA/FACMOD
      COMMON/VOL/V,NHST
      DATA PIE/3.14159/
      DATA GEE,NIONS,ILIM,NHST/0.5,44,4,9/
      DATA (TCHI(I),I=1,9)/58.5,62.25,64.,62.,60.75,61.5,62.,
     1 63.,64./
      DATA BETA/93.65/
      DATA (ANAME(I),I=1,9)/2HND,2HSM,2HEU,2HGD,2HTB,2HDY,
     1 2HHO,2HER,2HTM/
      DATA(TA(I),I=1,9)/9.72,9.67,9.68,9.65,9.63,9.61,9.58,
     1 9.57,9.55/
      DATA(TB(I),I=1,9)/6.60,6.55,6.53,6.53,6.51,6.49,6.47,
     1 6.47,6.45/
      DATA(TC(I),I=1,9)/7.90,7.96,7.96,7.92,7.89,7.87,7.84,
     1 7.84,7.82/
      DATA (UCP(I),I=1,36)/.25,.1521,.25,.75,.3769,.25,
     1 .0587,.837,.2601,.2813,.0471,.5432,.1423,.4254,.0888,
     1 .4406,.2988,.1058,.272,.92,.605,.364,.082,.608,
     3 .174,.484,.987,.117,.548,.14,.534,.322,.149,.476,
     4 .258,.002/
C
      CONV = PIE/180.
      BET = BETA*CONV
C
      I = NHST
      A = TA(I)
      C = TB(I)
      B = TC(I)
      CHI = TCHI(I)*CONV
      SB = SIN(BET)
      CC = COS(CHI)
      SC = SIN(CHI)
      CD = COS(BET - CHI)
      SD = SIN(BET - CHI)
      V = A*B*C*SB
C
      DO 217 I = 1,3
      J = I + 3
      P(1,I) = UCP(I)
      P(3,I) = UCP(J)
      P(2,I) = 1. - P(1,I)
      P(4,I) = 1. - P(3,I)
```

```
 217 CONTINUE
     J = 1
     DO 15 I = 5,41,4
     J = J + 1
     I61 = 3*J + 1
     I62 = I61 + 1
     I63 = I61 + 2
     P(I,1) = UCP(I61)
     P(I,2) = UCP(I62)
     P(I,3) = UCP(I63)
C
     K = I + 1
     P(K,1) = 1. - P(I,1)
     P(K,2) = 1. - P(I,2)
     P(K,3) = 1. - P(I,3)
     L =I + 2
     P(L,1) = 0.5 - P(I,1)
     P(L,2) = P(I,2)
     P(L,3) = 0.5 - P(I,3)
C
     M = I + 3
     P(M,1) = 0.5 + P(I,1)
     P(M,2) = 1.0 - P(I,2)
     P(M,3) = 0.5 + P(I,3)
  15 CONTINUE
C
     DO 9999 ITRIP = 1,1
     IF(ITRIP.EQ.1) ISITE = 1
     IF(ITRIP.EQ.2) ISITE = 3
     IF(ITRIP.EQ.3) ISITE = 5
     IF(ITRIP.GT.3) ISITE = ISITE + 4
C
     AAN = P(ISITE,1)
     BBN = P(ISITE,2)
     CCN = P(ISITE,3)
     DO 999 I9 = 1,44
     XO(I9) = P(I9,1) - AAN
     ZO(I9) = P(I9,2) - BBN
     YO(I9) = P(I9,3) - CCN
C
C
     DO 510 L = 1,3
     DIRQM(L) = 0.
     RECQM(L) = 0.
     DO 500 M = 1,3
     DIRPO(L,M) = 0.
     RECPO(L,M) = 0.
  500 CONTINUE
  510 CONTINUE
C
     DO 100 I = 1,ILIM
     AL = FLOAT(I) - 1.
 2000 CONTINUE
     DO 95 J = 1,ILIM
```

```
      AM = FLOAT(J) - 1.
 1000 CONTINUE
      DO 90 K = 1,ILIM
      ANN = FLOAT(K) - 1.
      TL = 2.*PIE*AL
      TM = 2.*PIE*AM
      TN = 2.*PIE*ANN
   20 R(1) = (AL + XO(I9))*A*CC + (AM + YO(I9))*B*CD
      R(2) = - (AL + XO(I9))*A*SC + (AM + YO(I9))*B*SD
      R(3) = (ANN + ZO(I9))*C
      G(1) = (TL*SD)/(A*SB) + (TM*SC)/(B*SB)
      G(2) = - (TL*CD)/(A*SB) + (TM*CC)/(B*SB)
      G(3) = TN/C
C
      TR(1) = R(1)
      TR(2) = R(2)
      TR(3) = R(3)
      TG(1) = G(1)
      TG(2) = G(2)
      TG(3) = G(3)
C
      RV = SQRT(R(1)**2 + R(2)**2 + R(3)**2)
      GV = SQRT(G(1)**2 + G(2)**2 + G(3)**2)
C
C
      SQP = SQRT(PIE)
      R5 = RV**5
      R7 = RV**7
      R9 = RV**9
      R11= RV**11
      G2 = GV**2
      G3 = GEE**3
      G5 = GV**5
C
C
      GRV = GEE*RV
      GR2 = (GEE*RV)**2
      GR4 = GR2**2
      GR6 = GR2**3
      GR8 = GR2**4
      IF(GR2.GT.100.) GO TO 888
      EXPD = EXP(-GR2)
      GO TO 889
  888 EXPD = 0.
  889 CONTINUE
C
      CALL ERFN(GRV,ERROR)
C
      FRONT = 2.*GRV*EXPD/SQP
      DO 776 L = 1,3
C
      IF(RV.EQ.0.) GO TO 80
      IF(ISITE.NE.1) GO TO 80
      DO 801 M = 1,3
```

```
      IF(L.EQ.M) DEL1 = 1.
      IF(L.NE.M) DEL1 = 0.
C
      FAC11=(16.*GR8+72.*GR6+252.*GR4+560.*GR2+945.)
     1 *FRONT + 945.*ERROR
      FAC12 = R(L)*(R(M)**4)/R11
      FAC21 = FRONT*(8.*GR6 + 28.*GR4 + 70.*GR2 + 105.) +
     1 105.*ERROR
      FAC22 = (4.*R(M)*DEL1 + 6.*R(L))*(R(M)**2)/R9
      FAC31 = FRONT*(4.*GR4 + 10.*GR2 + 15.) + 15.*ERROR
      FAC32 = (12.*R(M)*DEL1 + 3.*R(L))/R7
      DIRPO(L,M)=DIRPO(L,M) - FAC11*FAC12 + FAC21*FAC22 -
     1 FAC31*FAC32
C
  801 CONTINUE
   80 CONTINUE
C
      IF(RV.EQ.0.) GO TO 81
C
      TERM1 = (FRONT*(105. + 70.*GR2 + 28.*GR4 + 8.*GR6) +
     1 105.*ERROR)*(R(L)**4)/R9
      TERM2 = (FRONT*(15. + 10.*GR2 + 4.*GR4) + 15.*ERROR)*
     1 6.*(R(L)**2)/R7
      TERM3 = (FRONT*(3. + 2.*GR2) + 3.*ERROR)*3./R5
      DIRQM(L) = DIRQM(L) + TERM1 - TERM2 + TERM3
C
   81 CONTINUE
  776 CONTINUE
C
C
      IF((AL.EQ.0.).AND.(AM.EQ.0.).AND.(ANN.EQ.0.))GGG = 0.
      IF(GGG.EQ.0.) GO TO 745
      GRAT = (GV/(2.*GEE))**2
      IF(GRAT.GT.100.)GO TO 788
      EXPG = EXP(-GRAT)
      GO TO 789
  788 EXPG = 0.
  789 CONTINUE
C
      CALL DOTPC(PROPC)
      CALL DOTEL(PROEL)
C
  745 CONTINUE
C
      DO 760 L = 1,3
      IF(GGG.EQ.0.) GO TO 755
      IF(ISITE.NE.1) GO TO 755
C
      DO 754 M = 1,3
C
      RECPO(L,M) = RECPO(L,M) + (PIE/V)*4.*G(L)*
     1 (G(M)**4)*PROEL*EXPG/G2
C
  754 CONTINUE
```

```
  755 CONTINUE
C
C
      IF(GGG.EQ.0.) GO TO 54
      RECQM(L)=RECQM(L)+(PIE/V)*4.*(G(L)**4)*PROPC*EXPG/G2
C
   54 CONTINUE
  760 CONTINUE
C
C
C
      GGG = 1.
      IF(ANN.LE.0.) GO TO 90
      ANN = - ANN
      TN = - TN
      GO TO 20
   90 CONTINUE
      IF(AM.LE.0.) GO TO 95
      AM = - AM
      TM = - TM
      GO TO 1000
   95 CONTINUE
      IF(AL.LE.0.) GO TO 100
      AL = - AL
      TL = - TL
      GO TO 2000
  100 CONTINUE
C
C
      DO 340 L = 1,3
      DO 330 M = 1,3
      PNM(L,I9,M) = DIRPO(L,M) + RECPO(L,M)
  330 CONTINUE
      QMNEW(I9,L) = DIRQM(L) + RECQM(L)
  340 CONTINUE
C
C
C
C
  999 CONTINUE
C
C
 9999 CONTINUE
C
      DO 820 I = 1,44
      DO 819 L = 1,3
      WRITE(18,810)(PNM(L,I,J),J=1,3)
  819 CONTINUE
  820 CONTINUE
  810 FORMAT(3(F13.8))
      DO 830 I = 1,44
      WRITE(18,810)(QMNEW(I,J),J=1,3)
  830 CONTINUE
C
```

```
C
C
      STOP
      END
      SUBROUTINE ERFN(GRV,ERROR)
      DATA  P/0.3275911/
      DATA A1/0.254829592/
      DATA A2/-0.284496736/
      DATA A3/1.421413741/
      DATA A4/-1.453152027/
      DATA A5/1.061405429/
C
      T = 1./(1. + P*GRV)
      IF ( GRV.GT.10. ) GO TO 50
      EX = EXP(-(GRV**2))
      GO TO 60
   50 EX = 0.
   60 CONTINUE
      SUM = A1*T + A2*T**2 + A3*T**3 + A4*T**4 + A5*T**5
      ERROR = 1. - SUM*EX
      ERROR = 1. - ERROR
      RETURN
      END
      SUBROUTINE DOTPC(PROPC)
      DIMENSION R(3),G(3),PRO(3)
      COMMON/ONE/G,R,PROD
C
      SPRO = 0.
      DO 10 I = 1,3
      PRO(I) = G(I)*R(I)
      SPRO = SPRO + PRO(I)
   10 CONTINUE
      PROPC = COS(SPRO)
      RETURN
      END
      SUBROUTINE DOTEL(PROEL)
      DIMENSION R(3),G(3),PRO(3)
      COMMON/ONE/G,R,PROD
C
      SPRO = 0.
      DO 10 I = 1,3
      PRO(I) = G(I)*R(I)
      SPRO = SPRO + PRO(I)
   10 CONTINUE
      PROEL = SIN(SPRO)
      RETURN
      END
```

Program CL34 is the RTH analogue of FL024.

```
      PROGRAM CL34(INPUT,OUTPUT,TAPE5)
      REAL WK(1450),ALIV(44,9),QMAT(12,44,9),NEWPR(12,12,9),
     1 QMDEL(12,44,9),PROD(12,44,9),ATEM(3,3),BTEM(3,3),
     3 ESS(44,3,3),QUPE(36,36),DIMO(44,3),ELF(36),E(44,3),
     4 AMXTEM(44,3,3),OFFDIA(4),EPS(4,3,3),ALTEM(4,3),
     5 B42EXP(9),DIA(4),DEL(12,44),ELPRO(44,3),TEEL3(44,3),
     6 ALRE(9),PNM(3,44,3),B40EXP(9),TEEL4(44,3)
      DIMENSION DELPOL(4),B44EXP(9),PNMNEW(3,44,3),QMNEW(44,3)
      EXTERNAL LEQT2F
      COMMON/FIELD/E,ELPRO,TEEL3,TEEL4
      COMMON/CHARGE/ETA
      COMMON/POINT/QMNEW,FACMOD,ANS1,ANS2,ANS3
      DATA (ALRE(I),I=1,9)/1.23,1.11,1.06,1.01,0.97,0.94,
C     ALRE(1) = 1.23  (EXPL FREE ION VALUE)
C     ALRE(3) = 1.06 (EXXPL FREE ION VALUE)
     1 0.90,0.86,0.83/
      DATA (OFFDIA(I),I=1,4)/0.0,0.0,0.00,0.00/
      DATA (B40EXP(I),I=1,9)/-.033,-.035,-.034,0.0000,-.037,
     1 -.035,-.033,-.036,-.035/
      DATA (B42EXP(I),I=1,9)/.035,.023,.034,.000,.024,.031,
     1 .052,.092,.054/
      DATA (B44EXP(I),I=1,9)/-.014,+.001,+.004,+.000,-.004,
     1 -.005,-.033,+.069,+.031/
      DATA ETA,ALCL,ALOX,ALHY/0.4,1.40,3.10,0.6/
      DATA NHST/9/
C
      DO 869 I = 1,12
      DO 868 J = 1,44
      DEL(I,J) = 0.
  868 CONTINUE
  869 CONTINUE
      DEL(1,1) = 1.
      DEL(2,3) = 1.
      J = 1
      DO 870 I = 3,12
      J = J + 4
      DEL(I,J) = 1.
  870 CONTINUE
C
      DO 820 ITRIP = 1,12
      DO 819 I9 = 1,44
      READ(5,810)(QMAT(ITRIP,I9,J),J=1,5)
      READ(5,811)(QMAT(ITRIP,I9,K),K=6,9)
  819 CONTINUE
  820 CONTINUE
      DO 830 ITRIP = 1,12
      IF(ITRIP.EQ.1) ISITE = 1
      IF(ITRIP.EQ.2) ISITE = 3
      IF(ITRIP.EQ.3) ISITE =5
      IF(ITRIP.GT.3) ISITE = ISITE + 4
      READ(5,812)(ELPRO(ISITE,J),J=1,3)
      READ(5,812)(TEEL3(ISITE,J),J=1,3)
      READ(5,812)(TEEL4(ISITE,J),J=1,3)
  830 CONTINUE
```

```
      DO 840 I9 = 1,44
      READ(5,813)(PNM(1,I9,J),J=1,3)
      READ(5,813)(PNM(3,I9,J),J=1,3)
  840 CONTINUE
C
      DO 899 I  = 1,44
      DO 898 L  = 1,3
      READ(5,812)(PNMNEW(L,I,J),J=1,3)
  898 CONTINUE
  899 CONTINUE
      DO 897 I  = 1,44
      READ(5,812)(QMNEW(I,J),J=1,3)
  897 CONTINUE
C
C
  810 FORMAT(5(F13.8))
  811 FORMAT(4(F13.8))
  812 FORMAT(3(F13.8))
  813 FORMAT(3(F13.8))
C
C
C
C
      DO 510 I  = 1,44
      DO 505 J  = 1,3
      DO 501 K  = 1,3
      ESS(I,J,K) = 0.
  501 CONTINUE
  505 CONTINUE
  510 CONTINUE
      DO 515 I  = 1,3,2
      DO 514 J  = 1,3
      ESS(I,J,J) = 1.
  514 CONTINUE
  515 CONTINUE
      DO 520 I  = 5,41,4
      DO 519 J  = 1,3
      ESS(I,J,J) = 1.
  519 CONTINUE
  520 CONTINUE
      DO 525 I  = 2,4,2
      DO 524 J  = 1,3
      ESS(I,J,J) = -1.
  524 CONTINUE
  525 CONTINUE
      DO 530 I  = 6,42,4
      DO 529 J  = 1,3
      ESS(I,J,J) = -1.
  529 CONTINUE
  530 CONTINUE
      DO 535 I  = 7,43,4
      DO 534 J  = 1,3,2
      ESS(I,J,J) = -1.
  534 CONTINUE
```

```
      ESS(I,2,2) = 1.
  535 CONTINUE
      DO 540 I = 8,44,4
      DO 539 J = 1,3,2
      ESS(I,J,J) = 1.
  539 CONTINUE
      ESS(I,2,2) = -1.
  540 CONTINUE
C
C
  400 CONTINUE
C
      DO 8040 IJO = 1,1
      ETA = 0.20 + 0.01*FLOAT(IJO)
      CALL CHARE
      CALL CHAEL
      DO 8035 IJ1 = 1,1
      ALTEM(1,2) = +0.59 - 0.01*FLOAT(IJ1)
      ALTEM(1,1) = ALTEM(1,2)
      ALTEM(1,3) = ALTEM(1,2)
      DO 8030 IJ2 = 1,1
      ALTEM(2,2) = 3.04 + 0.01*FLOAT(IJ2)
      ALTEM(2,1) = ALTEM(2,2)
      ALTEM(2,3) = ALTEM(2,2)
      DO 8025 IJ3 = 1,1
      ALTEM(3,2) = 3.81 - 0.02*FLOAT(IJ3)
      ALTEM(3,1) = ALTEM(3,2)
      ALTEM(3,3) = ALTEM(3,2)
      DO 8024 IJ4 = 1,1
      ALTEM(4,2) =    0.411 + 0.001*FLOAT(IJ4)
      ALTEM(4,1) = ALTEM(4,2)
      ALTEM(4,3) = ALTEM(4,2)
C
      DO 8020 IK1 = 1,1
      OFFDIA(1) = +1.00 -1.00*FLOAT(IK1)
      DO 8019 IK2 = 1,1
      OFFDIA(2) = + 0.33 + 0.01*FLOAT(IK2)
      DO 8018 IK3 = 1,1
      OFFDIA(3) = 2.0 + 0.22*FLOAT(IK3)
      DO 8017 IK4 = 1,1
      OFFDIA(4) = + 0.029  + 0.002*FLOAT(IK4)
C
C
      ELF(1) = E(1,1)
      ELF(2) = E(1,2)
      ELF(3) = E(1,3)
      ELF(4) = E(3,1)
      ELF(5) = E(3,2)
      ELF(6) = E(3,3)
      I = 6
      DO 3 J = 5,41,4
      DO 2 K = 1,3
      I = I + 1
      ELF(I) = E(J,K)
```

```
    2 CONTINUE
    3 CONTINUE
C
      DO 270 I = 1,4
      DO 269 J = 1,3
      DO 268 K = 1,3
      EPS(I,J,K) = 0.
  268 CONTINUE
  269 CONTINUE
  270 CONTINUE
C
      DO 2000 KK = 1,4
      DIA(KK) = ALTEM(KK,1)*ALTEM(KK,3) - OFFDIA(KK)**2
      IF(DIA(KK).EQ.0.) DIA(KK) = DIA(KK) +,0.001
      EPS(KK,1,1) = ALTEM(KK,3)/DIA(KK)
      EPS(KK,2,2) = 1./ALTEM(KK,2)
      EPS(KK,3,3) = ALTEM(KK,1)/DIA(KK)
      EPS(KK,1,3) = - OFFDIA(KK)/DIA(KK)
      EPS(KK,3,1) = EPS(KK,1,3)
 2000 CONTINUE
C
C
      DO 220 I = 1,44
      IF(I.LE.2) ISUB = 1
      IF((I.GT.2).AND.(I.LE.8)) ISUB = 2
      IF((I.GT.8).AND.(I.LE.20)) ISUB = 3
      IF((I.GT.20).AND.(I.LE.44)) ISUB = 4
      DO 230  J = 1,3
      DO 240 K = 1,3
      AMXTEM(I,J,K) = EPS(ISUB,J,K)
  240 CONTINUE
  230 CONTINUE
  220 CONTINUE
C
      DO 215 I = 1,44
      L = 0
      DO 213 J = 1,3
      DO 211 K = 1,3
      L = L + 1
      ALIV(I,L) = AMXTEM(I,J,K)
  211 CONTINUE
  213 CONTINUE
  215 CONTINUE
C
      DO 40 L = 1,12
      DO 35 I = 1,9
      DO 25 K = 1,44
      QMDEL(L,K,I) = ALIV(K,I)*DEL(L,K) - QMAT(L,K,I)
   25 CONTINUE
   35 CONTINUE
   40 CONTINUE
C
C
      DO 500 I = 1,12
```

```
      DO 495 J = 1,44
      DO 490 K = 1,9
      PROD(I,J,K) = 0.
  490 CONTINUE
  495 CONTINUE
  500 CONTINUE
C
      DO 485 I = 1,36
      DO 480 J = 1,36
      QUPE(I,J) = 0.
  480 CONTINUE
  485 CONTINUE
C
C
C
      DO 58 I = 1,12
      DO 56 J = 1,44
      K = 0
      DO 54 L = 1,3
      DO 53 M = 1,3
      K = K + 1
      ATEM(L,M) = QMDEL(I,J,K)
   53 CONTINUE
   54 CONTINUE
      DO 52 L = 1,3
      DO 51 M = 1,3
      BTEM(L,M) = 0.
   51 CONTINUE
   52 CONTINUE
      DO 50 L = 1,3
      DO 49 M = 1,3
      DO 48 N = 1,3
      BTEM(L,M) = BTEM(L,M) + ATEM(L,N)*ESS(J,N,M)
   48 CONTINUE
   49 CONTINUE
   50 CONTINUE
      KK = 0
      DO 47 L = 1,3
      DO 46 M = 1,3
      KK = KK + 1
      PROD(I,J,KK) = BTEM(L,M)
   46 CONTINUE
   47 CONTINUE
   56 CONTINUE
   58 CONTINUE
C
C
      DO 70 I = 1,12
      DO 65 J = 1,12
      DO 60 K = 1,9
      NEWPR(I,J,K) = 0.
   60 CONTINUE
   65 CONTINUE
   70 CONTINUE
```

```
      DO 75 I = 1,12
      DO 74 J = 1,9
      DO 73 K = 1,2
      NEWPR(I,1,J) = NEWPR(I,1,J) + PROD(I,K,J)
   73 CONTINUE
      DO 72 K = 3,4
      NEWPR(I,2,J) = NEWPR(I,2,J) + PROD(I,K,J)
   72 CONTINUE
      K = 1
      DO 771 L = 3,12
      K = K + 4
      M = K + 3
      DO 770 N = K,M
      NEWPR(I,L,J) = NEWPR(I,L,J) + PROD(I,N,J)
  770 CONTINUE
  771 CONTINUE
   74 CONTINUE
   75 CONTINUE
      DO 95 I = 1,12
      DO 93 J = 1,12
      DO 89 K = 1,3
      DO 87 L = 1,3
      II = 3*(I - 1) + K
      JJ = 3*(J - 1) + L
      M = L + 3*(K - 1)
      QUPE(II,JJ) = NEWPR(I,J,M)
   87 CONTINUE
   89 CONTINUE
   93 CONTINUE
   95 CONTINUE
C
C
      IDGT = 0
C
      CALL LEQT2F(QUPE,1,36,36,ELF,IDGT,WK,IER)
C
      DO 200 I = 1,44
      DO 195 J = 1,3
      DIMO(I,J) = 0.
  195 CONTINUE
  200 CONTINUE
C
      DO 110 I = 1,2
      DO 105 J = 1,3
      DO 100 K = 1,3
      DIMO(I,J) = DIMO(I,J) + ESS(I,J,K)*ELF(K)
  100 CONTINUE
  105 CONTINUE
  110 CONTINUE
C
C
C
      DO 125 I = 3,4
      DO 120 J = 1,3
```

```
      DO 115 K = 1,3
      L = K + 3
      DIMO(I;J) = DIMO(I,J) + ESS(I,J,L)*ELF(K)
  115 CONTINUE
  120 CONTINUE
  125 CONTINUE
C
      K = 1
      DO 140 I = 3,12
      K = K + 4
      M = K + 3
      DO 137 J = K,M
      DO 134 L = 1,3
      DO 131 N = 1,3
      K2 = 3*(I - 1) + N
      DIMO(J,L) = DIMO(J,L) + ESS(J,L,N)*ELF(K2)
  131 CONTINUE
  134 CONTINUE
  137 CONTINUE
  140 CONTINUE
C
C
C
  150 CONTINUE
C
      EPO1 = 0.
      EPO2 = 0.
      EPO3 = 0.
      IF(ETA.EQ.1.) IDO = 20
      IF(ETA.LT.1.) IDO = 44
      DO 160 I = 1,IDO
      DO 155 J = 1,3
      EPO1 = EPO1 + DIMO(I,J)*PNMNEW(J,I,3)
      EPO2=EPO2+DIMO(I,J)*(PNMNEW(J,I,2)-PNMNEW(J,I,1))
      EPO3 = EPO3 + DIMO(I,J)*(PNMNEW(J,I,1) +
     1 PNMNEW(J,I,2) - 0.75*PNMNEW(J,I,3))
  155 CONTINUE
  160 CONTINUE
C
      ANS21 = - FACMOD*EPO1/192.
      ANS22 = - FACMOD*EPO2/48.
      ANS23 = - FACMOD*EPO3/48.
C
      BTOTO = ANS1 + ANS21
      BTOT2 = ANS2 + ANS22
      BTOT4 = ANS3 + ANS23
      DIFFO = BTOTO - B40EXP(NHST)
      DIFF2 = BTOT2 - B42EXP(NHST)
      DIFF4 = BTOT4 - B44EXP(NHST)
C
      PRINT 170,NHST,ANS1,ANS21,BTOTO,B40EXP(NHST),DIFFO
      PRINT 170,NHST,ANS2,ANS22,BTOT2,B42EXP(NHST),DIFF2
      PRINT 170,NHST,ANS3,ANS23,BTOT4,B44EXP(NHST),DIFF4
  170 FORMAT(1X,I1,5(E10.3,1X))
```

```
C
C
C
 8017 CONTINUE
 8018 CONTINUE
 8019 CONTINUE
 8020 CONTINUE
 8024 CONTINUE
 8025 CONTINUE
 8030 CONTINUE
 8035 CONTINUE
 8040 CONTINUE
 8021 CONTINUE
C
      STOP
      END
      SUBROUTINE CHARE
      DIMENSION TE(4,3),QMNEW(44,3)
      COMMON/POINT/QMNEW,FACMOD,ANS1,ANS2,ANS3
      COMMON/CHARGE/ETA
C
      DO 5 I = 1,4
      DO 4 J = 1,3
      TE(I,J) = 0.
    4 CONTINUE
    5 CONTINUE
C
      DO 10 I = 1,2
      TE(1,1) = TE(1,1) + QMNEW(I,3)/192.
      TE(1,2) = TE(1,2) + (QMNEW(I,2) - QMNEW(I,1))/48.
      TE(1,3) = TE(1,3) + (QMNEW(I,1) + QMNEW(I,2) -
     1 0.75*QMNEW(I,3))/48.
   10 CONTINUE
C
      DO 15 I = 3,8
      TE(2,1) = TE(2,1) + QMNEW(I,3)/192.
      TE(2,2) = TE(2,2) + (QMNEW(I,2) - QMNEW(I,1))/48.
      TE(2,3) = TE(2,3) + (QMNEW(I,1) + QMNEW(I,2) -
     1 0.75*QMNEW(I,3))/48.
   15 CONTINUE
C
      DO 20 I = 9,20
      TE(3,1) = TE(3,1) + QMNEW(I,3)/192.
      TE(3,2) = TE(3,2) + (QMNEW(I,2) - QMNEW(I,1))/48.
      TE(3,3) = TE(3,3) + (QMNEW(I,1) + QMNEW(I,2) -
     1 0.75*QMNEW(I,3))/48.
   20 CONTINUE
C
      DO 25 I = 21,44
      TE(4,1) = TE(4,1) + QMNEW(I,3)/192.
      TE(4,2) = TE(4,2) + (QMNEW(I,2) - QMNEW(I,1))/48.
      TE(4,3) = TE(4,3) + (QMNEW(I,1) + QMNEW(I,2) -
     1 0.75*QMNEW(I,3))/48.
   25 CONTINUE
```

```
C
      E1 = TE(1,1)*(+3.) + TE(2,1)*(-1.) +
     1 (-2.*ETA)*TE(3,1) + ETA*TE(4,1)
      E2 = TE(1,2)*(+3.) + TE(2,2)*(-1.) +
     1 (-2.*ETA)*TE(3,2) + ETA*TE(4,2)
      E3=TE(1,3)*3.-TE(2,3)-2.*ETA*TE(3,3)+ETA*TE(4,3)
C
      R2 = 1.515*(0.529**4)
      CONV = 116195.62
C
C     FACTOR 0.033/169. TEMPORARY ONLY
C
      FACMOD =(CONV*29.9*R2/60.)*0.33/169.
      ANS1 = - FACMOD*E1
      ANS2 = - FACMOD*E2
      ANS3 = - FACMOD*E3
C
      PRINT 40,  E1,E2,E3
      PRINT 40,ANS1,ANS2,ANS3
   40 FORMAT(1X,*A VALUES*,2X,3(E15.5,2X))
C
      RETURN
      END
      SUBROUTINE CHAEL
      DIMENSION E(44,3),ELPRO(44,3),TEEL3(44,3),TEEL4(44,3)
      COMMON/FIELD/E,ELPRO,TEEL3,TEEL4
      COMMON/CHARGE/ETA
C
C
      DO 20 I = 1,12
      IF(I.EQ.1) ISITE = 1
      IF(I.EQ.2) ISITE = 3
      IF(I.EQ.3) ISITE = 5
      IF(I.GE.4) ISITE = ISITE + 4
      DO 15 J = 1,3
      E(ISITE,J) = ELPRO(ISITE,J) - 2.*ETA*TEEL3(ISITE,J) +
     1 ETA*TEEL4(ISITE,J)
   15 CONTINUE
   20 CONTINUE
C
      RETURN
      END
```

REFERENCES

1. H. Bethe, Ann. Physik 3, 133 (1929).
2. B. N. Figgis, "Introduction to Ligand Fields" (New York: Interscience, 1966), p. 2.
3. H. A. Buckmaster, R. Chatterjee, and Y. H. Shing, Can. J. Phys. 50, 991 (1972).
4. A. Abragam and B. Bleaney, "Electron Paramagnetic Resonance of Transition Ions" (Oxford: Clarendon Press, 1970).
5. K. W. H. Stevens, Proc. Phys. Soc. A. 65, 209 (1952).
6. G. H. Dieke, "Spectra and Energy Levels of Rare-Earth Ions in Crystals" (New York: Interscience, 1968).
7. J. S. Griffith, "The Theory of Transition Metal Ions" (New York: Cambridge University Press, 1961).
8. H. Margenau and G. M. Murphy, "The Mathematics of Physics and Chemistry," 2nd ed. (Princeton: Van Nostrand, 1956).
9. M. T. Hutchings, Sol. State Phys. 16, 234, (1964).
10. C. P. Poole and H. A. Farach, "The Theory of Magnetic Resonance" (New York: Interscience, 1972).
11. A. R. Edmonds, "Angular Momentum in Quantum Mechanics" (Princeton: Princeton University Press, 1957).
12. K. N. R. Taylor and M. I. Darey, "Physics of Rare Earth Solids" (London: Chapman and Hall, 1972).
13. E. U. Condon and G. H. Shortley, "The Theory of Atomic Spectra" (New York: Cambridge University Press, 1963).
14. E. U. Condon and H. Obadasi, "Atomic Structure" (New York: Cambridge University Press, 1980), p. 173.

15. B. G. Wybourne, Phys. Rev. 148, 317 (1966).

16. D. J. Newman and W. Urban, J. Phys. C 5, 3101 (1972).

17. D. J. Newman and W. Urban, Adv. Phys. 24, 793 (1975).

18. D. J. Newman, J. Phys. C 8, 1862 (1975).

19. E. J. Bijvank and H. W. den Hartog, Bull. Mag. Res. 2, 165 (1980).

20. E. J. Bijvank and H. W. den Hartog, Phys. Rev. B 22, 4121 (1980).

21. E. J. Bijvank and H. W. den Hartog, Phys. Rev. B 22, 4133 (1980).

22. S. E. Barnes, K. Baberschke, and M. Hardiman, Phys. Rev. B 18, 2409 (1978).

23. S. Adam, G. Adam, and A. Corciovei, Phys. Stat. Sol. (b) 105, 85 (1981).

24. D. J. Newman, Adv. Phys. 20, 197 (1971).

25. C. A. Hutchison, B. R. Judd, and D. F. D. Pope, Proc. Phys. Soc. B70, 1514 (1957).

26. B. G. Wybourne, J. Chem. Phys. 43, 4506 (1966).

27. G. E. Stedman and D. J. Newman, J. Phys. C 7, 2347 (1974).

28. G. E. Stedman and D. J. Newman, J. Phys. C 8, 1070 (1975).

29. D. J. Newman, Aust. J. Phys. 29, 263 (1976).

30. A. Edgar and D. J. Newman, J. Phys. C 8, 4023 (1975).

31. S. K. Misra, P. Mikolajczak, and N. R. Lewis, Phys. Rev. B 24, 3729 (1981).

32. N. R. Lewis and S. K. Misra, Phys. Rev. B 25 (In press)

33. S. K. Misra, P. Mikolajczak, and S. Korczak, J. Chem. Phys. 74(2), 922 (1981).

34. S. K. Misra, J. Magn. Reson. 23, 403 (1976).

35. A. Zalkin, D. H. Templeton, and T. E. Hopkins, Inorg. Chem. 5, 1466 (1966).

36. S. K. Misra and G. R. Sharp, J. Phys. C 10, 897 (1977).

37. S. K. Misra and P. Miklojczak, J. Magn. Reson. 35, 87 (1979).

38. J. Y. Buzaré, M. Fayet-Bonnet, and J. C. Fayet, J. Phys. C. 14, 67 (1981).

39. P. P. Ewald, Ann. Phys. (Leipzig) 64, 253 (1921).

40. M. Faucher, J. Dexpert-Ghys, and P. Caro, Phys. Rev. B 21, 3689 (1980).

41. A. P. Cracknell, "Group Theory in Solid State Physics" (London: Taylor and Francis, 1975), p. 11.

42. C. Kittel, "Introduction to Solid State Physics," 5th Ed. (New York: John Wiley, 1976), p. 410.

43. R. Kubo and T. Nagamiya (Ed.), "Solid State Physics" (New York: McGraw-Hill, 1969), p. 643, p. 655.

44. B. Z. Malkin, Z. I. Ivanenko, and I. B. Aizenberg, Sov. Phys. Solid State 12, 1491 (1971).

45. A. L. Larionov and B. Z. Malkin, Opt. Spectrosc. 39, 637 (1975).

46. L. A. Bumagina, B. N. Kazakov, B. Z. Malkin, and A. L. Stolov, Sov. Phys. Solid State 19, 624 (1977).

47. G. A. Bogomolova, L. A. Bumagina, A. A. Kaminskii, and B. Z. Malkin, Sov. Phys. Solid State 19, 1428 (1977).

48. G. Burns and A. M. Glazer, "Space Groups for Solid State Scientists" (New York: Academic, 1978), p. 172.

49. "International Tables for X-Ray Crystallography" (Birmingham, England: The Kynoch Press, 1952).

50. R. R. Birge, J. Chem. Phys. 72, 5312 (1980).

51. B. G. Dick and A. W. Overhauser, Phys. Rev. 112, 90 (1958).

52. H. J. Juretschke, "Crystal Physics" (Reading, Mass.:

W. A. Benjamin, 1974), p. 17.

53. Ibid., p. 50.

54. M. Satoh and T. Taki, Phys. Rev. B 23, 6711 (1981).

55. A. Cohen, Phys. Lett. 68, 166 (1979).

56. W. B. Mims, "The Linear Electric Field Effect in Paramagnetic Resonance" (Oxford: Clarendon Press, 1976).

57. P. O. Lowdin, Adv. Phys. 5, 1 (1956).

58. N. R. Lewis and S. K. Misra (To be published)

59. G. Burns, Phys. Rev. 128, 2121 (1962).

60. L. Pauling, "The Nature of the Chemical Bond," 3rd ed. (Ithaca, N. Y.: Cornell University Press, 1960).

61. G. S. Koerber, "Properties of Solids" (Englewood Cliffs, N. J.: Prentice-Hall, 1962).

62. K. M. S. Saxena and S. Fraga, J. Chem. Phys. 57, 1800 (1972).

63. J. R. Tessman, A. H. Kahn, and W. Shockley, Phys. Rev. 92, 890 (1953).

64. J. D. H. Donnay and G. Donnay, "Crystal Determinative Tables," 2nd ed. (New York: American Crystallographic Association, 1962).

65. E. E. Havinga, Phys. Rev. 119, 1193 (1960).

66. J. M. Ziman, "Principles of the Theory of Solids" (London: Cambridge University Press, 1965).

67. J. W. Weenk and H. A. Harwig, J. Phys. Chem. Solids 38, 1047 (1977).

68. S. K. Misra and N. R. Lewis, J. Chem. Phys. 71, 1033 (1979).

69. Abragam and Bleaney, Op. cit., p. 666.

70. Condon and Obadasi, Op. cit., p. 149.

71. E. P. Wigner, "Group Theory" (New York: Academic, 1959), p. 331.

72. M. Marezio, H. A. Plettinger, and W. H. Zachariasen, Acta Cryst. 14, 234 (1961).